TECHNISCHE UNIVERSITÄT WIEN
Vienna University of Technology

UNIVERSITY OF CALGARY

# DIPLOMA THESIS

## Synthesis and Study of Novel Carbazole- and Indolocarbazole-Functionalized Dithienophosphole Oxides as Bipolar Functional Organic Materials

Conducted at the

**Department of Chemistry & Centre for Advanced Solar Materials**

At the **University of Calgary,** in **Calgary, Canada** (1)

And the

**Institute of Applied Synthetic Chemistry**

At the **Vienna University of Technology,** in **Vienna, Austria** (2)

Under the supervision of

[1] Univ.Prof. Dipl.Chem. Dr.rer.nat. Thomas **Baumgartner**

And

[2] Univ.Prof. Dipl.-Ing. Dr.techn. Johannes **Fröhlich**

Advised by

[2] Univ.Ass. Dipl.-Ing. Dr.techn. Daniel **Lumpi**
[2] Univ.Ass. Dipl.-Ing. Paul **Kautny**

By

Hannes **Puntscher**, BSc.

Matr.Nr.: 0825609

Schleifmühlgasse 15/14, A – 1040 Wien

Vienna, May 24, 2014

Bazinga. – *Sheldon Cooper*

# Danksagung, Acknowledgment

Zunächst möchte ich *Univ.Prof. Dipl.Chem. Dr.rer.nat. Thomas Baumgartner* und *Univ.Prof. Dipl.-Ing. Dr.techn. Johannes Fröhlich* danken, die es mir ermöglicht haben an dieser Diplomarbeit in Calgary und Wien zu arbeiten. Das Auslandsjahr in Kanada und die Zusammenarbeit dieser Forschungsgruppen waren eine großartige, unvergessliche Erfahrung für mich.

*Univ.Ass. Dipl.-Ing. Dr.techn. Daniel Lumpi* und *Univ.Ass. Dipl.-Ing. Paul Kautny* danke ich herzlich für die hervorragende fachliche Betreuung und Unterstützung zeitweise aus einigen tausend Kilometern Entfernung. *Univ.Ass. Dipl.-Ing. Paul Kautny* danke ich außerdem auch für die Aufnahme von Absorptions- und Emissionsspektren.

Furthermore, I'd like to thank my lab colleagues at the University of Calgary, *Thomas Wang MSc*, *Monika Stolař BSc*, *Dr. He Xiao-Ming*, *Alva Woo MSc*, *Huy Huynh BSc* and *Emad Hajar BSc*, for the very warm welcome and all their support especially during intense hours of my project.

*Ass.Prof. Dipl.-Ing. Dr. Christian Hametner* danke ich für die Aufnahme von NMR-Spektren und die Hilfe bei deren Auswertung und *Univ.Ass. Dipl.-Ing. Dr.techn. Berthold Stöger* für die Durchführung der Kristallstrukturanalysen.

Auch bei meinen Laborkollegen an der TU Wien möchte ich mich herzlich für die schöne gemeinsame Zeit und all die ernsten, sowie etwas weniger ernsten Diskussionen bedanken: *Univ.Ass. Dipl.-Ing. Brigitte Holzer*, *Dipl.-Ing. Florian Glöcklhofer* und *Markus Lunzer BSc*, sowie *Barbara Sohr BSc*. Letzterer möchte ich an dieser Stelle ganz besonders danken für die vielen gemeinsamen produktiven Arbeits- und Lernstunden und die großartige freundschaftliche Unterstützung während des ganzen Studiums. Ohne sie wäre mit Sicherheit vieles deutlich schwerer gefallen - danke, liebe Babsolina!

Außerdem möchte ich auch meinen *engsten Frœunden* danken, die immer für mich da waren und sind und mir stets mit Rat und positiven Worten zur Seite standen. So vor allem *Sabrina Mayr*, die mich regelmäßig mit Kaffee versorgt hat und meine lieben Mitbewohner in Calgary und Wien *Volker Mayer*, *Max Kosok* und *Claudia Pichler*.

Ganz besonders herzlich möchte ich mich bei meinen Eltern *Othmar* und *Veronika* bedanken, die mir das ganze Studium erst ermöglicht haben und immer mit viel Interesse, aber auch Geduld hinter mir stehen, stets motivierend und verständnisvoll. Danke an meine ganze Familie, insbesondere an meinen Bruder *Florian*, meiner Tante *Sonja* und meiner Oma *Klara*.

## ABSTRACT

Bipolar functional organic materials are increasingly gaining attention due to their good and balanced charge transport properties, which are crucial for the efficiency and stability of organic electronic devices such as Organic Light-Emitting Diodes (OLEDs). [1]

Within this work, the strongly blue fluorescent dithienophosphole oxide (DTPOX) building block was functionalized with various triarylamine systems (Ph-Cbz, ICz, fig.1).

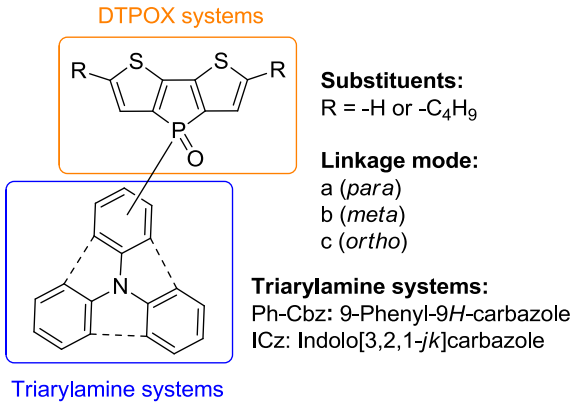


**Fig.1: General structure of the synthesized triarylamine functionalized dithieno[3,2-*b*:2', 3'-*d*]phosphole oxides (DTPOXs)**

The influence of different triarylamine systems (more and less panarized), their linkage mode (*para*, *meta*, *ortho*) and *n*-Bu-substituents at the DTPOX-system on the electrochemical and photophysical properties of the novel materials was investigated.

The synthesis of various triarylamine based precursor systems (D-$PCl_2$) was realized by Ullmann condensation and lithiation of bromo-precursors in order to introduce the phosphorus center. By linking these precursors with the corresponding 3,3'-dibromo-2,2'-bithiophenes (R at positions 5 and 5' on the thiophene rings =H or =$C_4H_9$) trivalent phosphorus compounds were formed and oxidized *in situ* with excess $H_2O_2$.

In order to characterize the photophysical properties absorption and emission spectra of the DTPOX compounds were recorded (fig.2).

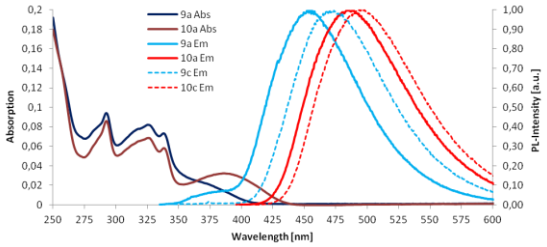


**Fig.2: Absorption and emission spectra of synthesized triarylamine functionalized dithieno[3,2-*b*:2',3'-*d*]phosphole oxides (DTPOX)**

The generally similar absorption spectra show distinctly red shifted onsets of absorption for compounds with R=$C_4H_9$ with respect to those with R=H. Analogously, red-shifted emission was observed for all *n*-Bu-substituted materials. In contrast, the triarylamine moiety does not influence the absorption onset or the emission characteristics with the exception of the species functionalized with the *ortho*-linked phenylcarbazole system (dashed lines: fig. 2, molecular structure: fig.3), which is attributed to intramolecular $\pi$-stacking.

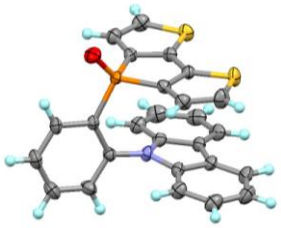

**Fig.3: Molecular structure of the *ortho*-linked phenylcarbazole functionalized DTPOX (obtained by X-ray crystallography)**

Furthermore, the electrochemical properties were investigated by cyclic voltammetry (CV). Both HOMO and LUMO levels indicate no significant injection barrier for charge carriers to adjacent layers in electro-optical devices. Based on these results the next step will be the incorporation of these materials in test-devices.

## KURZFASSUNG


Bipolare funktionelle organische Materialien gewinnen immer mehr an Bedeutung aufgrund ihrer Eigenschaft sowohl positive als auch negative Ladungsträger zu transportieren. Für die technische Anwendung dieser Materialien im Bereich der organischen Elektronik ist dies ausschlaggebend für die Effizienz und Stabilität der Bauteile, wie z.B. organischer Leuchtdioden (OLEDs). [1]

Im Zuge dieser Arbeit wurde das intensiv blau fluoreszierende Dithienophospholoxid (DTPOX) mit verschiedenen Triarylamin-Systemen funktionalisiert (Ph-Cbz, ICz, Abb.1).

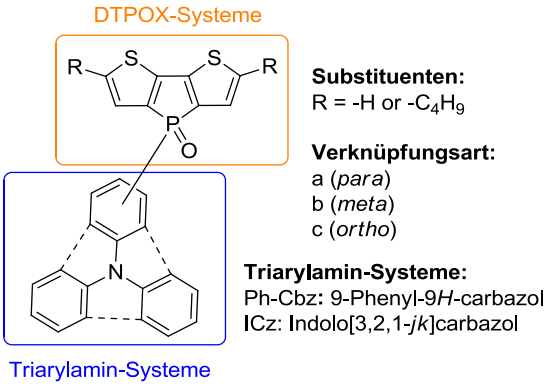


**Abb.1: Allgemeine Struktur der synthetisierten Triarylamin-funktionalisierten Dithieno[3,2-*b*:2',3'-*d*]phospholoxide (DTPOXs)**

Der Einfluss unterschiedlich planarer Triarylamin-Systeme, der Verknüpfungsart (*para*, *meta*, *ortho*) und der *n*-Bu-Substituenten am DTPOX-System auf elektrochemische und photophysikalische Eigenschaften der neuen Materialien wurde untersucht.

Die Synthese der verschiedenen Triarylamin-Vorstufen (D-$PCl_2$) wurde über Ullmann Kondensation und die Lithiierung der Bromo-Spezies realisiert, um dann das Phosphoratom einzuführen. Durch das Zusammenführen dieser Vorstufen mit den entsprechenden 3,3'-Dibromo-2,2'-bithiophenen (R an Position 5 u 5' =H oder =$C_4H_9$) konnten Phosphor(III)-Verbindungen erhalten werden, welche *in situ* mit einem $H_2O_2$-Überschuss oxidiert wurden.

Die photophysikalischen Eigenschaften der Zielsubstanzen wurden durch ihre Absorptions- und Emissionsspektren charakterisiert (Abb.2).

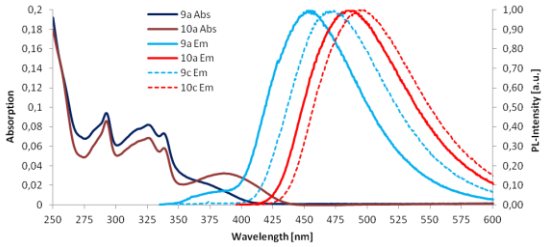


**Abb.2: Absorptions- und Emissionsspektren von Triarylamin-funktionalisierten Dithieno[3,2-*b*:2',3'-*d*] phospholoxiden (DTPOX)**

Die Absorptionsspektren zeigen klar rot-verschobene Absorptionsansätze für Substanzen mit R=$C_4H_9$ verglichen mit denen mit R=H. Auch die Emissionsmaxima der *n*-Bu-substituierten Verbindungen sind rot-verschoben. Das Triarylamin-System scheint hingegen keinen Einfluss auf diese Eigenschaften zu haben. Lediglich für Substanzen mit *ortho*-verknüpften Phenylcarbazol-Systemen zeigt sich eine zusätzliche Rotverschiebung. Intramolekulares *π*-Stacking könnte dies verursachen (gestrichelte Linie: Abb.2, Molekülstruktur: Abb.3).

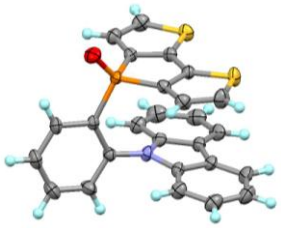

**Abb.3: Molekülstruktur des *ortho*-verknüpften Phenylcarbazol-funktionalisierten DTPOX (ermittelt mittels Einkristallstrukturanalyse)**

Elektrochemische Eigenschaften wurden mittels Cyclovoltammetrie (CV) untersucht, um HOMO und LUMO Werte der Substanzen zu ermitteln. Aufgrund der positiven Ergebnisse können diese Materialien in Test-Bauteilen verbaut und weiter untersucht werden.

# Abbreviations

Besides common abbreviations in the English language and chemical element symbols the below listed short forms are used.

| | |
|---|---|
| BuLi | Butyllithium |
| Cbz | Carbazole |
| DCM | Dichloromethane |
| DMF | Dimethylformamide |
| D-A system | Donor-acceptor system |
| EA | Ethylacetate |
| eq. | (molar) Equivalent |
| Hex | Hexanes |
| HOMO | Highest occupied molecular orbital |
| ICz | Indolocarbazole |
| LUMO | Lowest unoccupied molecular orbital |
| Ph-Cbz | Phenylcarbazole |
| $T_B$ | Boiling Point |
| $T_g$ | Glass transition temperature |
| *t*-Bu | *tert*-butyl |
| *t*-Bu-Cl | 2-Chloro-2-methylpropane |
| THF | Tetrahydrofuran |
| tmsCl | Trimethylsilyl chloride |
| TLC | Thin layer chromatography |
| TPA | Triphenylamine |

# General remarks

## Labeling of substances

Identification of substances is achieved by sequential numbering. Structurally similar substances receive same numbers combined with additional small letters of the Latin alphabet for further differentiation. Substances previously reported in the literature receive Arabic numbers, whereas substances unknown to the literature are labeled in roman numbers.

## References to literature citations

References to literature are given within the text by Arabic numbers in square brackets.

## Nomenclature

The nomenclature of chemical compounds not described in the literature is based on the rules of Chemical Abstracts. Other compounds, reagents and solvents may be described by simplified terms, trivial or trade names.

# Table of contents

# A. Formula scheme

# A.1 Synthesis of OLED compounds – donor systems

## A.1.1 Synthesis of the carbazole-based bromo-precursors

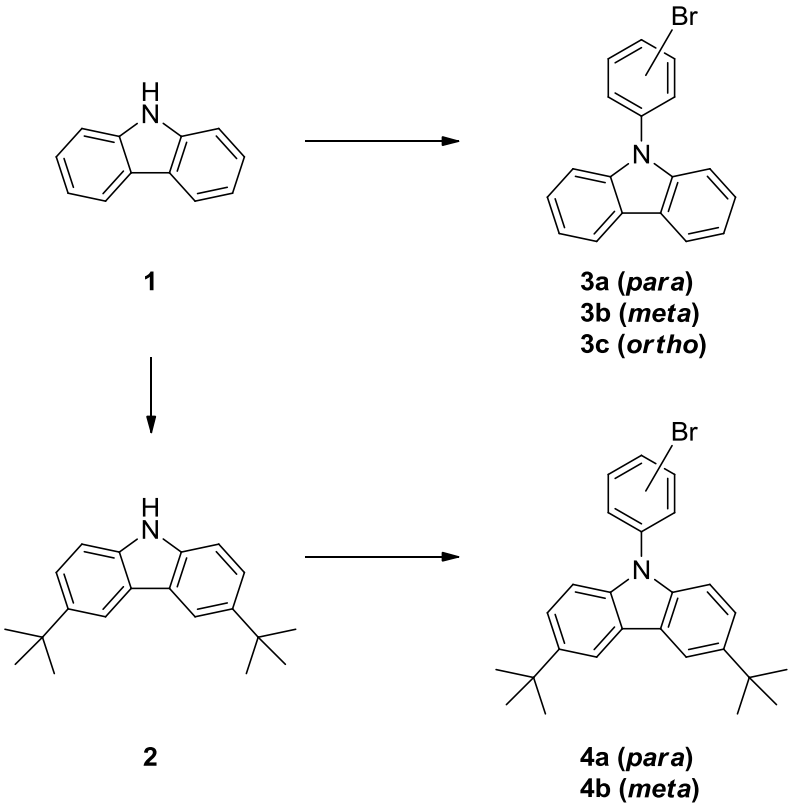


**1** **3a (*para*)**
**3b (*meta*)**
**3c (*ortho*)**

**2** **4a (*para*)**
**4b (*meta*)**

## A.1.2 Lithiation trial of a brominated triarylamine system

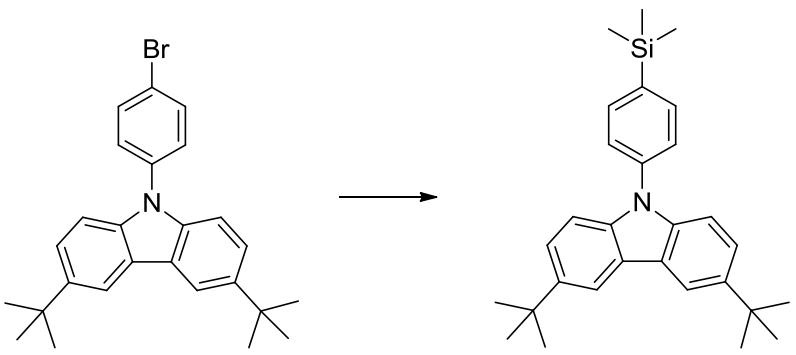


**4a** **T1**

## A.1.3 Preparation of the phosphine reagent

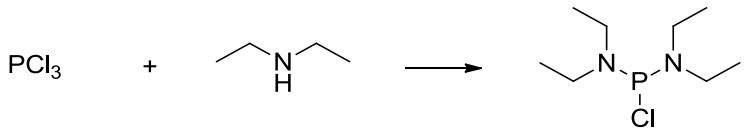


**5** **6** **7**

## A.1.4 Synthesis of the dichlorophosphine precursors

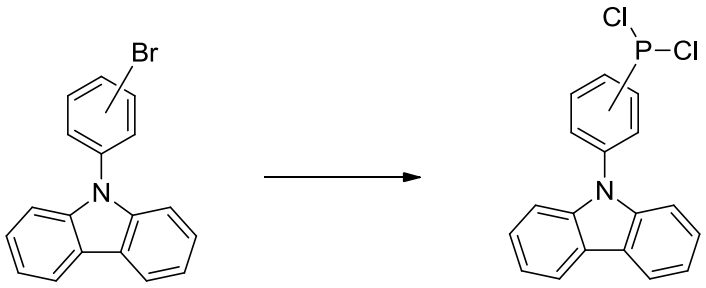


**3a (*para*)**
**3b (*meta*)**
**3c (*ortho*)**

**Ia (*para*)**
**Ib (*meta*)**
**Ic (*ortho*)**

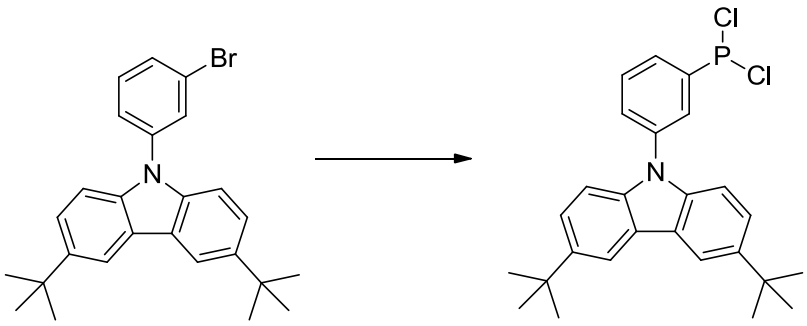


**4b (*meta*)**

**IIb (*meta*)**

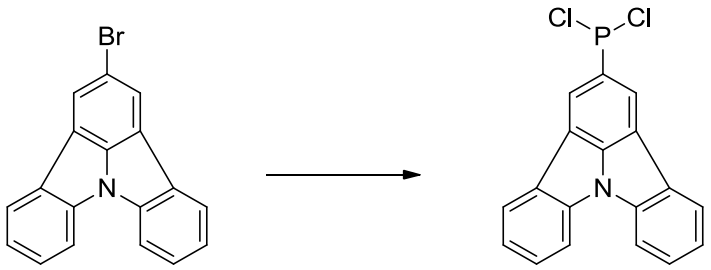


**8a (*para*)** **IIIa (*para*)**

## A.2 Synthesis of OLED compounds – acceptor systems

### A.2.1 Synthesis of bithiophene systems

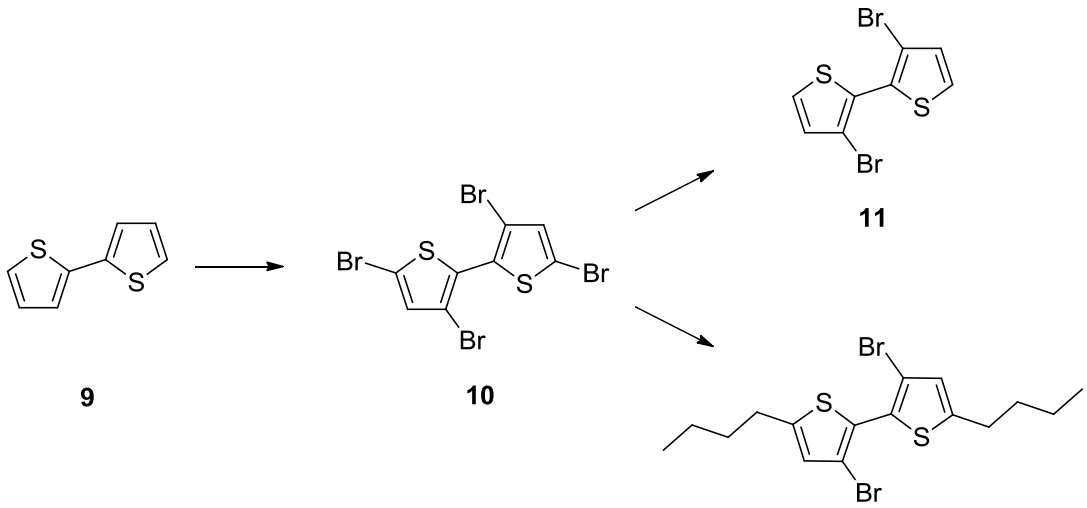


**9** **10** **11** **12**

### A.2.2 Test reaction - Synthesis of a basic dithienophosphole oxide

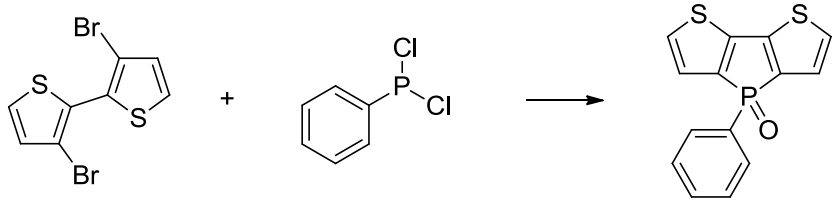


**11** **13** **14**

## A.3 Synthesis of dithienophosphole oxides

### A.3.1 2,2'-Bithiophene-based dithienophosphole oxides

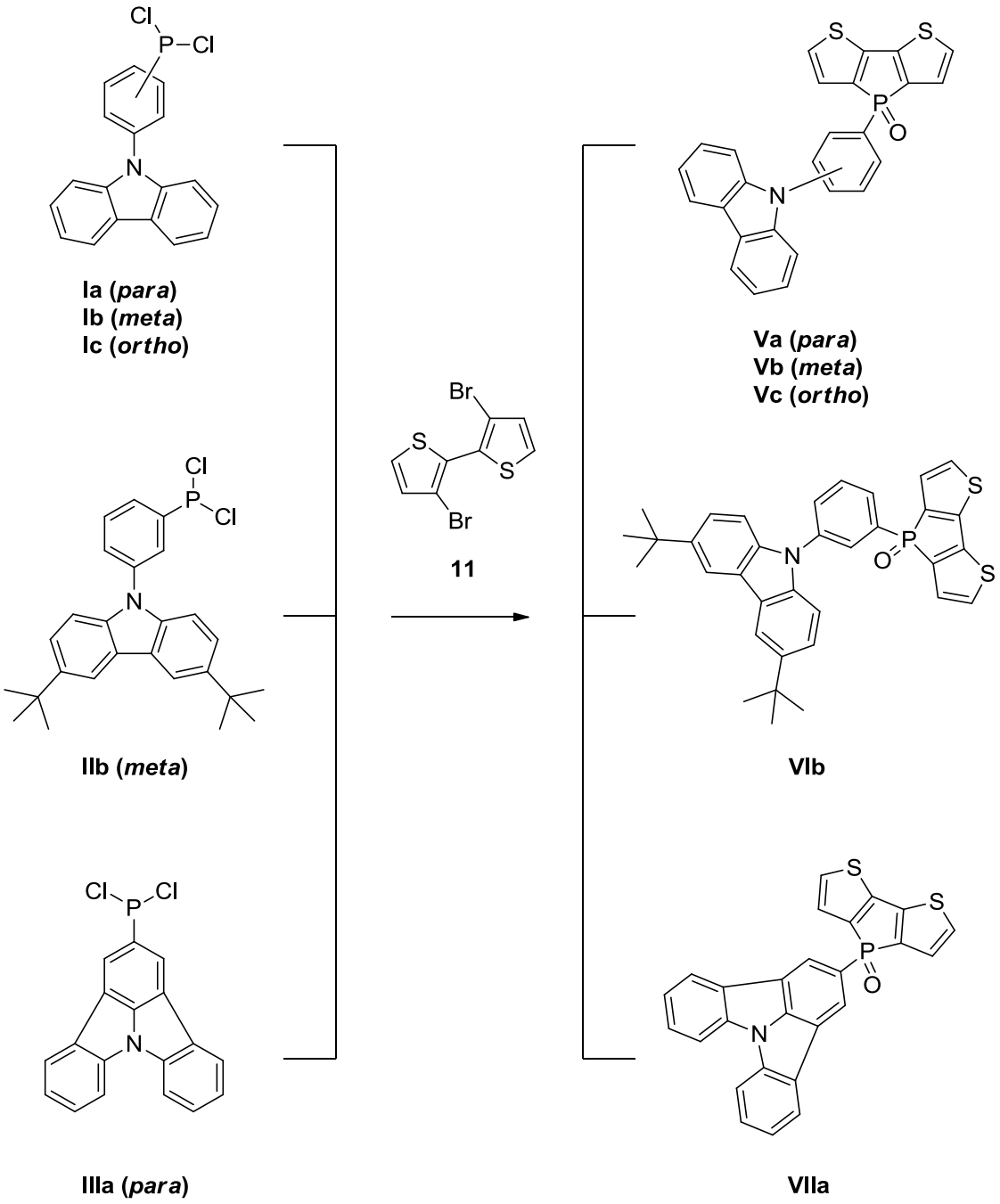

## A.3.2 5,5'-Dibutyl-2,2'-bithiophene-based dithienophosphole oxides

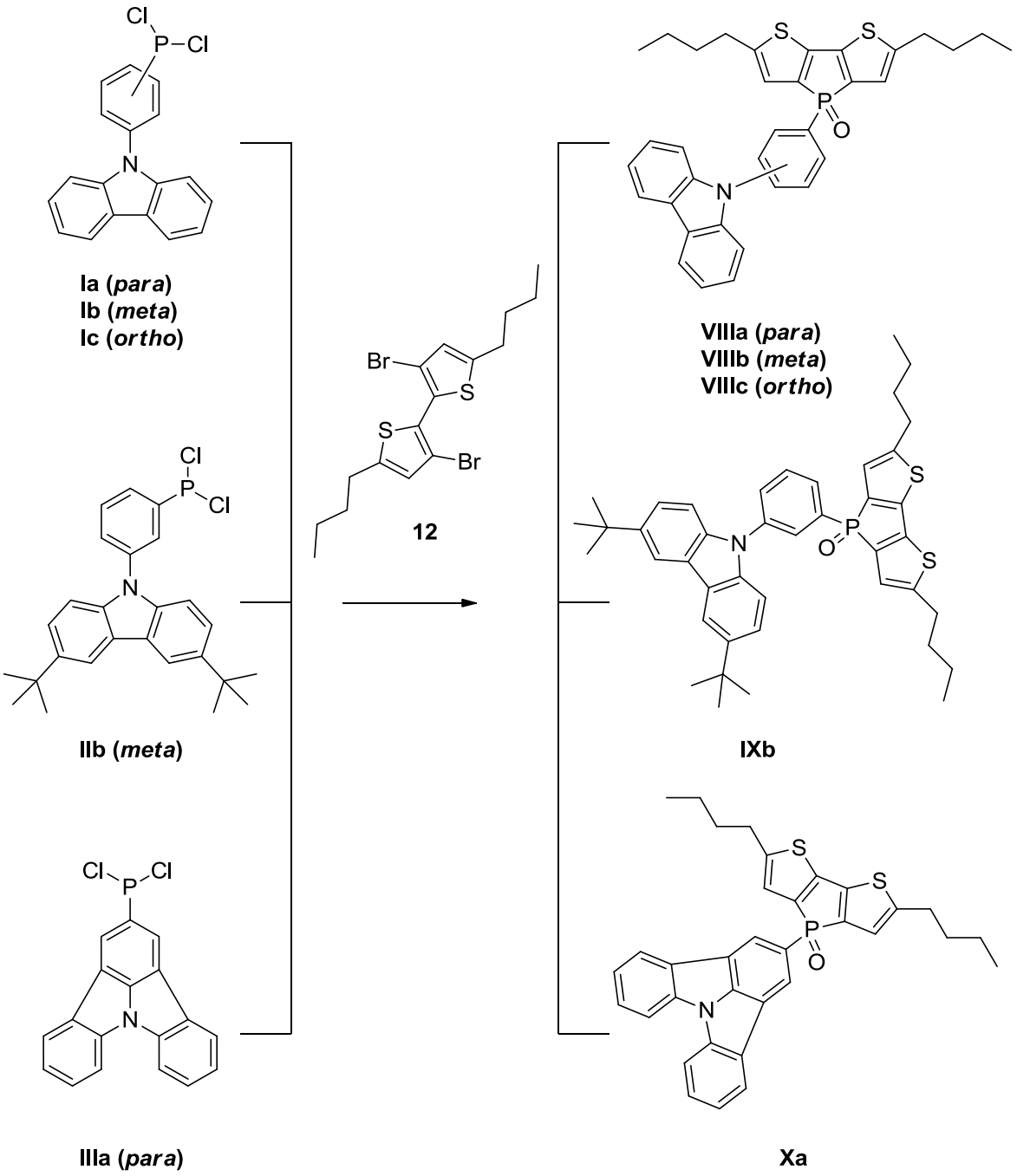

# B. General part

## B.1 Organic Electronics – Introduction

Organic Electronics is the field of electronics and materials science, which deals with carbon-based semiconductive small molecules and polymers. The synthesis and tuning of the functional organic materials, as well as the fabrication of the electronic devices and their optimization are parts of this large research field.

Organic $\pi$-conjugated materials are increasingly gaining attention from both academia and industry due to their exceptionally widespread applicability in organic electronics, which includes Organic Light-Emitting Diodes (OLEDs), Organic Field-Effect Transistors (OFETs), and Organic Photovoltaics (OPVs), but also as highly sensitive chromophores in the area of molecular sensing. [2]

A major advantage of organic materials is the fact that their properties are highly tunable by chemical modification using an elaborate building block approach. Also the incorporation of heteroelements like main group elements such as B, Si, and P can have an interesting effect on the $\pi$-conjugated materials' properties as recent research has shown. [3]

A variety of devices based on organic electronics have already entered the market, most notable may be the display applications. This technology will lead to an entirely new generation of lightweight, compact and even flexible and (partly) transparent electronic devices in the offing. The advantages of these functional organic materials with regard to synthesis and low-cost processability by spin coating and printing technologies may allow for new applications performing functions that are traditionally provided by conventional and more expensive semiconductor materials, such as silicon. [4]


Figure B- 1: OLED-based TV-display [5]

## B.2 OLEDs

### B.2.1 Set-up and function

Organic light-emitting diodes (OLEDs) have attracted broad attention over the last two decades because of their potential applications in full-color flat panel displays and solid state lighting. [1b, 6]

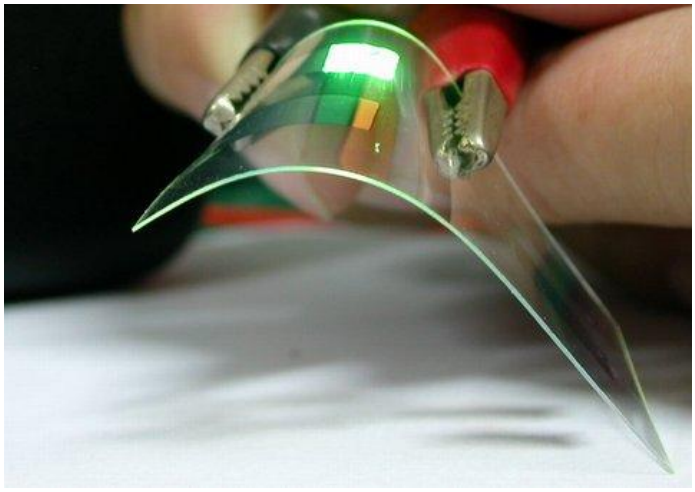

Figure B- 2: OLED test device [7]

OLEDs are electronic devices, in which an emissive layer consisting of an organic functional material emits light in response to an applied voltage. Two electrodes inject charge carriers into the organic material due to the applied voltage: The cathode injects electrons and the anode injects holes (positive charge carriers). The recombination of these opposite charges ideally in the central layer of the device forms so called excitons, formally uncharged electron-hole pairs, which can be converted to light.

The simplest set-up of an OLED device is the Single Layer Device, in which one single emissive layer based on an organic functional material is arranged between the two electrodes (Scheme B- 1).

While a metal cathode induces negative charges (electrons) to the LUMO of the organic material as soon as voltage is applied, the anode induces positive charges (holes) to the HOMO. In order to allow for effective electron injection, metals with low work function are used as cathodes. Alkaline-earth metals (Ca, Mg) as well as metals co-deposited or coated with alkali elements (Li, Cs), meet this requirement. However, they are chemically highly reactive and easily oxidize in the presence of oxygen and moisture. This obviously leads to

limitations with regard to the fabrication, which must be carried out in an inert atmosphere. (At ambient conditions sufficiently stable aluminum cathodes are commonly used in test devices.) Also, an encapsulation of the devices with barrier-coatings after fabrication is necessary, which increases both the cost and complexity of the device architectures. [8] The anode often consists of ITO (indium tin oxide), a transparent, non-stochiometric composite of $SnO_2$ and $In_2O_3$. Seeing that the generated light needs to somehow exit the device, the transparency of at least one electrode is a crucial requirement for any application. [9]

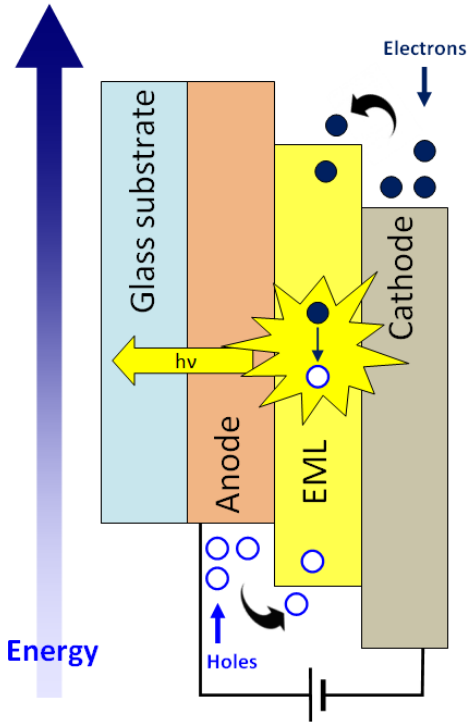


Scheme B- 1: Set-up and working principle of a Single Layer OLED device
EML... emissive layer

Due to the applied voltage, the induced, opposite charges converge and recombine forming excitons. These excitons lead to emission of light by the relaxation of the electrons from the LUMO to the lower lying HOMO, the position of the induced holes. Consequently, the emitted energy corresponds to the specific HOMO-LUMO energy band gap of the organic material. Electrochemical properties like HOMO and LUMO energy levels determine the applicability of organic materials in the field of organic electronics.

Alternatively to the light emission, the electron can relax non-radiatively converting the energy to heat, which is an undesired process. [10]

Since intrinsic technical limits with regard to adequate supply of both charge carriers keep the efficiency of such a single layer device low, most highly efficient OLEDs have multilayer device configurations (Scheme B- 2), in order to reach an improved injection and more balanced transport of charge carriers. Furthermore, a high conversion efficiency of excitons to light can be achieved, which is crucial for a successful OLED device. [1b, 11]

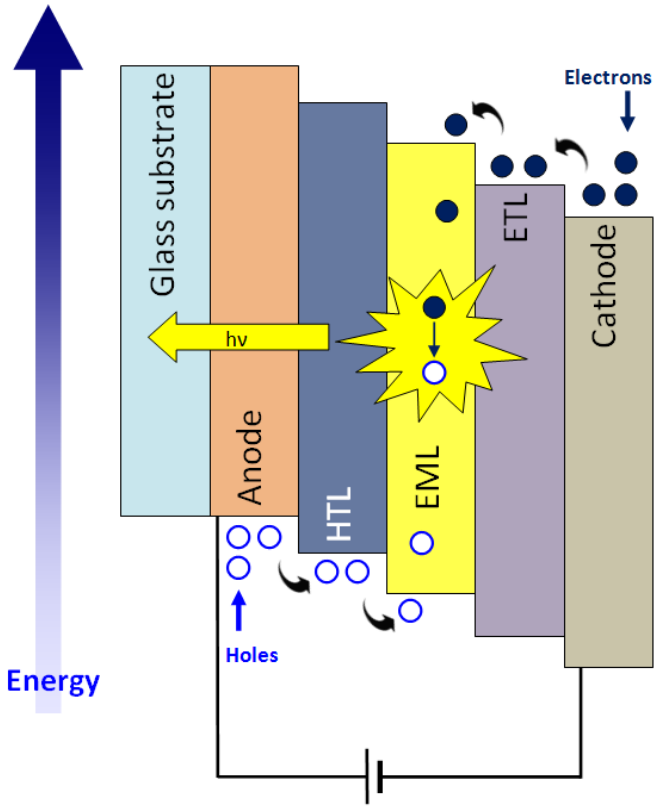


Scheme B- 2: Set-up and working principle of a Multi Layer OLED device
HTL... hole transport layer; EML... emissive layer; ETL... electron transport layer

Additional layers between electrodes and the central emissive layer shall not only improve the injection, but also the transport of charges. The better LUMO levels along the electron-transfer pathway and HOMO levels along the hole-transfer pathway are matched between adjacent materials, the better the charge supply to the emissive layer will be provided.

Therefore, the emissive layer (EML) is usually sandwiched between a hole-transport layer (HTL) and an electron-transport layer (ETL). Some devices also have additional hole-injection and electron-injection layers as well as hole- or electron-blocking layers. Charge-injection layers shall improve the charge injection from the (inorganic) electrodes to adjacent organic charge-transport layers. [1b]

Trapping charge carriers in the emissive layer can improve the efficiency of a device by enhancing the probability of charge carrier recombination. Therefore, so called blocking layers are used to prevent at least one of the charge carriers from leaving the emissive layer again. [10]

## B.2.2 Fluorescent and phosphorescent OLEDs

By electrical excitation of an organic functional material both singlet and triplet excitons are formed with an approximate ratio of 1:3. [12] Purely fluorescent emitters are able to convert singlet excitons to light, but not triplet excitons. In this case the relaxation from triplet states is quantum-mechanically forbidden and thus very unlikely. Therefore, purely fluorescent OLED devices cannot reach an internal quantum efficiency higher than 25%.

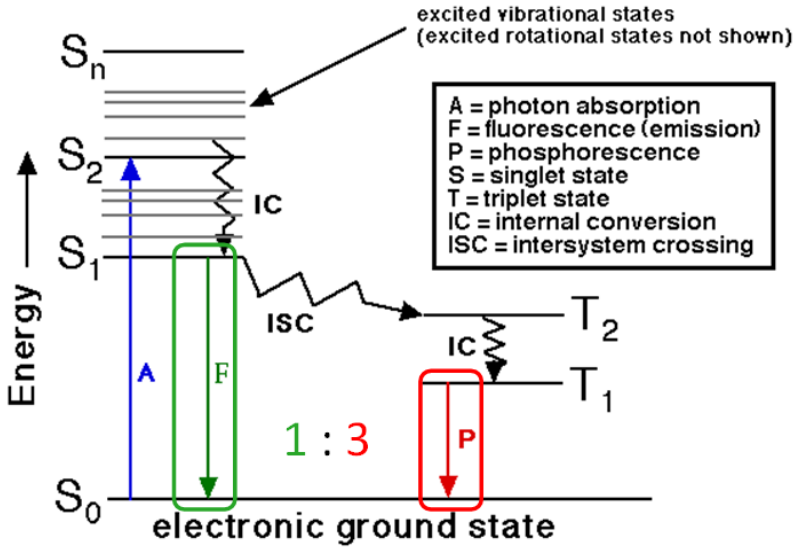


Scheme B- 3: Term diagram showing absorption (A), fluorescence (F), internal conversion (IC), intersystem crossing (ISC) and phosphorescence (P) processes. Adapted from [13]

The concept of phosphorescent OLEDs, so called PhOLEDs, allows for harvesting both singlet and triplet excitons simultaneously. With this major breakthrough, a theoretical internal quantum efficiency of 100% was realized. [1b, 6, 14]

PhOLEDs take advantage of heavy transition metal complexes as phosphorescent emitters. Especially chelate-complexes incorporating Ru(II), Os(II), Pt(II) and Ir(III) (Scheme B- 4) show interesting photophysical properties. By modification of the ligand-systems the metal-chelate bonding interaction can be tuned, which is directly related to the emitted wavelength. [15]

Because of spin-orbit coupling phenomena in these heavy atom phosphors, the non-spin-conserving and therefore usually forbidden triplet relaxation is possible and leads to phosphorescence.[15a] In contrast to spin-conserving singlet transitions responsible for fluorescence, phosphorescence is a rather slow process.[1b, 15a] This fact can be disadvantageous since the long lifetime (scale of microseconds) of these excited triplet states can lead to dominant triplet-triplet ($T_1$-$T_1$) annihilation at high current rates, as well as non-radiative exciton quenching in adjacent layers because of exciton diffusion with a range of even more than 100 nm. [1b, 16]

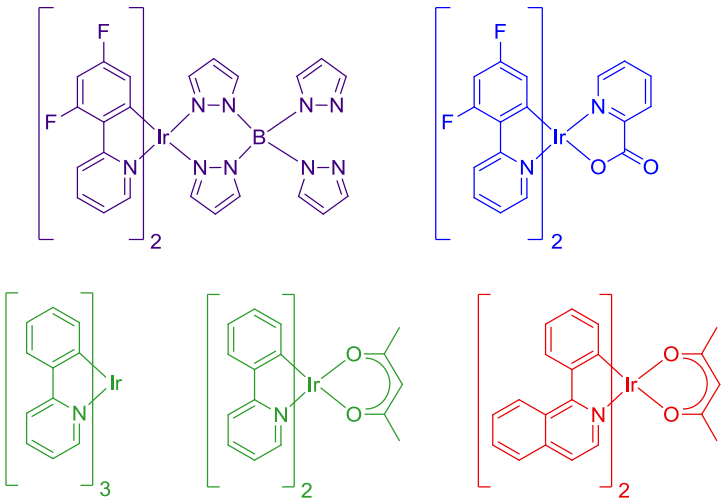

Scheme B- 4: Molecular structures of widely investigated (blue, green and red) Ir(III) triplet emitters [1b]

In order to prevent these undesired processes, which would lower the external quantum efficiency significantly, phosphorescent emitters are widely dispersed into organic host matrices. [1b] Separating the excited triplet states from each other by embedding them in a host material prevents quenching processes.

Even though fluorescent OLEDs are limited to an internal quantum efficiency of 25% due to the statistical distribution of excited states, devices based on fluorescent materials are still of great interest and subject of ongoing research. Promising advantages compared to PhOLEDs partly compensate this intrinsic drawback.

Some fairly stable fluorescent emitters may not require host matrices. In that case, the whole challenge of the synthesis of a matching host-guest system and the related more complex device fabrication is not necessary. But, depending on the design and the properties of the

emitters, such as bipolarity, conductivity, aggregation-induced emission shift, etc., the embedding into a host material may be advantageous or even necessary also for fluorescent emitters. [17]

Generally, a lower driving voltage is needed for fluorescent OLEDs (to emit light of the same wavelength) compared to PhOLEDs, which implies a lower energy consumption of the devices. Particularly in blue PhOLED devices, a higher degradation rate of the incorporated materials may be the result of the required, higher driving voltage. This is necessary to overcome the higher triplet energy levels of the host materials applied in PhOLEDs. The reasons, why host materials generally require higher triplet energy levels and therefore the devices operate at higher driving voltages, is discussed in Chapter B.2.4. [17]

Due to many advantages and promising characteristics of OLED devices, there is a strong demand to improve their durability and performance. Currently, the most successful devices exhibit red, but also green phosphors. However, blue emitting devices are still not as efficient and stable – one reason is the lack of accurately fitting host materials in PhOLEDs. [18]

By combining red, green and blue emitters, it is possible to realize OLED devices which emit white light. This technology is a highly interesting alternative to commonly used light sources (e.g. light bulbs) as well as display (backlight) applications. [19] Especially for this application blue phosphors need to be as effective as the corresponding red and green ones.

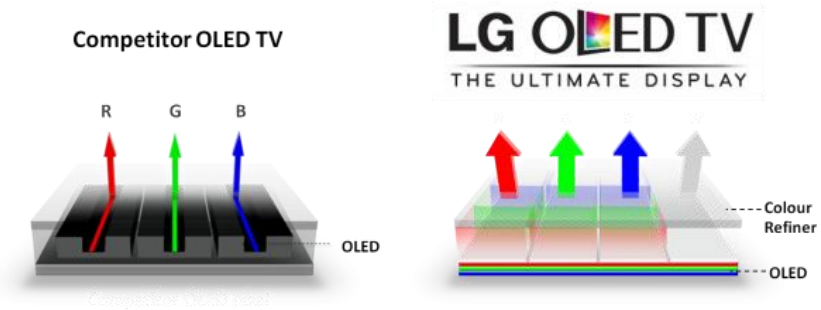


Figure B- 3: Example for a multicolor OLED device [5]

## B.2.3 Emission processes in PhOLEDs

Generally, in PhOLEDs phosphorescent materials show phosphorescence because of the radiative decay of triplet excitons. The host material used to disperse the phosphor is not

intended to convert the excited states to fluorescence, but needs to transfer the energy to the embedded dopant.

Due to the relatively lower abundance of dopant in the host/guest system, charge carriers recombine mainly in the host material (as singlet (25%) and triplet (75%) excitons) and excitons are then transferred to the dopant.

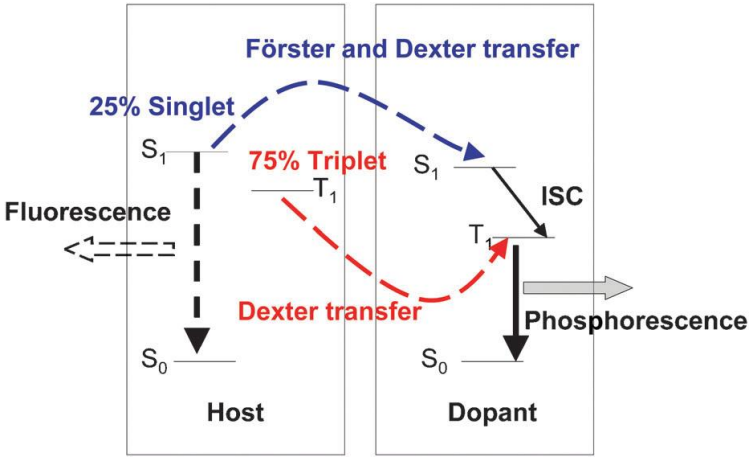


Scheme B- 5: Energy-transfer and light-emission processes in host-dopant systems [1b]

The following three routes lead to the excitation of the dopant, and thus to phosphorescence (Scheme B- 5). [1b, 2d, 15a]

(i) Singlet excitons formed on the host can be transferred to the phosphor *via* Förster and Dexter energy transfer, where they are converted to triplet excitons by efficient intersystem crossing.

(ii) Triplet excitons formed on the host can be transferred to the phosphor through Dexter energy transfer.

(iii) Excitons can be formed directly on the dopant. [20]

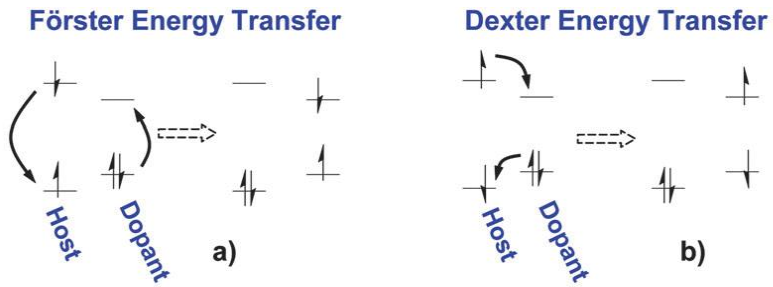


Scheme B- 6: Schematic representation of Förster (a) and Dexter Energy Transfer (b) [1b]

"*Förster energy transfer is a Coulombic interaction between the host exciton and the dopant, which is a fast (~$10^{-12}$ s) and long-range process (up to 10 nm) while Dexter energy transfer is an electron-exchange interaction between the host exciton and the dopant, which is a short distance process (1.5–2.0 nm). For the Förster transfer, the emission spectrum of the host matrix needs to overlap significantly with the absorption spectrum of the dopant, whereas efficient Dexter transfer requires the match of energies of the singlet and triplet excitons on the host with the exciton energies on the guest.*" [1b] (Scheme B- 6)

## B.2.4 Host materials in PhOLEDs

A general requirement for host materials is a higher triplet energy compared to the dopant emitters (Scheme B- 7 c) in order to prevent reverse energy transfer from the dopant back to the host.

Quite challenging is the synthesis of host materials for blue emitters (requiring relatively high triplet energy values of ≥ 2.65 eV) since a large π-conjugation, which is necessary for good charge transport properties as well as thermal and morphological stability, generally leads to lower triplet energies. [1b] [21]

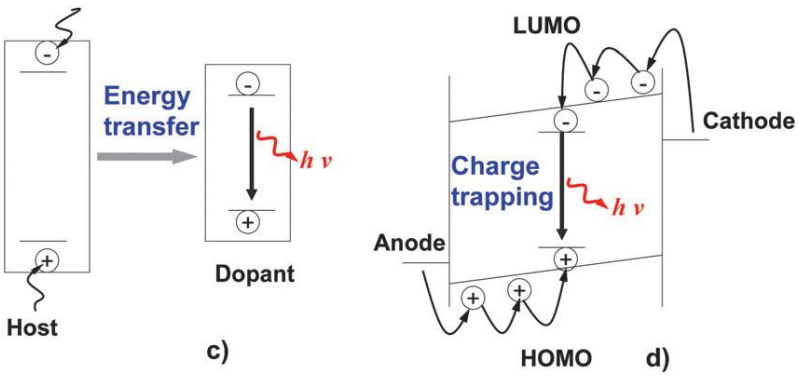


Scheme B- 7: Schematic representation of host-dopant energy transfer (c) and charge trapping (d) [1b]

In order to increase the probability of the formation of excitons in the first place, charge carriers are trapped in the emissive layer by the insertion of blocking layers as described in Chapter B.2.1 (Scheme B- 7 d).

An effective transfer of electrons and holes to the emissive layer requires well-matched HOMO (for the transfer of holes) and LUMO (for the transport of electrons) levels of the

adjacent layers. By realizing rather "small steps" between the molecular orbitals of the materials charge carrier injection barriers are lowered and, as a consequence, the driving voltages of the device. [10]

Another important requirement for host materials is good and balanced charge-carrier transport properties.

Host materials, which preferentially transport just one of the charge carriers, electrons *or* holes, due to their electronic structure, generally reach lower efficiencies of light emission. Due to the poor or inefficient transport of one type of charge carriers, the latter cannot disperse properly in the material of the emissive layer. As a consequence, rather narrow zones of recombination and light emission are established, which causes the lowered efficiency. These zones are located close to the interface of the EML and one of the transport layers (Scheme B- 8). [1b, 22]

This is one reason why bipolar host materials transporting both electrons and holes are desirable and came more and more into focus of latest research.

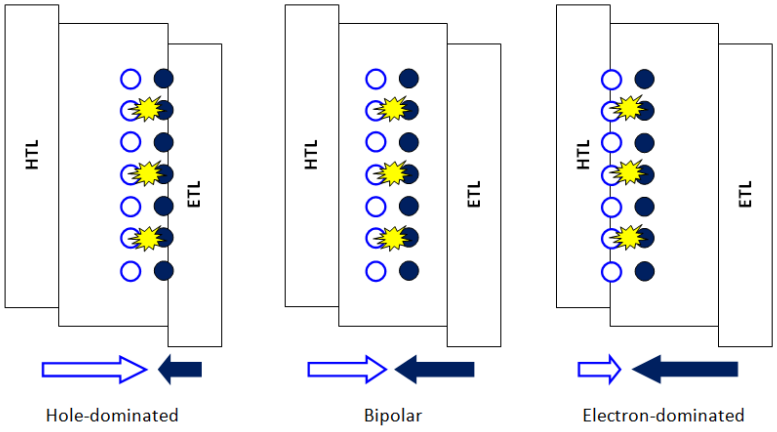


**Scheme B- 8: Schematic representation of the organic layers of OLEDs in which a host material possesses different degrees of charge balance: hole-dominated, (am-) bipolar, electron-dominated [22]**

Alternative strategies to broaden and improve the emission zone are

- the use of double emissive layers arranging a hole- and an electron-transporting host material next to each other or
- mixed host system layers.

Both concepts could improve the emission efficiency, but lead at the same time to a more complicated fabrication of the devices. [1b, 23]

Good thermal and morphological stabilities are crucial features for host materials, as well as any other organic functional material in an electronic device. Phase separation upon heating or any kind of chemical degradation (e.g. oxidation etc.) will shorten the operational device lifetime.

Generally, materials with a rather high glass transition temperature, which are able to form morphologically stable and uniform films because of their bulky and sterically hindered molecular configuration, are preferable.

### B.2.5 Bipolar organic functional materials

Ambipolar or bipolar hosts or generally bipolar functional organic materials are promising compounds for applications in OLED devices due to their good and balanced electron- and hole-transport features and the resulting simplification of the device structures.

A particularly intriguing strategy toward this kind of compounds involves the combination of donor- and acceptor-building blocks within the same π-conjugated scaffold. [1a, 2]

While typical donors providing hole transport are electron-donating moieties such as arylamines (e.g. triphenylamine, carbazole,...), typical acceptors providing electron transport are electron-withdrawing moieties like oxadiazole, triazole, pyridine, phosphine oxide ect. (Scheme B- 9).

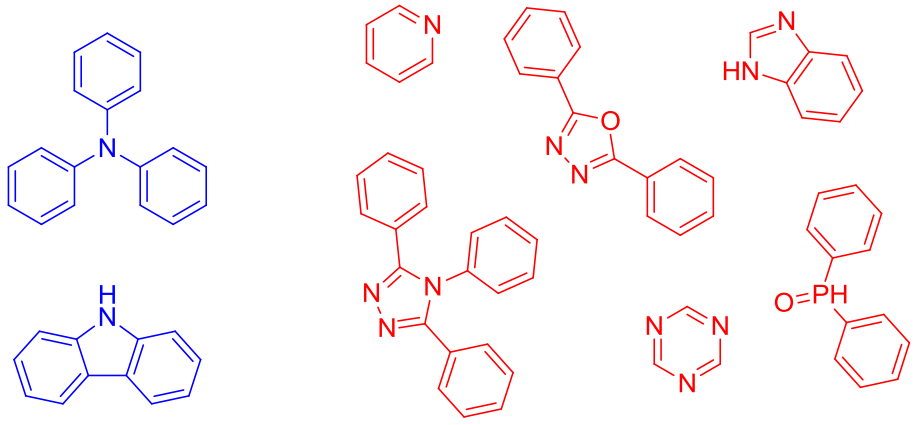


Scheme B- 9: Donor- (blue) and acceptor- (red) building block examples

The fact that positive and negative charges are transported by the very same π-conjugated molecule implies the risk of intramolecular charge transfer phenomena which lower unavoidably the singlet and triplet energy levels of the material. This restricts the applicability of the material to OLEDs with emitters of higher wavelengths.

To avoid these undesired effects, it is necessary to minimize the donor-acceptor interaction by interruption of the π-conjugation. Several strategies were found dealing with specific linkage modes between donor- and acceptor-systems in order to achieve this aim. They can be summarized to two main concepts:

- The introduction of a spacer between donor and acceptor unit, such as fluorene [24], a sterically demanding methyl group [25] or a $sp^3$-hybridized atom [26] [27] (flexible non-conjugated σ-bond linkage [28])
- *Meta*-/*ortho*-linkage instead of *para*-linkage [29] (linkage with torsion)

## B.3 Goal of this thesis

All the requirements for functional organic materials for OLED devices on the one hand and the possible applications in organic electronics on the other hand, make this field of research a pretty challenging but also very promising one.

The goal of this thesis is the synthesis of novel bipolar organic functional materials and the study of their photophysical and electrochemical properties. Positive results with regard to synthesis and characterizations may lead to the incorporation of the materials in fluorescent or phosphorescent OLED test devices. Following the approach of combining donor- and acceptor-systems, building blocks with suitable properties regarding triplet energy values and charge transfer were chosen (Scheme B- 12).

Electron rich arylamines are known to be good donor systems. 4,4'-Bis[N-(p-tolyl)-N-phenylamino]biphenyl (TPD) for instance is a commonly used hole transport material in OLED technology [1b] (HOMO -5.4 eV, LUMO -2.4 eV, triplet energy 2.34 eV, [30]). Due to its chemical structure and the resulting, relatively low glass transition temperature ($T_g$) of 65 °C, it tends to crystallize and lacks thermal and morphological stability. [10]

N,N'-Di(1-naphthyl)-N,N'-diphenylbenzidine (NPB), one of the most widely used hole transport materials, incorporates the sterically more demanding naphthyl moiety, which leads to an improved $T_g$ (95 °C). [10] Even though it shows very similar HOMO and LUMO levels compared to TPD, the triplet energy is slightly lower at 2.29 eV. [30]

An example for a hole transport material incorporating carbazole moieties is 4,4',4''-tris(N-carbazolyl)triphenylamine (TCTA, $E_T$: 2.76 eV, HOMO/LUMO: -5.7/-2.4 eV) [31]. Its high triplet energy allows for application even in PhOLEDs and the $T_g$ value is as high as 151 °C due to its star shaped structure that impedes crystallization. [10]

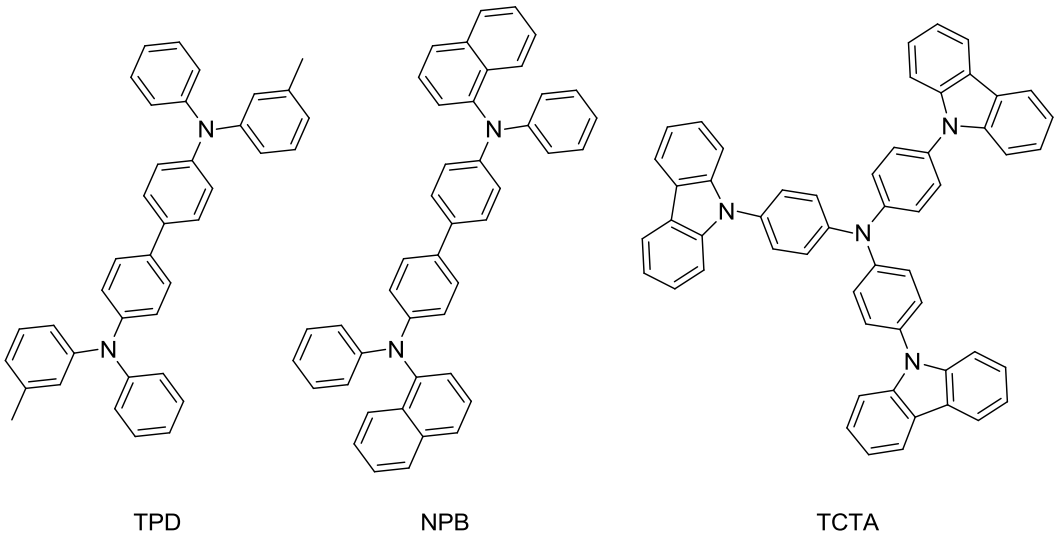


Scheme B- 10: Examples of commonly used hole transport materials in OLED technology

As recently published results of Prof. Fröhlich's research group showed, the electrochemical and photophysical properties as well as the morphological stability of triarylamine-incorporating organic functional materials are related to the degree of planarization of the chemical structures. [32] According to this study, increasingly planarized triarylamine structures lead to improved morphological stability and elevated singlet and triplet energy values, due to steric effects (increased torsion of chemical bonds reduces intramolecular charge transfer effects) and the reduced donor strength of the planarized arylamine structures.

Following this concept, indolocarbazole was applied as a donor moiety for dithienophosphole oxides, in order to investigate the material's properties compared to those of the phenylcarbazole species.

The dithieno[3,2-*b*:2',3'-*d*]phosphole oxide (DTPOX) building block was developed in Prof. T. Baumgartner's group. Generally, phospholes (five-membered heterocycles incorporating one phosphorus atom, which adopts a pyramidal geometry) have drawn interest because of their peculiar electronic characteristics. [3c] The electron lone pair of the phosphorus atom within the phosphole structure has high s-character that hinders efficient interaction with the π-system. Therefore, the aromaticity of phospholes is diminished compared to other five-membered heterocycles, such as pyrrole, thiophene or furan. Nevertheless, interactions between the σ*-orbital of the exocyclic bond and the π*-system of the ring lead to a degree of aromaticity and a high polarizability of the phosphole system and thus, to a high tunability of photophysical and electrochemical properties by chemical modification. [33]

In 2004, Prof. Baumgartner's group published the synthesis of the dithieno[3,2-*b*:2',3'-*d*]phosphole. This fused system shows extraordinary chemical versatility and outstanding photophysical properties, which have led to series of contributions in the fields of light-emitting materials [1a, 34], polymers [35], coordination compounds [36], and supra-molecular chemistry [37], among others.

In the work of C. J. Chua [34d], also conducted in Prof. T. Baumgartner's research group, dithienophospholes were functionalized at the phosphorus center with triphenylamine (TPA) moieties.

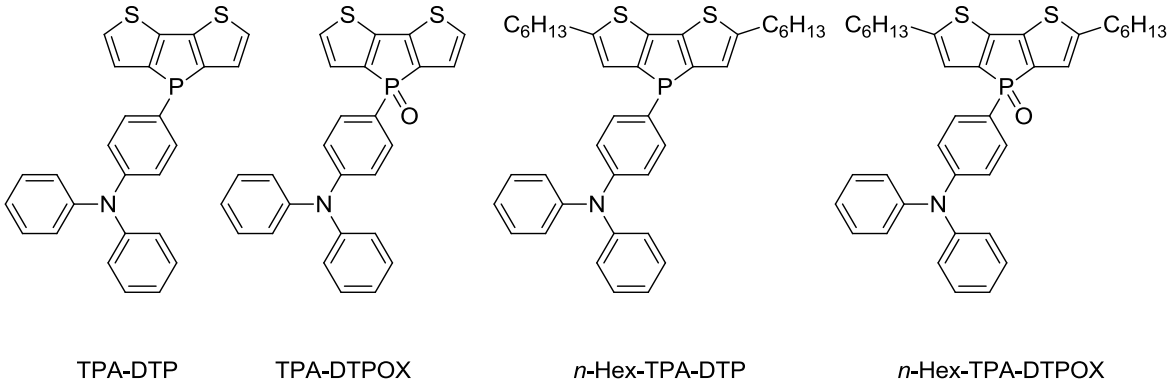


**Scheme B- 11: Unsubstituted (left) and *n*-hexyl-substituted (right) triphenylamine-functionalized dithienophospholes (DTP) and dithienophosphole oxides (DTPOX) synthesized by C. J. Chua in Prof. T. Baumgartner's group [34d]**

As a part of that work, charge transfer effects were investigated manipulating photophysical and electrochemical properties *via* oxidation of the phosphorus center and alkylation of the

dithienophosphole system. The oxidation from trivalent to a pentavalent species proved to increase the acceptor-properties of the dithienophosphole building block and thus the charge transfer character of the compounds. More surprisingly however, charge transfer effects could be suppressed by installation of alkyl substituents at the 2,6-position of the dithienophosphole scaffold.

Following the concept of combining acceptor- and donor-building blocks with suitable properties (Scheme B- 12), within this work, a series of new π-conjugated donor–acceptor (D/A) materials should be synthesized.

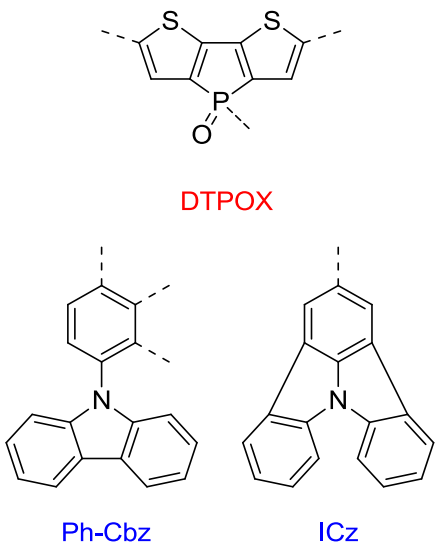


**Scheme B- 12: Acceptor and donor building blocks**
**DTPOX: dithieno[3,2-*b*:2',3'-*d*]phosphole oxide (acceptor)**
**PhCbz: phenylcarbazole, ICbz: indolo[3,2,1-*jk*]carbazole (donors)**

Furthermore, the influence of the linkage mode (*para*, *meta*, *ortho*) between the building blocks and the *n*-Bu-substituents at the DTPOX-system on electrochemical and photophysical properties of the novel materials should be investigated.

Particularly, *meta*- and *ortho*- linkage modes between the building blocks as well as the incorporation of the planarized triarylamine system ICz were supposed to suppress intramolecular charge transfer effects due to interruption of the conjugated π-system and lead to higher triplet energy values.

# C. Specific part

## C.1 General

In the course of this master thesis, the applied reactions will be presented in the specific part, while subsequently, photophysical and electrochemical properties of the final products will be discussed in the spectroscopic part (Chapter D). Detailed information on reaction procedures as well as the characterization of all synthesized compounds are presented in the experimental part (Chapter E).

## C.2 General synthetic strategy

In order to synthetically access triarylamine-functionalized dithienophosphole oxides, corresponding precursors for both building blocks of these π-conjugated systems were synthesized.

In detail, functionalized dithienophosphole oxides are accessible, according to the retro synthetic analysis (Scheme C- 1), *via* the ring closing reaction of 3,3'-dibromo-2,2'-bithiophene species and dichlorophosphine species functionalized with the desired triarylamine moiety. As soon as the two building blocks are connected forming the phosphole flanked by two thiophene rings, the dithienophosphole system, the trivalent phosphorus center can be oxidized forming the desired dithienophosphole oxide species.

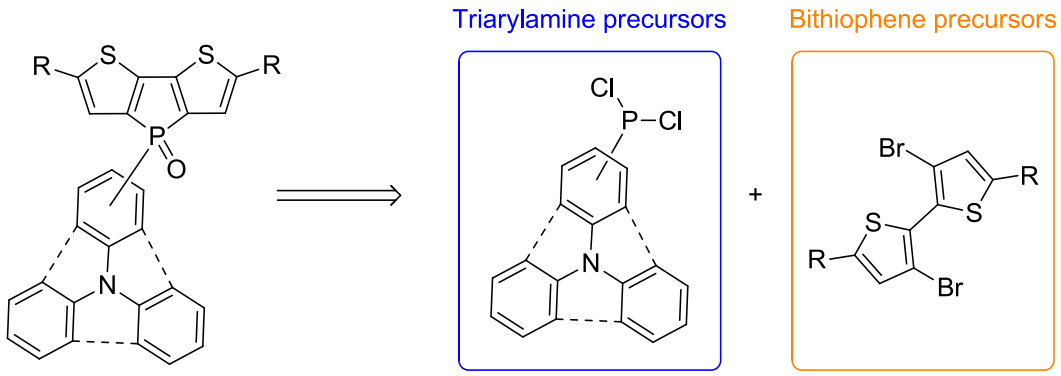


Scheme C- 1: Retro synthetic analysis of phenylcarbazole functionalized dithienophosphole oxides

The triarylamine systems used within this work were mostly phenylcarbazoles. In order to compare the effects of an even more rigid scaffold to these kind of donor moieties regarding photophysical properties, indolo[3,2,1-*jk*]-carbazole was introduced as an alternative donor moiety.

# C.3 Synthesis of the donor precursor systems

## C.3.1 Synthesis of the carbazole-based triarylamine systems

Brominated phenylcarbazole precursors were synthesized by Ullmann condensation starting from 9*H*-carbazole (**1**) and the corresponding dibromobenzene (Scheme C- 2). Depending on the substitution pattern of the dibromobenzene, the linkage mode between triarylamine and dithienophosphole oxide system will be *para* (**a**), *meta* (**b**) or *ortho* (**c**).

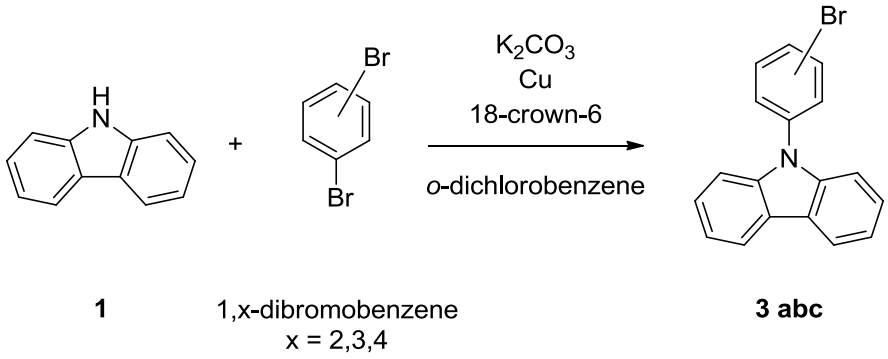


Scheme C- 2: Synthesis of 9-(x-bromophenyl)-9*H*-carbazole, x= 4 (*para*), 3 (*meta*), 2 (*ortho*)

For this reaction, 9*H*-carbazole (**1**), the corresponding dibromobenzene, $K_2CO_3$, copper powder and 18-crown-6 as a ligand were added to the high-boiling solvent *o*-dichlorobenzene ($T_B$ = 180.5 °C) and refluxed under inert conditions for about 24 hours (procedure on basis of [38]).

In order to compare solubility, as well as electrochemical and photophysical properties of the final products, phenylcarbazole precursors with *t*-Bu-substituents at the positions 3 and 6 of the Cbz scaffold (**4 a,b**) were synthesized as well (Scheme C- 3).

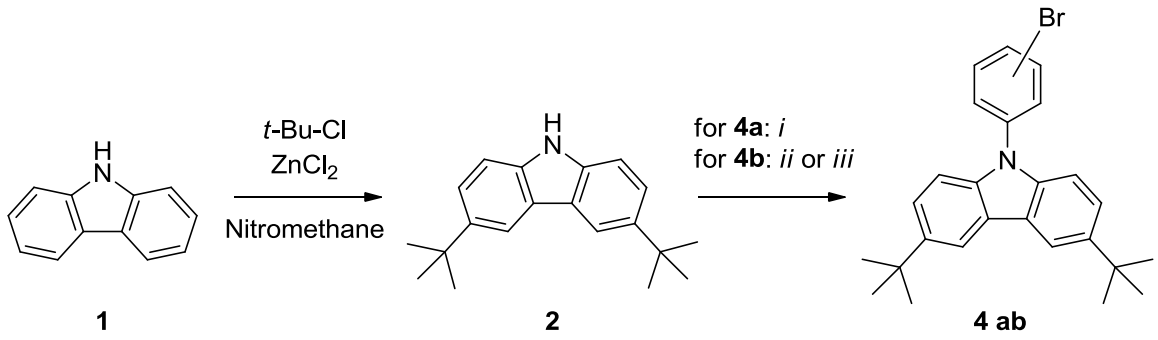


Scheme C- 3: Synthesis of 9-(x-bromophenyl)-3,6-di-*tert*-butyl-9*H*-carbazole, x= 4 (*para*), 3 (*meta*);
*i*: 1,4-dibromobenzene, $K_2CO_3$, copper powder and 18-crown-6 in o-dichlorobenzene
*ii*: 1,3-dibromobenzene, $K_2CO_3$, copper powder and 18-crown-6 in o-dichlorobenzene
*iii*: 1-bromo-3-iodobenzene, $K_2CO_3$, copper powder and 18-crown-6 in DMF

The modification of **1** was realized by Friedel-Crafts alkylation using 2-chloro-2-methylpropane and $ZnCl_2$ as a Lewis acid catalyst (procedure according to [38]). The quite polar solvent nitromethane allowed for dissolving both the organic starting materials and sufficient amounts of inorganic catalyst. The amount of catalyst used for the reaction was reduced from 3 eq. (according to [38]) to 1 eq. after some trial reactions, since it was noticed visually that a significant fraction was not dissolving, anyways.

Due to the positive mesomeric effect of the nitrogen atom, *ortho*- and *para*- positions relative to it are favored for the alkylation. Furthermore, the *t*-Bu-group is sterically demanding, so that the reaction at positions 3 and 6 of (**1**) is most likely.

The Ullmann condensation of the *para*-substituted compound **4a** gave the product as a white solid with a yield of 58%. (**2**), 1,4-dibromobenzene, $K_2CO_3$, copper powder and 18-crown-6 were refluxed in o-dichlorobenzene (Scheme C- 3, *i*) in analogous fashion to the compounds without *t*-Bu-groups at the Cbz.

However, the *meta*-substituted compound **4b** was formed just once under these conditions with the corresponding 1,3-dibromobenzene (Scheme C- 3, *ii*) (with a yield of 40%). The reaction was repeated several times with exact the same and different conditions (more and less $K_2CO_3$, in DMF, in toluene), but it did not lead to the same product again. Instead, NMR and MS confirmed that during every reaction but the first one the product shown in Scheme C- 4 was formed:

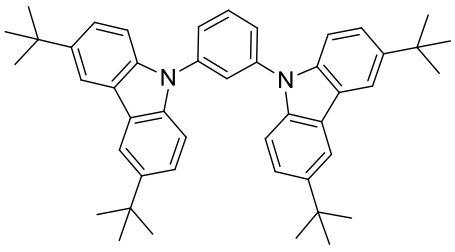


1,3-bis(3,6-di-*tert*-butyl-9*H*-carbazol-9-yl)benzene
$C_{46}H_{52}N_2$
632,92

Scheme C- 4: Undesired product

After many trials another procedure on basis of [39] was applied. In this case (Scheme C- 3, *iii*) the 1,3-dibromobenzene was replaced with 1-bromo-3-iodobenzene and DMF was used as a solvent. Since iodine is more reactive than bromine with regard to the oxidative addition within the catalytic cycle of the Ullmann condensation, the undesired competitive reaction did

not occur again. Furthermore, lower reaction temperatures ($T_B$ of DMF = 153 °C) are sufficient for these starting materials. The desired product was given as a white solid with a yield of 66%.

### C.3.2 Lithiation trial of a brominated triarylamine system

To make sure that the lithiation of brominated triarylamine systems is applicable and well working, one test compound (**4a**) was dissolved in THF, lithiated at -78 °C and quenched with trimethylsilyl chloride (tmsCl) (Scheme C- 5). This product being stable in the presence of oxygen and moisture could be characterized and quantified easily.

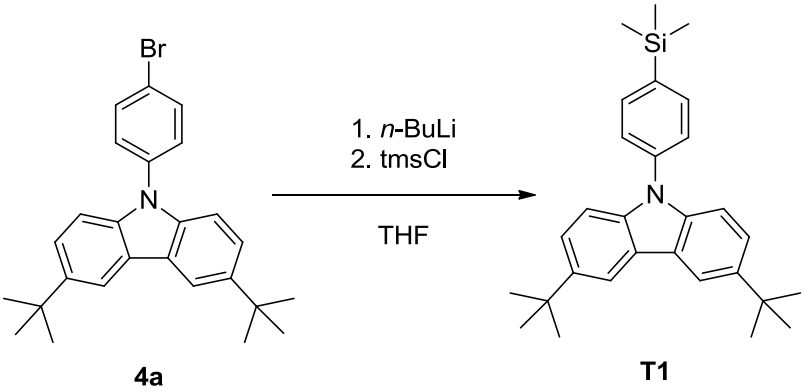


Scheme C- 5: Lithiation trial of brominated triarylsystem

It turned out that a liquid-liquid extraction of the reaction solution gave the product almost quantitatively as a white slightly yellowish product without any purification steps.

### C.3.3 Preparation of the phosphine reagent

The reagent for the introduction of the phosphorus center (**7**) was synthesized by the addition of 4 equivalents of diethyl amine (**6**) to phosphorus trichloride (**5**) in THF at low temperatures (-78 °C) (Scheme C- 6) (procedure according to [40]). The product was separated from the diethylammonium chloride by filtration and purified by distillation giving a colorless liquid in good yield (86%).

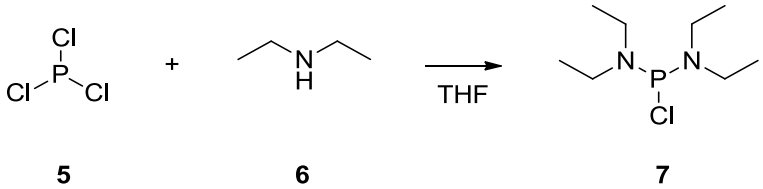


Scheme C- 6: Synthesis of bis(diethylamino)chlorophosphane (7)

## C.3.4 Synthesis of the carbazole-based dichlorophosphine precursors

In the next step (Scheme C- 7), the bromine functionality on the prepared triarylamine precursors was replaced with the trivalent dichlorophosphine species (procedure on basis of [34d]), which is necessary for the ring closing reaction forming the desired phospholes. These trivalent species are prone to oxidation, which is the reason why all following procedures need to be done under exclusion of oxygen and moisture.

First, the brominated precursors were lithiated with *n*-BuLi following the generally known metal-halogen-exchange procedure at low temperatures (-78 °C). After 1-2 hours at constantly low temperatures the lithiated species was quenched with bis(diethylamino)chlorophosphane (**7**). The reaction mixture was allowed to warm up to room temperature at this point. This step leads to the corresponding N,N,N,N-tetraethylphosphinediamine and the formation of LiCl salt. Finally, the no longer necessary protecting diethylamine groups could be removed from the phosphorus center by the use of HCl in dry diethyl ether replacing them with chlorine.

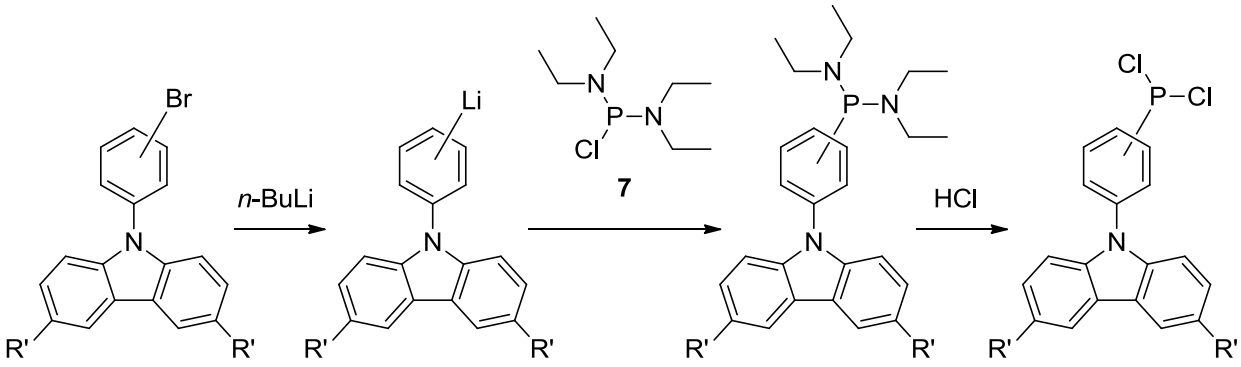


Scheme C- 7: Synthesis of ((dichlorophosphino)phenyl)-9*H*-carbazole species

The formed diethylammonium chloride as well as the LiCl from the step right beforehand were separated *via* filtration under inert conditions. Even filter paper with the smallest porosity available could not separate the superfine precipitate.

Hence, the reaction mixture was filtered through an aluminum oxide plug, a glass frit filled with dry aluminum oxide (Scheme C- 8). In order to keep the reaction mixture under inert conditions, it was transferred from the original Schlenk flask through the cannula to the glass

frit applying a difference in pressure between the vessels. A cannula is a hollow and flexible tube made of chemically resistant stainless steel or PTFE (Teflon).

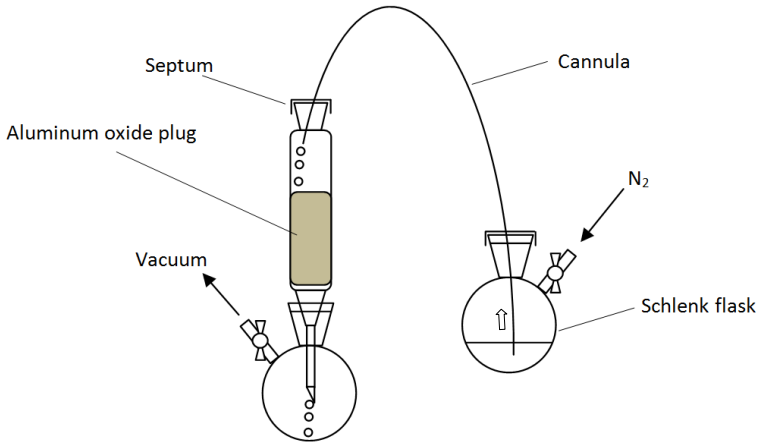


**Scheme C- 8: Filtration through an aluminum oxide plug using a cannula for transferring the reaction mixture under inert conditions**

However, lithium salts in general are quite soluble in THF, partly soluble in diethyl ether and possibly even in DCM. They are not soluble in non-polar solvents such as hexanes.

This fact showed to make the filtration of the reaction mixture quite tricky, since the used solvent was either THF or diethyl ether. The desired compound showed to be poorly soluble in hexanes which is why the solvent of the reaction mixture could not be exchanged fully.

In order to find a compromise, a mixture of hexanes and diethyl ether was believed to be the best choice, even though smaller amounts of precipitate, which appeared like salt residues, could be found in the filtrate flask after removing the solvent *in vacuo*.

One more problem was that these rather large molecules could not be distilled for purification as similar, more volatile compounds in earlier projects of Prof. Baumgartners research group. The boiling point of the chemically similar compound 4-(dichlorophosphino)-N,N-diphenylaniline was calculated using Advanced Chemistry Development (ACD/Labs) Software V11.02 (© 1994-2013 ACD/Labs) to be close to 461.3±28.0 °C at atmospheric pressure. [Scifinder]

This would mean, the boiling point of the even more rigid molecular scaffold of the synthesized compounds could not be expected lower than 250 °C, even when applying reduced pressure of an oil vacuum pump. Therefore, a distillation could not be considered as an applicable method of purification.

However, $^{1}H$ and $^{31}P$-NMR spectra showed quite good results. Hence, the synthesized precursors were used crude without any further purification for the next steps.

### C.3.5 Synthesis of the Indolocarbazole-based dichlorophosphine precursor

Like the rest of the brominated triarylamine precursors (see Chapter C.3.4) 2-bromoindolo[3,2,1-*jk*]carbazole was converted to the dichlorophosphine species following the analogue procedure (Scheme C- 9).

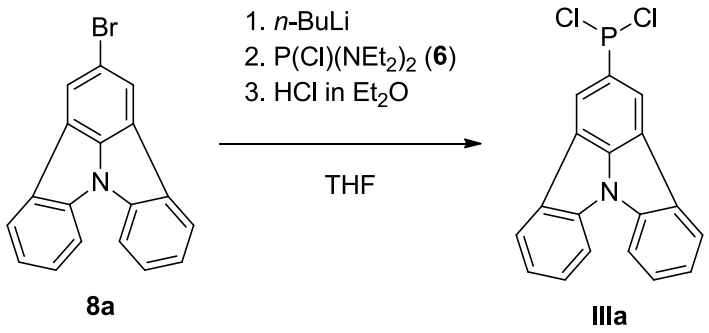


Scheme C- 9: 2-(Dichlorophosphino)indolo[3,2,1-*jk*]-carbazole (IIIa)

## C.4 Synthesis of the acceptor precursor systems

Commercially available 2,2'-bithiophene was freshly distilled and brominated with molecular bromine in chloroform and glacial acetic acid (procedure according to [41]). The halide is activated by the acid and attacks the aromatic system in an electrophilic aromatic substitution reaction. Due to a higher number of resonance structures and thus higher stability, positions 5 and 5' as well as 3 and 3' are brominated first.

By lithiation using *n*-BuLi at low temperatures and quenching of the lithiated species with water or 1-bromobutane the dibromo-species could be obtained with the corresponding R-substituents in positions 5 and 5': H for quenching with water (**11**) (procedure according to [42]) and *n*-Bu for quenching with 1-bromobutane (**12**) (procedure based on [34d]).

A direct bromination of positions 3 and 3' of the bithiophene (**9**) to synthesize **11** in one step is not possible due to the relatively higher reactivity of positions 5 and 5'.

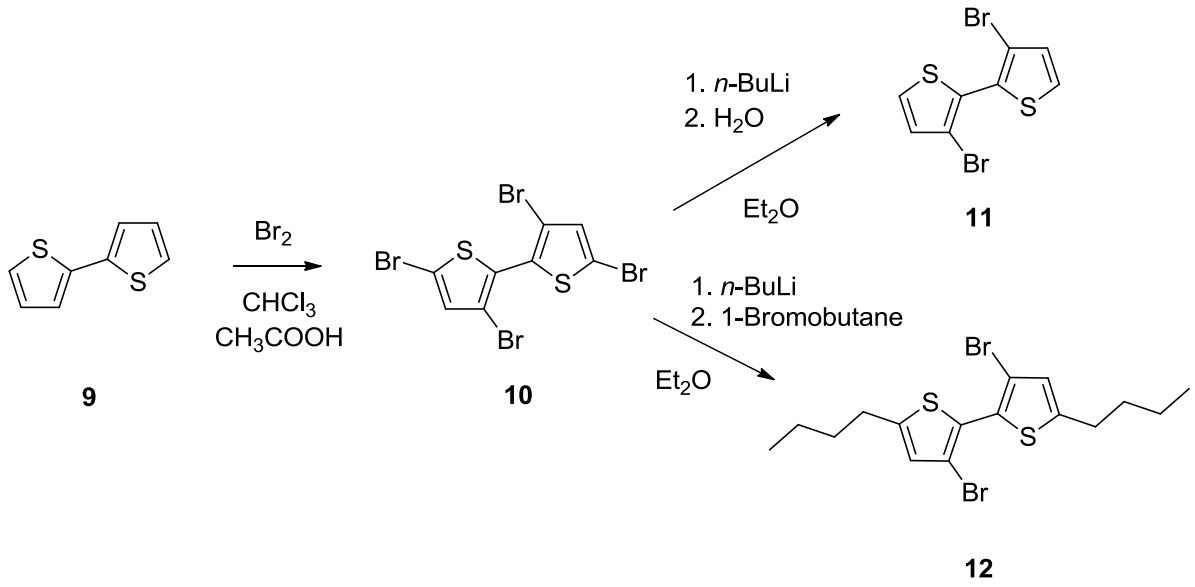


Scheme C- 10: Synthesis of the dibrominated bithiophene systems

## C.5 Synthesis of dithienophosphole oxides

As soon as the needed acceptor and donor precursors were prepared, the desired functionalized dithienophosphole oxides could be synthesized (procedure according to [34d]).

First of all, the dibromobithiophene species (**11** or **12**) were lithiated (in diethyl ether or THF) with *n*-BuLi at low temperatures (-78 °C). After 1.5 hours a solution of the crude dichlorophosphine species in THF was added *via* a syringe. The reaction mixture was then quickly warmed to room temperature replacing the dewar vessel containing dry ice in aceton with a warm water bath.

While the highly reactive lithium species reacts pretty fast with the first chlorine of the dichlorophosphine species, the second pair of reaction partners is pointing to opposite directions. This makes a ring closing reaction less likely.

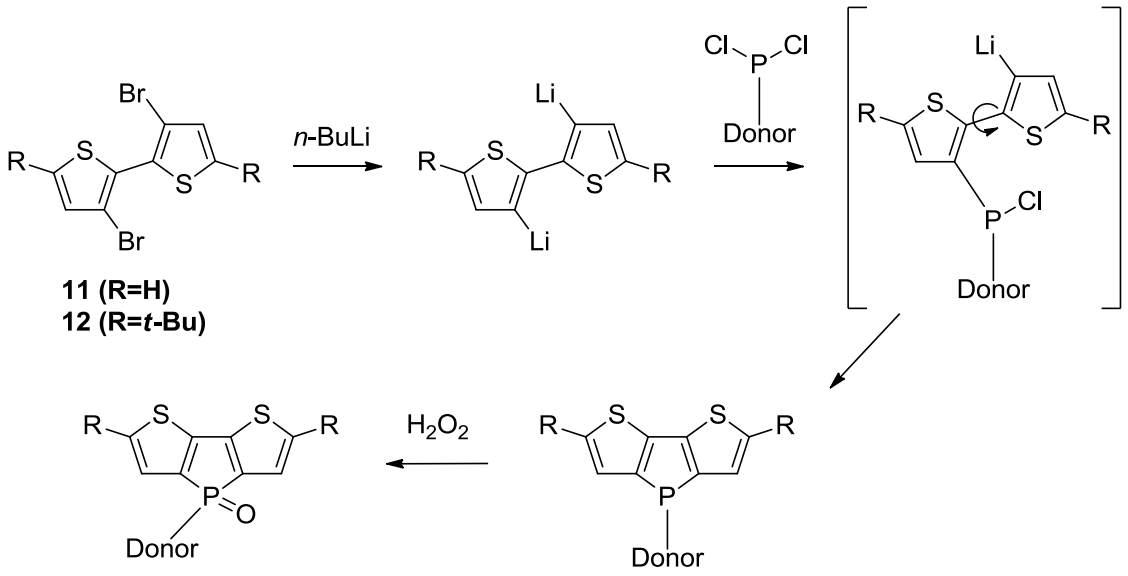


Scheme C- 11: Synthesis of functionalized dithienophosphole oxides

Keeping the overall concentration of the reaction mixture rather low, the probability of competitive intermolecular reactions should remain low compared to the desired intramolecular reactions.

As a final step, the dithienophospholes were dissolved in chloroform and stirred with excess $H_2O_2$ (30%) for 2 hours at room temperature, in order to oxidize the phosphorus atom.

# D. Spectroscopic part

# D.1 Absorption and emission spectra

## D.1.1 Experimental parameters of the absorption and emission spectra

The photophysical properties of the new DTPOXs (**Vabc, VIIIabc, VIb, VIIa, IXb, Xa**) were studied *via* UV-Vis absorption and fluorescence emission spectroscopy.

Absorption spectra were recorded on a Perkin Elmer Lambda 750 UV-Vis spectrometer. Fluorescence spectra were recorded on an Edinburgh FLS920 system. All spectra were taken at room temperature from solutions in DCM (HPLC grade) at concentrations of 5 nmol/ml using quartz glass cuvettes. For the fluorescence spectra the excitation wavelength was the corresponding absorption maxima.

## D.1.2 The recorded absorption and emission spectra

The following Scheme D- 1-5 show the obtained spectra of the dithienophosphole oxides.

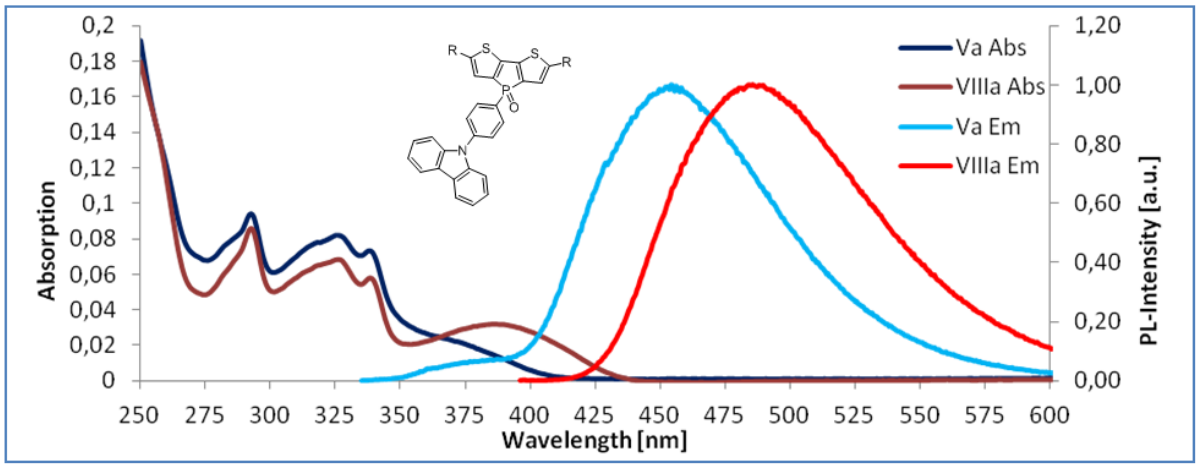


Scheme D- 1: Absorption (Abs) and emission (Em) spectra of compounds Va and VIIIa

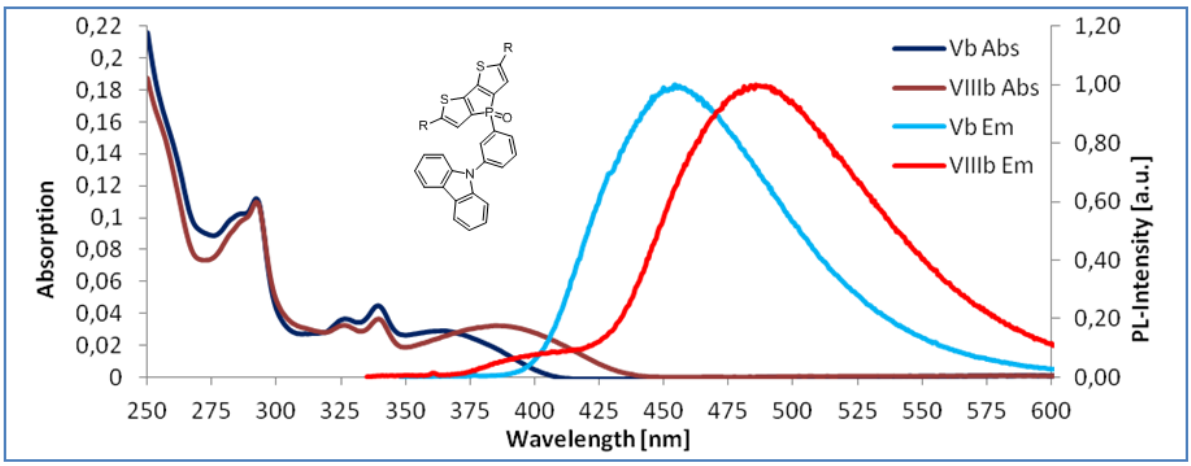


Scheme D- 2: Absorption (Abs) and emission (Em) spectra of compounds Vb and VIIIb

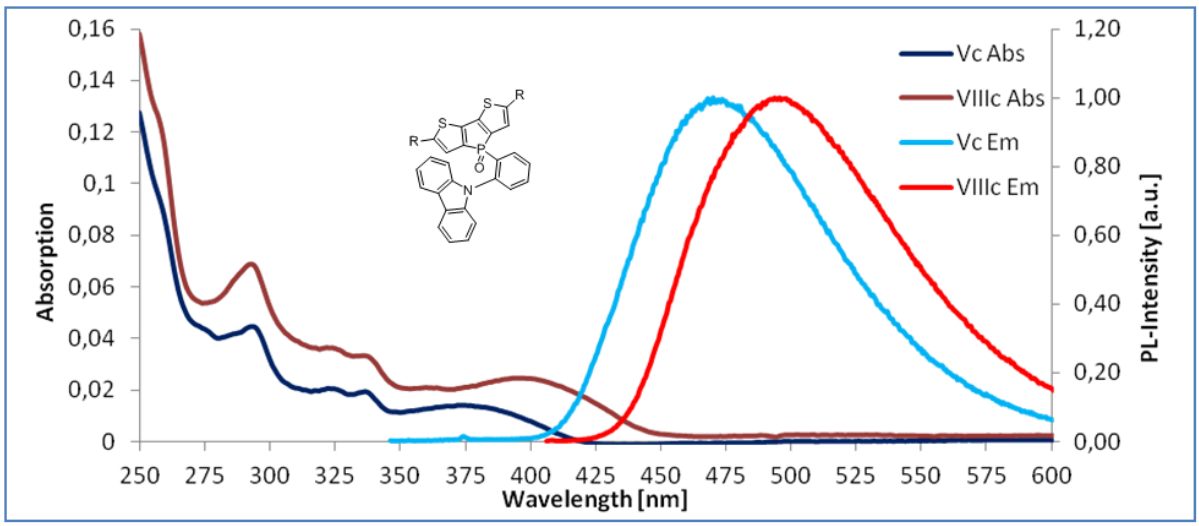


Scheme D- 3: Absorption (Abs) and emission (Em) spectra of compounds Vc and VIIIc

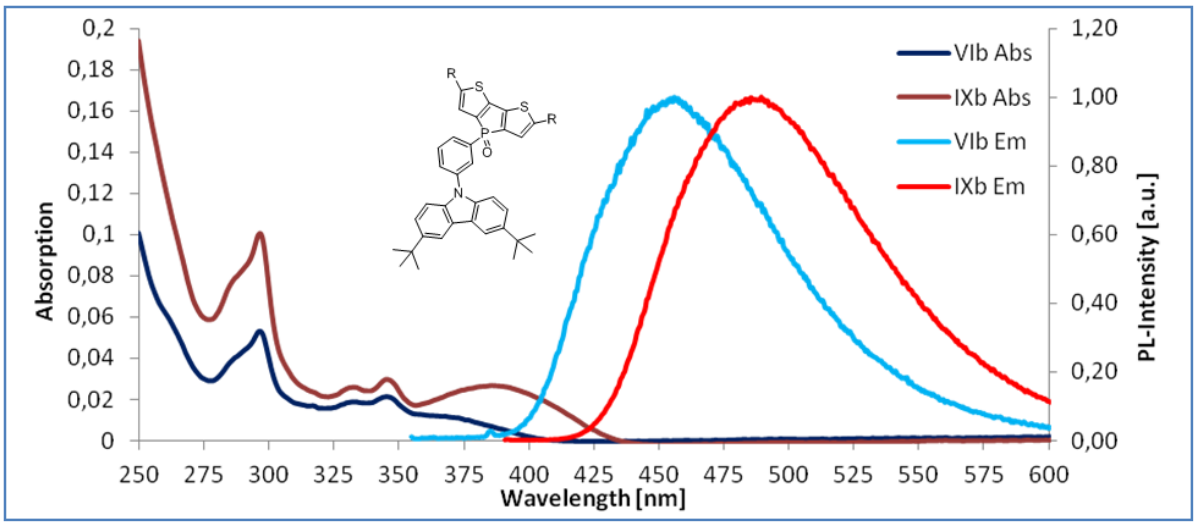


Scheme D- 4: Absorption (Abs) and emission (Em) spectra of compounds VIb and IXb

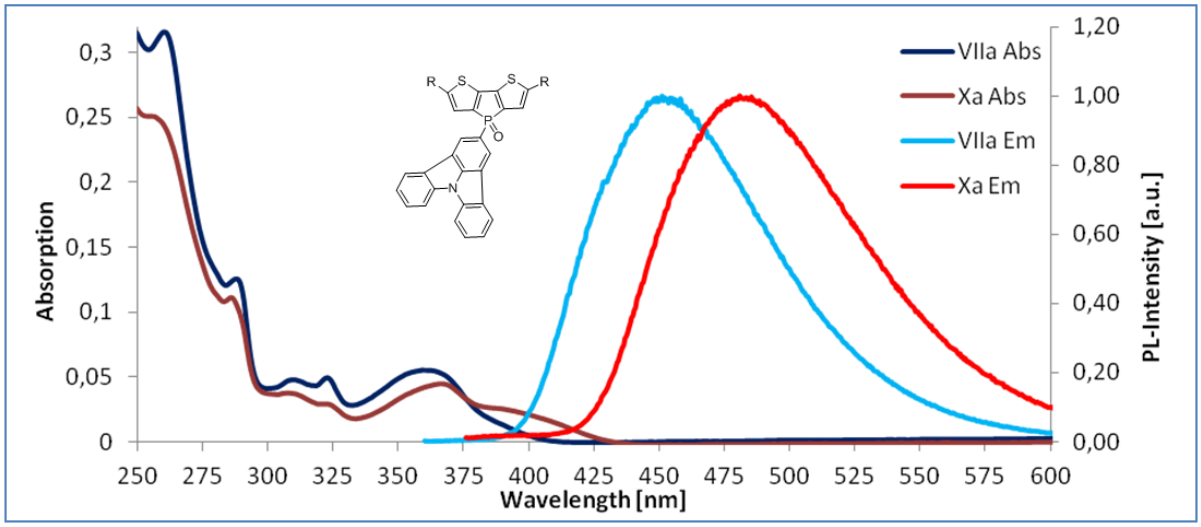


Scheme D- 5: Absorption (Abs) and emission (Em) spectra of compounds VIIa and Xa

In the following table (Table 1) maxima of absorption and emission spectra of the dithienophosphole oxides are listed.

Table 1: Spectroscopic data of the new dithienophosphole oxides
[a] UV-Vis absorption maxima in DCM
[b] Emission maxima in DCM
((sh) for shoulder band)

| Compound | $\lambda_{abs}$ [nm] [a] | | | | | $\lambda_{em}$ [nm] [b] |
|---|---|---|---|---|---|---|
| Va | 364 (sh) | 338 | 325.5 | 292 | | 454 |
| VIIIa | 386 | 338 | 326 | 292.5 | | 485.5 |
| Vb | 364.5 | 339 | 326.5 | 292 | | 454.5 |
| VIIIb | 385.5 | 339 | 326 | 292 | | 485.5 |
| Vc | 373.5 | 337 | 322.5 | 293 | | 470 |
| VIIIc | 397 | 336 | 322 | 293 | | 495.5 |
| VIb | 364 (sh) | 345.5 | 333 | 297 | | 456 |
| IXb | 386 | 345.5 | 333 | 297 | | 489.5 |
| VIIa | 360 | 323 | 310 | 288 | 260.5 | 451 |
| Xa | 366.5 | 321 | 308 | 286 | 255 | 481 |

## D.1.3 Discussion of the results - absorption

At first sight it is notable that overlapping areas of absorption and emission spectra of each compound are very small. This leads to the suggestion that self-absorption of these materials is generally low and almost zero in the region of maximum emission intensity.

All absorption spectra of the dithienophosphole oxide compounds show quite similar maxima.

The compounds incorporating Cbz show an absorption maximum close to 292.5 nm, which lies within a typical range reported for Cbz. [25, 32] Both compounds **VIb** and **IXb**, having *t*-Bu substituents at the positions 3 and 6 of the Cbz, show this maximum slightly red-shifted at 297 nm. In contrast, the more distant DTPOX system and its H- or *n*-Bu-substituents do not have an influence on this absorption maximum. Scheme D- 6 shows the direct comparison of Cbz and t-Bu-substituted Cbz incorporating compounds.

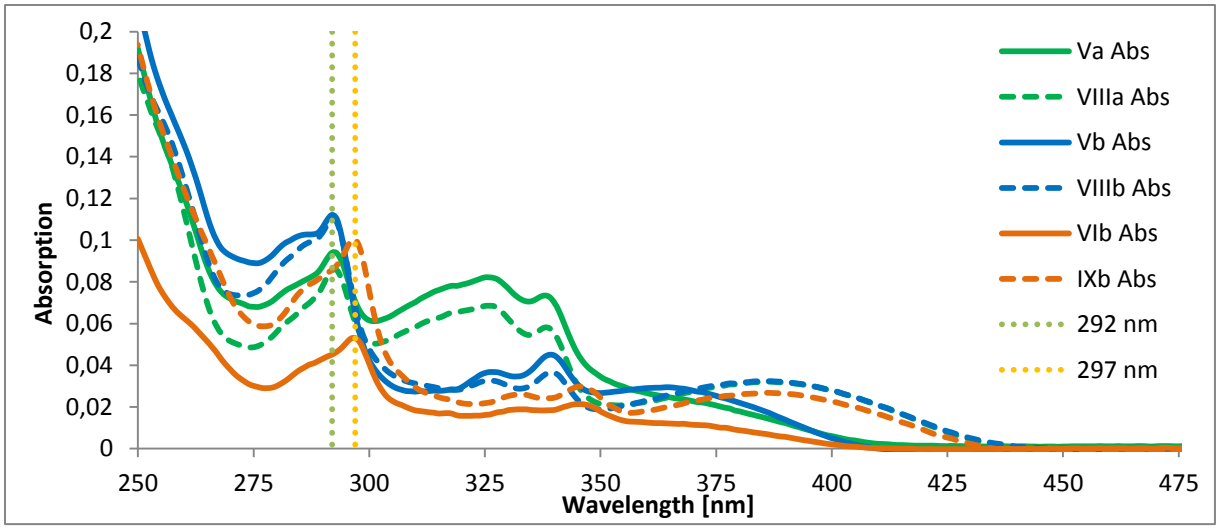


Scheme D- 6: Comparison of absorption spectra
Compounds incorporating Cbz (green: Va, VIIIa; blue: Vb, VIIIb) and *t*-Bu substituted Cbz (orange: VIb, IXb)

**VIIa** and **Xa**, the compounds with ICz as a donor system instead of a phenylcarbazole species, show absorption maxima at 288 (**VIIa**) and 286 (**Xa**) nm (Scheme D- 7).

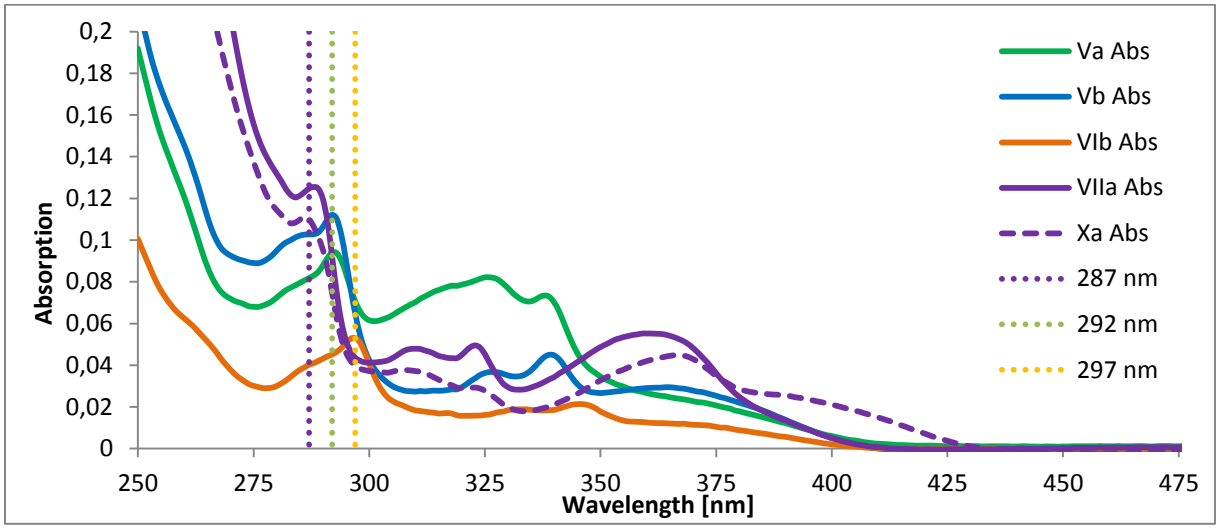


Scheme D- 7: Comparison of absorption spectra
Compounds incorporating ICz (VIIa, Xa: purple), Cbz (Va: green; Vb: blue) and *t*-Bu substituted Cbz (orange: VIb)

Maxima between 330 and 350 nm can be attributed to transitions, typically for dithienophospholes directly linked to a phenyl-ring at the phosphorus atom [34d] and found in all recorded spectra. With increasing donor strength of the triarylamine systems these absorption bands are more and more red-shifted: ICz (average: 322 and 309 nm) < Cbz (average: 338 and 325 nm) < *t*-Bu-Cbz (average: 345 and 333 nm) (Scheme D- 7). *n*-Bu-substituents do not have an influence on this absorption as can be seen in Scheme D- 6 and Scheme D- 8.

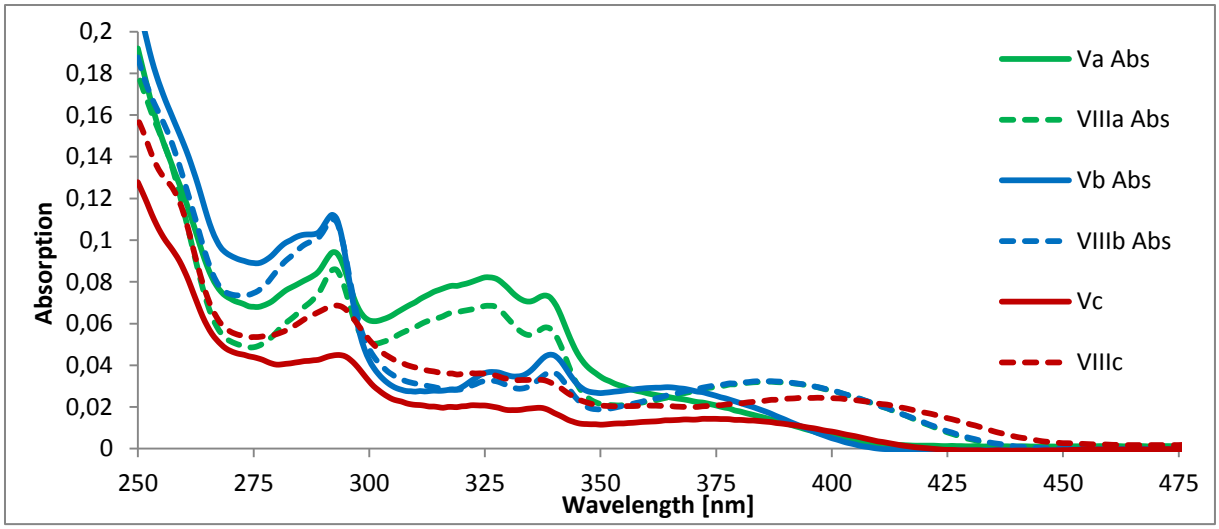


Scheme D- 8: Comparison of absorption spectra
Compounds with *para*- (a, green), *meta*- (b, blue) and *ortho*- (c, red) linkage between Ph-Cbz and DTPOX systems

Most notable is the influence of the *n*-Bu-substituents on the DTPOX system on the absorption onset and hence the most red-shifted absorption band (Scheme D 1-5, Scheme D- 9).

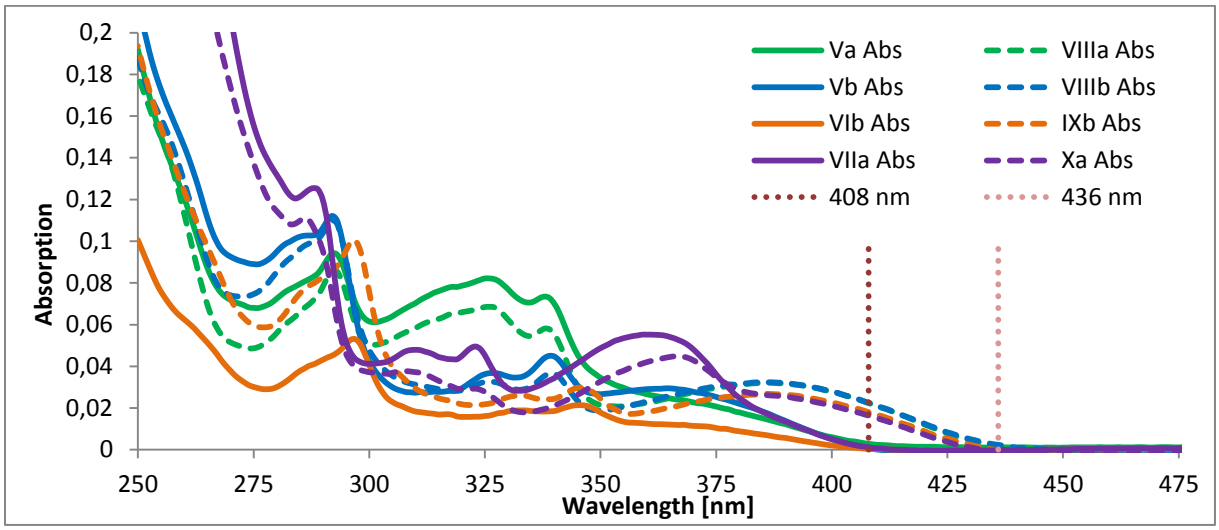


Scheme D- 9: Comparison of absorption onsets

The absorption onset of compounds with *n*-Bu-substituents on the DTPOX system is distinctly red-shifted with respect to those without. The calculations of the optical bandgap of the substances were based on the absorption onset values, both presented in the following table (Table 2).

Table 2: Absorption onset values and optical bandgap of the dithienophosphole oxides

| Compound | Absorption onset [nm] | Resulting optical bandgap [eV] |
|---|---|---|
| Va | 408.1 | 3.04 |
| VIIIa | 436.0 | 2.84 |
| Vb | 408.5 | 3.04 |
| VIIIb | 436.4 | 2.84 |
| Vc | 422.5 | 2.93 |
| VIIIc | 447.8 | 2.77 |
| VIb | 408.2 | 3.04 |
| IXb | 435.6 | 2.85 |
| VIIa | 407.2 | 3.04 |
| Xa | 434.2 | 2.86 |

The values for all *n*-Bu-substituted and all unsubstituted compounds respectively are similar. This means that the triarylamine system does not influence the absorption onset, that is the optical band gap. Generally, the bandgap of *n*-Bu-substituted materials is smaller (average: 2.85 eV) compared to that of unsubstituted materials (average: 3.04 eV). There is just one exception: **Vc** and **VIIIc**, the *ortho*-linked phenylcarbazole functionalized species, show additionally red-shifted values and therefore also smaller optical bandgaps (2.93 and 2.77 eV, respectively).

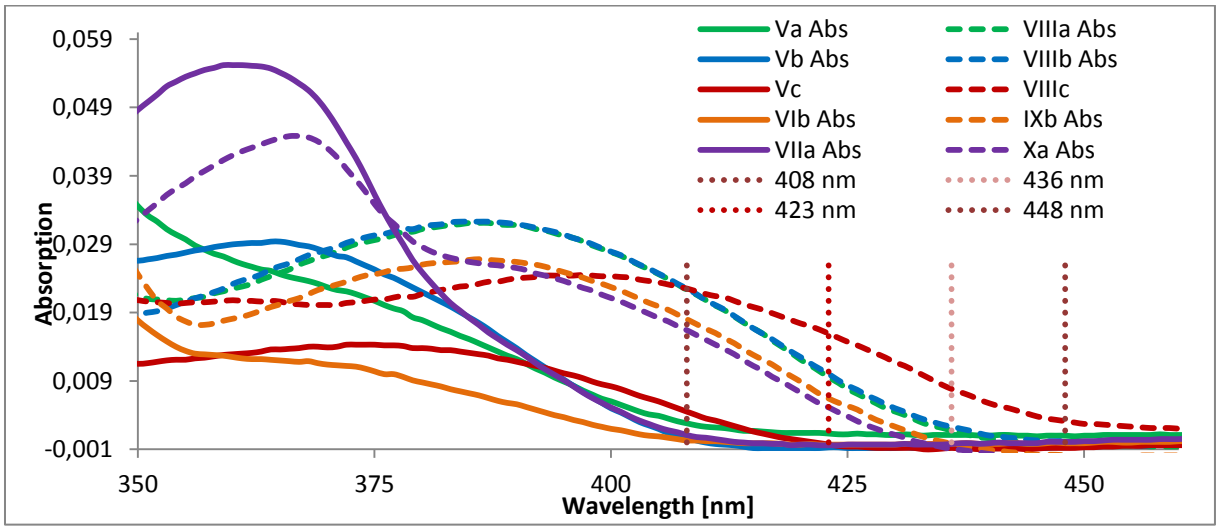


Scheme D- 10: Comparison of absorption onsets

X-ray crystallography revealed that the *ortho*-linkage allows for intramolecular π-stacking between the planar annelated-ring systems (Scheme D- 11), which might be a reason for slightly different band gap values.

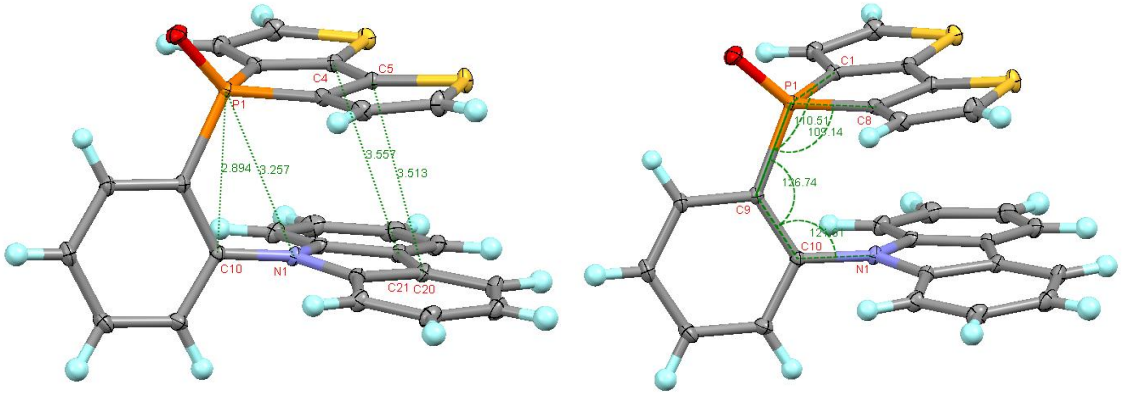


**Scheme D- 11: Molecular structure of Vc. C (grey), N (blue), S (yellow), P (orange), and O (red) atoms are represented by ellipsoids drawn at 50% probability levels, H atoms by spheres of arbitrary radius. Selected distances between the labeled atoms (figure on the left, [Å]) and selected bond angles (figure on the right, [deg]). Single crystals, suitable for X-ray-crystallography, were obtained by slow evaporation from a $CD_2Cl_2$-solution.**

The distance between the two almost parallel planes amounts approximately 3 Ångström (Å): The distance amounts 2.9 Å between atom P1 and C10 and increases slightly towards periphery. The bond angles between the planar systems allowing for this configuration are [deg]: C1-P1-C9, 110.52(4); C8-P1-C9, 109.14(4); P1-C9-C10, 126.74(6); C9-C10-N1, 121.61(7); Selected bond lengths [Å]: C1-P1, 1.8061(10); C8-P1, 1.7979(9); P1-C9, 1.8167(8); C9-C10, 1.4142(12); C10-N1, 1.4237(11).

Single crystals, suitable for X-ray-crystallography, were obtained by slow evaporation from a $CD_2Cl_2$-solution. All data were collected on a Bruker APEX II diffractometer with κ geometry, equipped with a CCD detector using Mo Kα radiation (λ = 0.71073 Å) at 100 K in a dry stream of nitrogen. Frame data were reduced to intensity values using SAINT-Plus and absorption correction was applied using the multi-scan method implemented by SADABS [43]. The structures were solved using charge-flipping implemented by SUPERFLIP [44] and refined against F values with JANA2006 [45]. H atoms were placed at calculated positions and refined as riding on the parent C atoms. More detail on data collection and refinement are compiled in Table 3.

**Table 3: Crystal data and details of the refinements of the compound Vc. The experiment was carried out at 100 K with Mo Kα radiation. Absorption was corrected by multi-scan methods, SADABS. H-atom parameters were constrained.**

| **Crystal data** | |
|---|---|
| Chemical formula | $C_{26}\ H_{16}\ N_1\ O_1\ P_1\ S_2$ |
| $M_r$ | 453.5 |
| Crystal system, space group | Monoclinic, P 2yb |
| a, b, c [Å] | 8.3295(6), 14.1464(10), 8.8132(6) |
| β [deg] | 103.1530(19) |
| V [$Å^3$] | 1011.24(12) |
| Z | 2 |
| Z' | - |
| μ [$mm^{-1}$] | 0.363 |
| Crystal size [mm] | 0.65 x 0.55 x 0.42 |

| **Data collection** | |
|---|---|
| Diffractometer | Bruker KAPPA APEX II CCD |
| $T_{min}$, $T_{max}$ | 0.79, 0.86 |
| No. Of measured, indipendent and observed [$I > 3\sigma(I)$] reflections | 41608 |
| $R_{int}$ | 0.0374 |
| $(\sin \theta/\lambda)_{max}$ [$Å^{-1}$] | 0.99 |

| **Refinement** | |
|---|---|
| $R[F^2>2\ \sigma(F^2)]$, $wR[F^2]$, S | 0.0198, 0.0272, 1.92 |
| No. of reflections | 7360 |
| No. of parameters | 281 |
| No. of restraints | 0 |
| $\Delta\rho_{max}$, $\Delta\rho_{min}$ [e $Å^{-3}$] | 0.28, -0.20 |

However, it is noteworthy to mention that the red-shift of the absorption onset values of all compounds with *n*-Bu-substituents on the dithienophosphole oxide system compared to the analogue compounds without those substituents respectively (including the compounds **Vc** and **VIIIc**), amounts approximately 27 nm in average. Therefore, the resulting values for the optical bandgaps show this constant difference of 0.19 eV in average as well.

The same effect on similar compounds (Scheme D- 12) was also found by C. J. Chua in Prof. T. Baumgartner's group. [34d] The *n*-hexyl-substituted triphenylamine-functionalized DTPOX showed red-shifted absorption onsets compared to the analogue unsubstituted compound (approximately 20-25 nm, depending on the solvent used for the measurement).

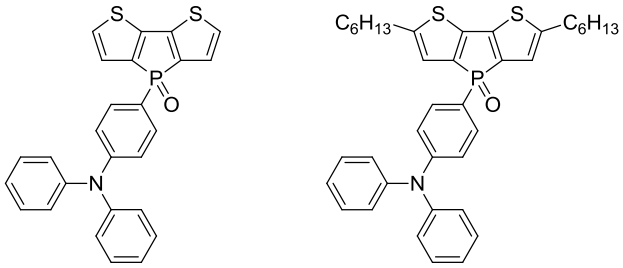


Scheme D- 12: *n*-Hexyl-substituted (right) and unsubstituted (left) triphenylamine-functionalized DTPOX compounds synthesized by C. J. Chua in Prof. T. Baumgartner's group [34d]

## D.1.4 Discussion of the results – emission

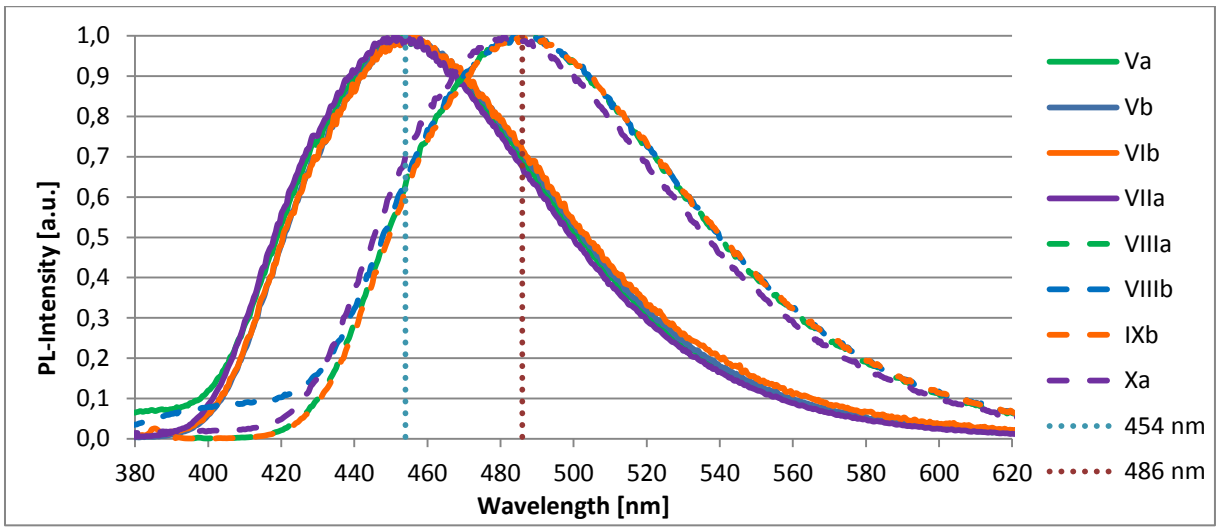


Scheme D- 13: Comparison of emission spectra

Analogously to the absorption onset discussed in the previous chapter, red-shifted emission maxima were observed for all compounds with *n*-Bu-substituents on the dithienophosphole oxide system (Scheme D- 13).

And again there was found one exception: **Vc** and **VIIIc**, the *ortho*-linked phenylcarbazole functionalized species, show additionally red-shifted values for the emission maxima (Scheme D- 14). This fits with the smaller optical band gap resulting from the red-shifted absorption onset.

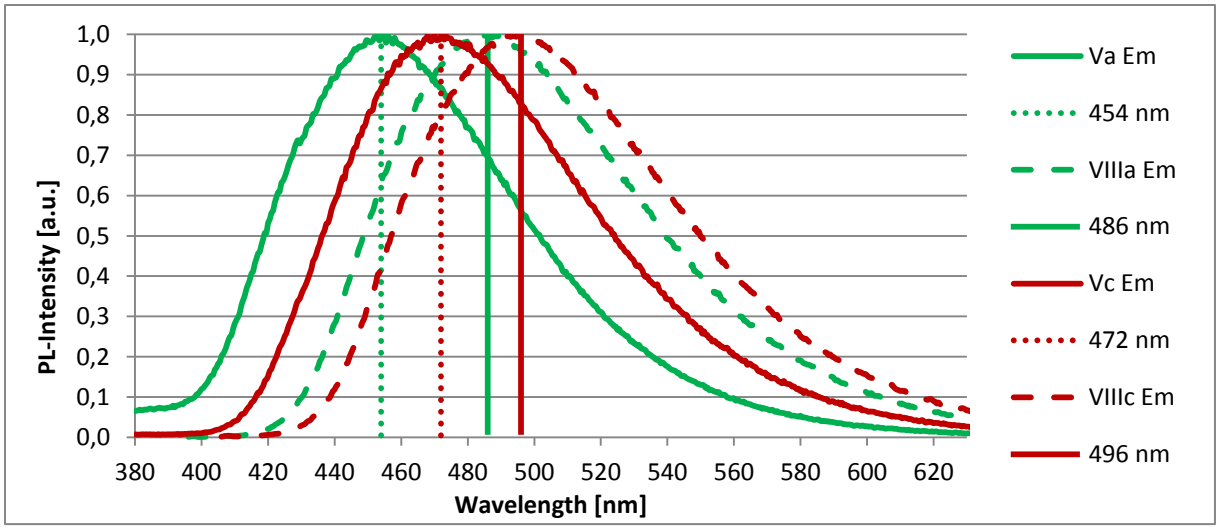


Scheme D- 14: Comparison of emission spectra; red-shifted Vc and VIIIc

Emission maxima of TPA-functionalized DTPOXs (C. J. Chua and T. Baumgartner [34d]) showed an inverse tendency: The unsubstituted compound had a red-shifted emission maximum (508 nm, measured in $CH_2Cl_2$) compared to the *n*-hexyl-substituted analog (472 nm, measured in $CH_2Cl_2$).

DFT calculations of the TPA-functionalized DTPOXs (Scheme D- 15) gave the HOMO and LUMO energies and orbital surfaces, which are in line with the emission measurements. [34d]

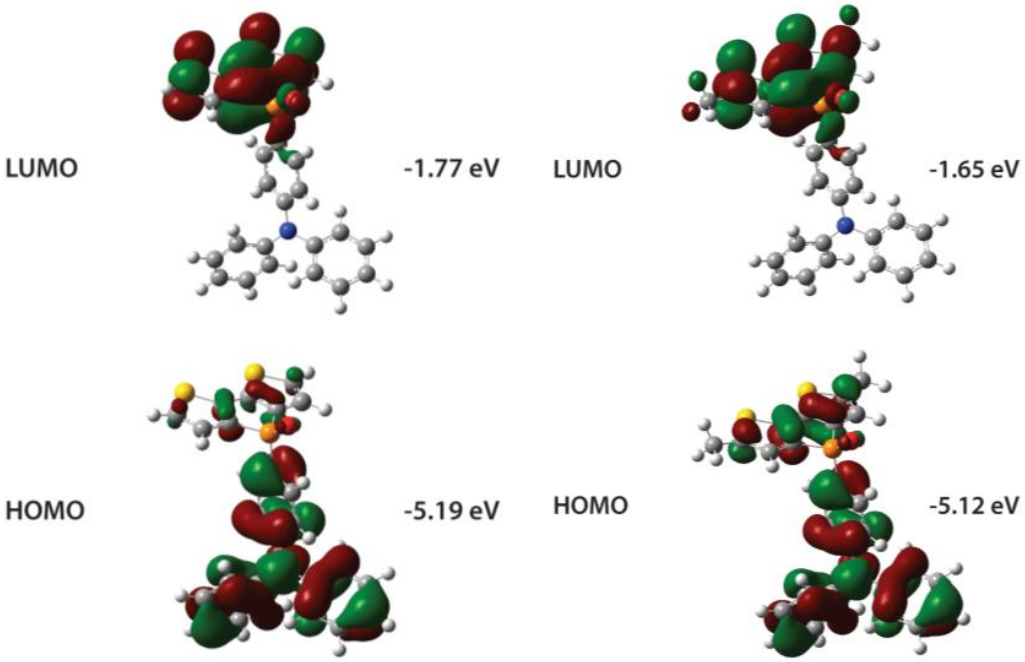


Scheme D- 15: Frontier HOMO and LUMO surfaces for TPA-DTPOX (left) and *n*-Hex-TPA-DTPOX (right) [34d]

The *n*-hexly substituents lead to higher HOMO and LUMO energy levels and due to the separated allocation (and thus different sensitivity) of the molecular orbitals, the LUMO is raised more compared to the HOMO energy level. As a result, HOMO-LUMO transitions for the unsubstituted TPA-DTPOX (3.42 eV) are slightly smaller compared to the substituted analog (3.47 eV). [34d]

The inverse tendency for phenylcarbazole and indolocarbazole functionalized DTPOXs may have to do with the weaker donor strength of the applied triarylamine systems compared to the triphenylamine system used by Chua.

As DFT calculations of compound **Vc**, the *ortho*-linked phenylcarbazole functionalized DTPOX, revealed (Scheme D- 16), the HOMO is located not only on the carbazole moiety but spreads also over the dithienophosphole plane, where the LUMO is located. The HOMO-1 surface shows an orbital lobe connecting the two almost parallel planes and confirms the presumption of an electronic interaction discussed in the previous chapter.

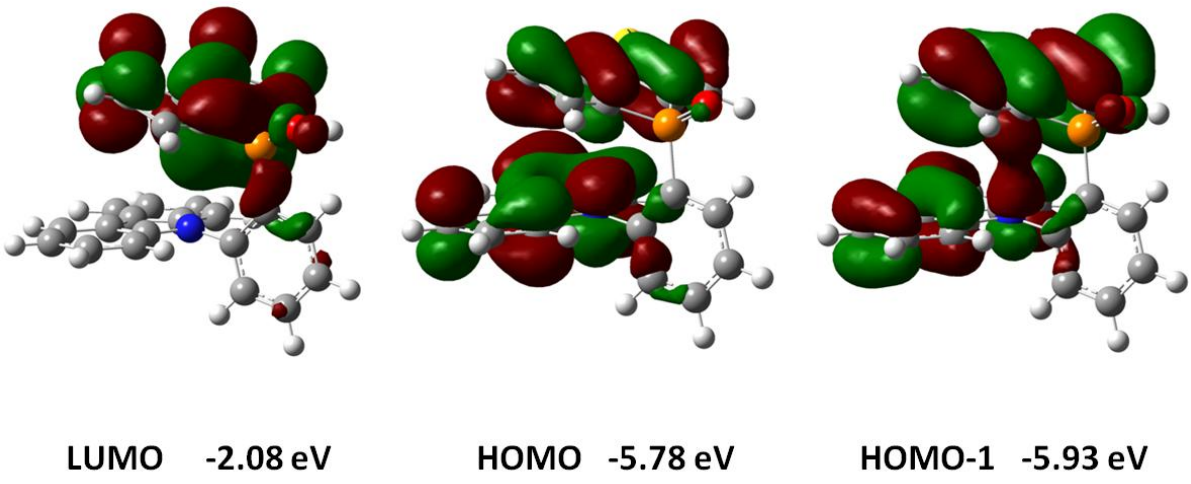


Scheme D- 16: Frontier LUMO, HOMO and HOMO-1 surfaces of the coumpound Vc (DFT calculation)

The spatial distribution of the HOMO may lead to relatively higher sensitivity towards the *n*-Bu-substituents and be responsible for the opposite property trend compared to TPA-functionalized DTPOXs studied by Chua.

If this theory can be applied on the synthesized DTPOX compounds is not confirmed at this point. Further studies, DFT calculations in particular, are necessary to clearly identify the origin of the red-shift of the emissions and to fully determine the electrochemical properties of the compounds.

## D.2 Electrochemical analysis

The HOMO energy levels of the 10 new dithienophosphole oxides (**Vabc, VIb, VIIa, VIIIabc, IXb, Xa**) were measured by cyclic voltammetry (CV) in order to investigate the influence of the different triarylamine functionalizations as well as the influence of alkyl-substituents at the DTPOX systems.

For the CV measurements a set-up of a working and a counter electrode (both platinum electrodes) and a reference electrode (a silver chloride coated silver wire) was used as can be seen in Scheme D- 17.

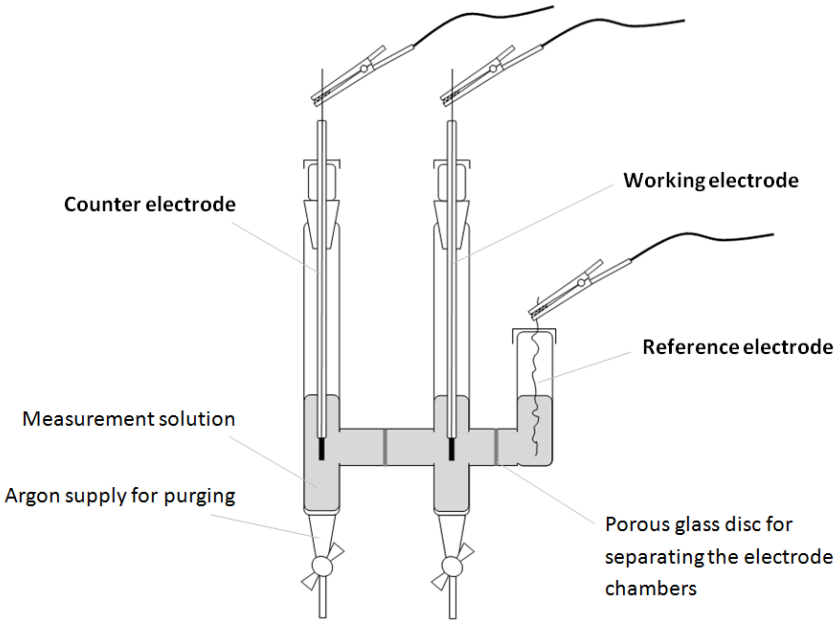


Scheme D- 17: Cyclic voltammetry cell

The resulting data were recorded using a Metrohm Autolab B.V equipment (PGSTAT128N, ADC164, DAC164, External, DI048 potentiostat).

Samples of the phosphole oxides were dissolved in anhydrous DCM (0.5 mmol/L), which is the same solvent used for recording the UV-Vis absorption spectra as well. Tetrabutylammonium tetrafluoroborate (*n*-$Bu_4NBF_4$, 0.1 mol/L) was added to each of the analyte solutions as a supporting electrolyte.

The measurement solutions were filled into the electrode chambers (Scheme D- 17) and purged with argon for 15 minutes prior to measurement.

Applying a voltage between the electrodes leads to the oxidation of the analyte molecules in the measurement solution. The HOMO energy levels can be calculated from the onset of oxidation, which was determined by the intersection of two tangents drawn at the signal background and at the rising of oxidation peaks. The tangents are shown in the corresponding diagrams used for the evaluation of the measurements (Scheme D- 19-28).

The electrode set-up was calibrated by external calibration. Ferrocene has a HOMO energy level of -4.80 eV and is a suitable material for external calibration showing a reversible oxidation (Scheme D- 18). The onset of the oxidation was used to reference the following measurement results.

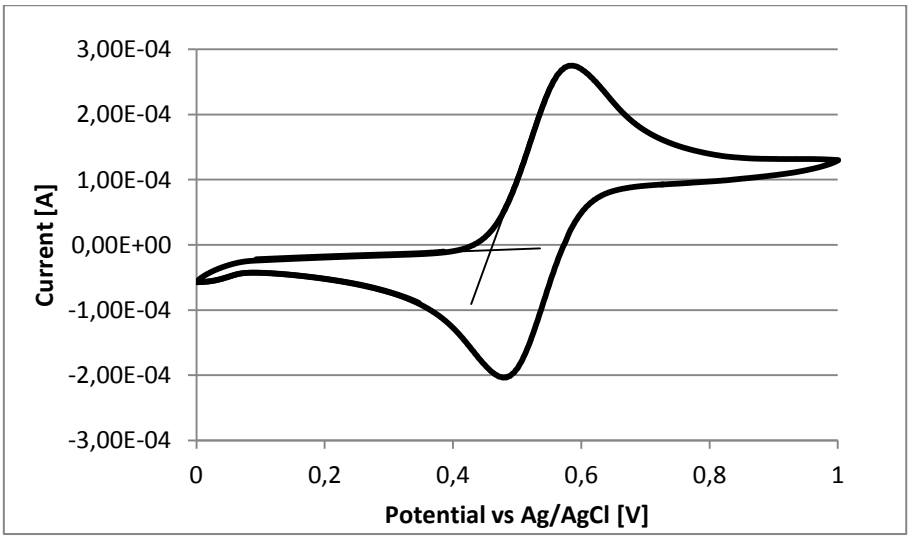


Scheme D- 18: CV measurement of the reversible oxidation of ferrocene (Fc/Fc+)

The CV-measurements of the dithienophosphole oxides are shown in Scheme D- 19-25. While HOMO energy levels were calculated from the onset of oxidation based on these CV-measurements, LUMO energy levels were calculated by addition of the optical bandgap energy to the HOMO energy levels (Table 4).

The values for the optical bandgaps were based on the recorded absorption spectra (Chapter D.1.3) and this resulted in quite plausible values for all substances. Undesired side reactions during CV measurements (oxidation), probably caused by the carbazole moieties, led to additional peaks before the actual oxidation onset of the compound and made the evaluation of the graphs quite difficult. In order to choose the right oxidation onset, the scale of the measured electrical current was taken into account.

Table 4: Optical bandgap [eV], HOMO and LUMO energy levels [eV] of the dithienophosphole oxides

| Compound | Optical bandgap [eV] | HOMO level [eV] | LUMO level [eV] |
|---|---|---|---|
| Va | 3.04 | -5.70 | -2.66 |
| VIIIa | 2.84 | -5.67 | -2.83 |
| Vb | 3.04 | -5.70 | -2.66 |
| VIIIb | 2.84 | -5.66 | -2.82 |
| Vc | 2.93 | -5.71 | -2.78 |
| VIIIc | 2.77 | -5.64 | -2.87 |
| VIb | 3.04 | -5.55 | -2.51 |
| IXb | 2.85 | -5.54 | -2.69 |
| VIIa | 3.04 | -5.90 | -2.86 |
| Xa | 2.86 | -5.82 | -2.96 |

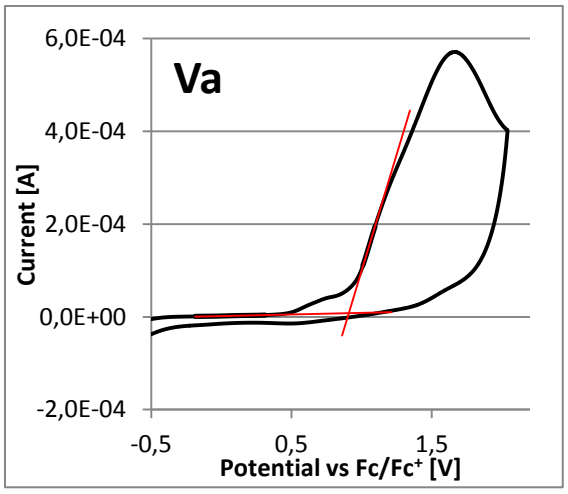


Scheme D- 19: CV measurement of oxidation of Va

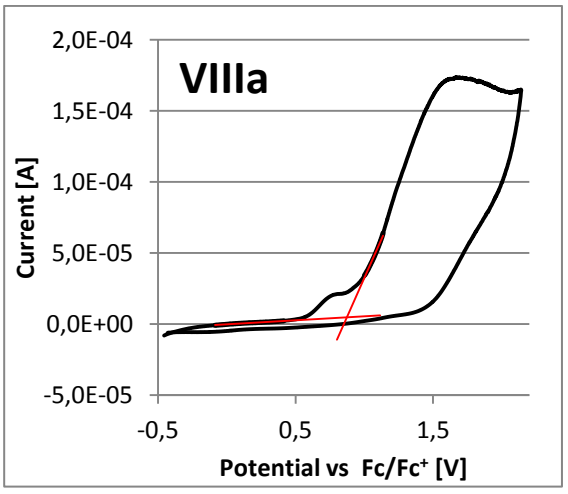


Scheme D- 20: CV measurement of oxidation of VIIIa

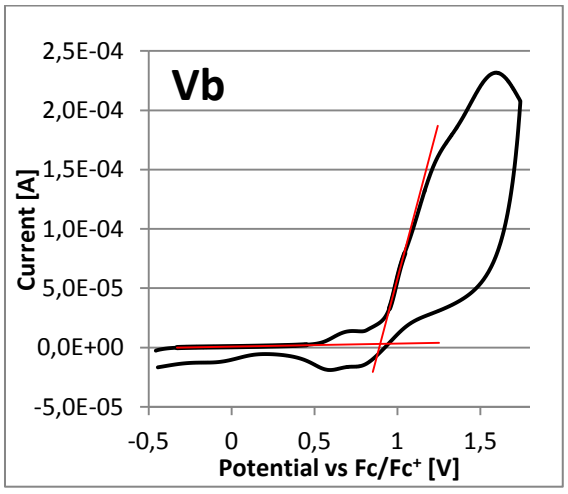


Scheme D- 21: CV measurement of oxidation of Vb

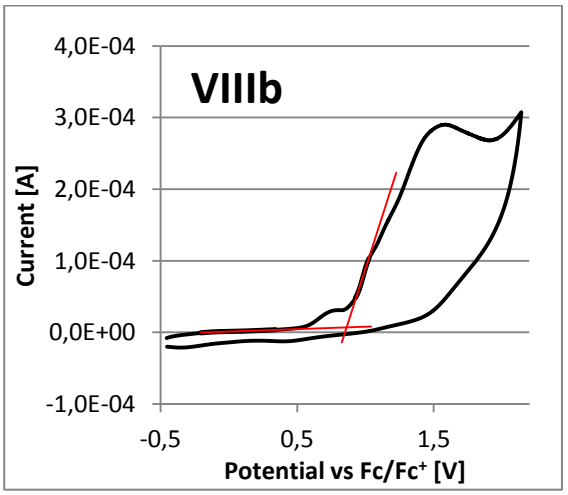


Scheme D- 22: CV measurement of oxidation of VIIIb

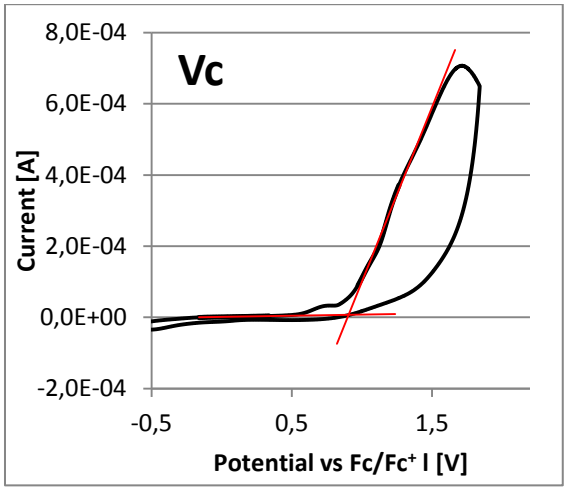


Scheme D- 23: CV measurement of oxidation of Vc

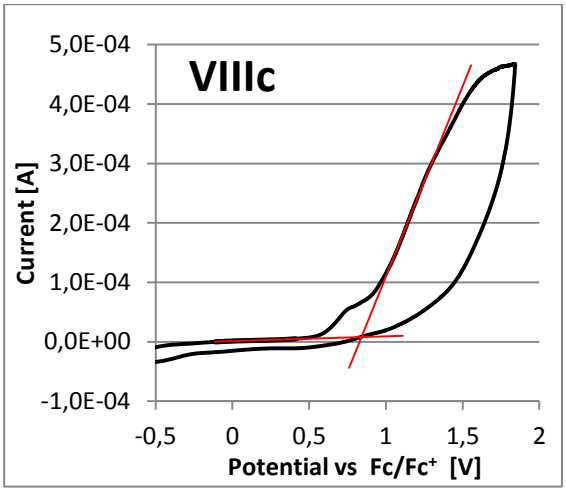


Scheme D- 24: CV measurement of oxidation of VIIIc

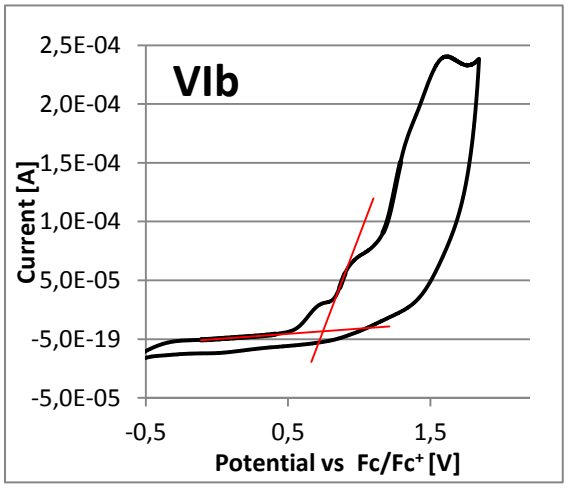


Scheme D- 25: CV measurement of oxidation of VIb

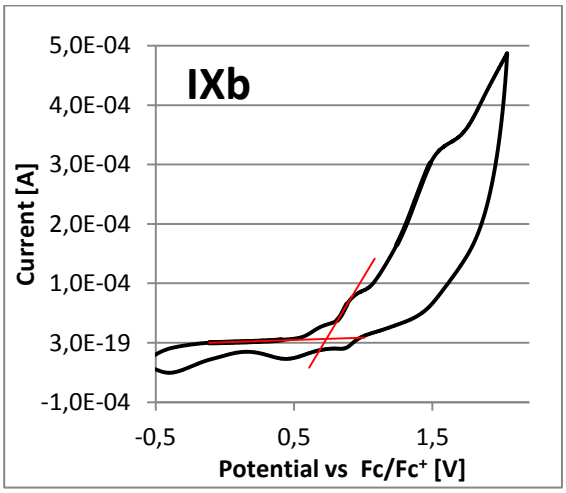


Scheme D- 26: CV measurement of oxidation of IXb

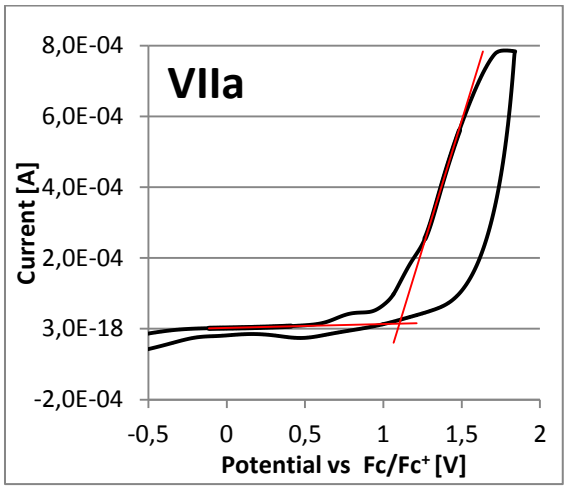


Scheme D- 27: CV measurement of oxidation of VIIa

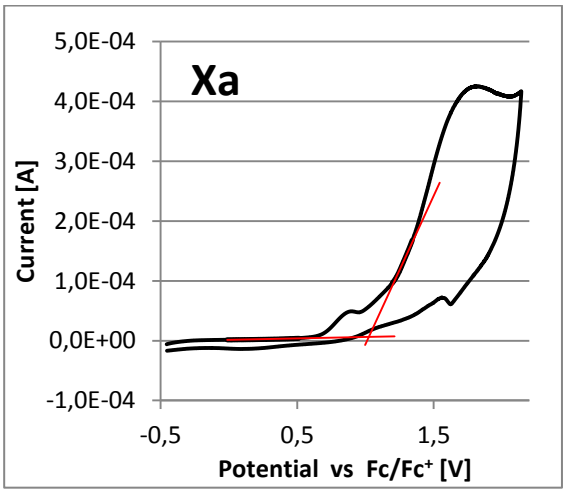


Scheme D- 28: CV measurement of oxidation of Xa

The obtained values for the compounds' HOMO levels are in a range of -5.90 to -5.54 eV.

The Ph-Cbz-functionalized compounds show fairly similar HOMO levels: **Vabc** close to -5.70 eV and **VIIIabc** close to -5.66 eV. There clearly was a discernible tendency between *n*-Bu-substituted DTPOX systems and those without, even though the difference is rather small. The *n*-Bu-substituents lead to higher HOMO levels, since their positive inductive effect causes a higher electron density in the molecule, which allows for easier oxidation of the compound.

Almost the same values were observed for the slightly higher lying HOMO levels of the two *t*-Bu-substituted Ph-Cbz species: -5.55 eV for **VIb** and -5.54 for **IXb**. Therefore, the *t*-Bu-substituents show the same, but an even stronger, effect as the just discussed *n*-Bu-substituents. This might be, because of the higher inductive effect of the branched alkyl-moieties.

In contrast to that, ICz-functionalized compounds showed slightly lower lying HOMO levels, -5.90 eV for **VIIa** and -5.82 eV for **Xa**. Considering the lower donor strength of this triarylamine moiety, the oxidation of the compound should be less easy compared to the other donor systems.

The location of both HOMO and LUMO levels indicate no significant injection barrier for charge carriers from and to adjacent layers in electro-optical devices. Therefore, the next step for further investigation is the incorporation of these materials in prototype-OLED devices.

# E. Experimental part

## E.1 General Remarks

All reagents from commercial suppliers were, unless otherwise noted, used without further purification. Anhydrous solvents like toluene, diethyl ether, dichloromethane and tetrahydrofurane were absolutized by an MBraun solvent purification system prior to use. The commercially available lithiation reagent *n*-BuLi was used without additional quantitative analyses, using the declared value.
All reactions were carried out under nitrogen atmosphere, employing standard Schlenk techniques.

## E.2 Chromatographic Methods

### E.2.1. Thin layer chromatography

Thin layer chromatography (TLC) was performed using TLC-aluminum foil (Merck, silica gel 60 $F_{254}$).

### E.2.2. Column chromatography

Preparative column chromatography was performed using standard flash chromatography.

For the purification of the dithienophosphole oxides (**Vabc**, **VIb**, **VIIa**, **VIIIabc**, **IXb**, **Xa**) a Büchi SepacoreTM Flash system was used, which was equipped with the following components:

- Pump-system: 2 Büchi pump modules C-605
  Büchi pump manager C-615
- Detector: Büchi UV photometer C-635
- Fraction collector: Büchi fraction collector C-660

The appropriate PP-cartridges were packed with silica gel (Merck, 40-63 µm).

## E.3 Analytical Methods

### E.3.1 NMR-Spectroscopy

NMR spectra were recorded using a Bruker Avance (-II, -III) 400 MHz spectrometers.

$^{1}$H- and $^{13}$C-spectra are given as stated: chemical shift in parts per million (ppm) referenced to the according residual non-deuterated solvent peaks ($^{1}$H: $CDCl_3$ δ = 7.26 ppm, $CD_2Cl_2$ δ = 5.32; $^{13}$C: $CDCl_3$ δ = 77.0 ppm, $CD_2Cl_2$ δ = 53.84) with tetramethylsilane (TMS) at δ = 0 ppm.

Chemical shifts of $^{31}$P-spectra were referenced to external 85% $H_3PO_4$.

Multiplicities of the signals are given as: $^{1}$H: s = singlet, bs = broad singlet, d = doublet, t = triplet, q = quartet, quin. = quintet, hex = hextet and m = multiplet: $^{13}$C: s = singlet, d = doublet.

### E.3.2 Absorption spectroscopy

Absorption spectra were recorded on a Perkin Elmer Lambda 750 UV-Vis spectrometer. All spectra were taken at room temperature from solutions in DCM (HPLC grade) at concentrations of 5 nmol/ml using quartz glass cuvettes.

### E.3.3 Fluorecence spectroscopy

Fluorescence spectra were recorded using an Edinburgh FLS920 fluorometer. All compounds were measured as solutions in dry DCM (5nmol/mL) in fused quartz cuvettes under standard laboratory conditions. For the fluorescence spectra the excitation wavelength was the corresponding absorption maxima.

### E.3.4 Cyclic voltammetry

For the cyclic voltammetry (CV) measurements a set-up of a working and a counter electrode (both platinum electrodes) and a reference electrode (a silver chloride coated silver wire) was used (Scheme D- 17). The resulting data were recorded using a Metrohm Autolab B.V equipment (PGSTAT128N, ADC164, DAC164, External, DI048 potentiostat).

Samples of the DTPOXs were dissolved in anhydrous DCM (0.5 mmol/L) and Tetrabutylammonium tetrafluoroborate (*n*-$Bu_4NBF_4$, 0.1 mol/L) was added to each of the analyte solutions as a supporting electrolyte.

The solutions were purged with argon for 15 minutes prior to measurement. HOMO energy levels were calculated from the onset of oxidation. The onset potential was determined by the intersection of two tangents drawn at the background and the rising of oxidation peaks.

## E.4 Synthesis of OLED compounds – donor systems

Detailed experimental procedures for the synthesis of each compound as well as their characterization are presented in the following chapters.

### E.4.1 Modification of 9*H*-carbazole

**3,6-Di-*tert*-butyl-9*H*-carbazole (2)**

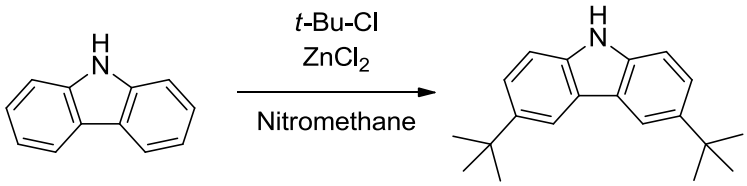


**1**
$C_{12}H_9N$
167,21

**2**
$C_{20}H_{25}N$
279,42

Procedure according to [38]. 9*H*-carbazole (**1**) (5.02 g, 30 mmol, 1 eq.), 100 mL of nitromethane, and $ZnCl_2$ (4.9 g, 36 mmol, 1.2 eq.) were added to a Schlenk flask under nitrogen atmosphere. 2-Chloro-2-methylpropane (8.33 g, 90 mmol, 3 eq.) was added dropwise at 0 °C. The mixture was stirred first at room temperature overnight and then at 50 °C for 24 hours before it was hydrolyzed with 100 mL of water. The product was extracted with DCM (3x50 mL). The organic layer was washed with water (2x50 mL), dried with $MgSO_4$, and evaporated under vacuum. The residue was purified by flash column chromatography (silica gel, 50% hexanes in EA) and recrystallized from hexanes to give compound **2** (7.05 g, 84%) as a white solid.

$R_f$: 0.71 (Hex:EA = 3/1)

$^1$H-NMR (400 MHz, $CDCl_3$): δ = 8.08 (d, J = 1.83 Hz, 2H), 7.83 (bs, 1H), 7.47 (dd, J = 8.51, 1.91 Hz, 2H), 7.33 (d, J = 8.50), 1.46 (s, 18H) ppm.

$^{13}$C NMR (400 MHz, $CDCl_3$) δ = 142.24, 138.04, 133.95, 123.51, 116.17, 109.97, 34.69, 32.03 ppm.

## E.4.2 Synthesis of the carbazole-based bromo-precursors

### 9-(4-Bromophenyl)-9*H*-carbazole (3a)

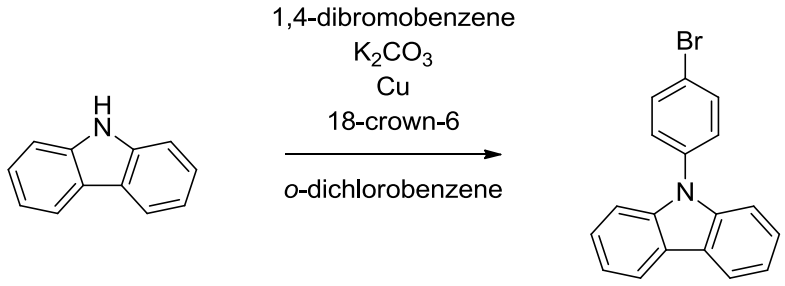


**1**
$C_{12}H_9N$
167,21

**3a**
$C_{18}H_{12}BrN$
322,20

Procedure on the basis of [38]. A mixture of 9*H*-carbazole (**1**) (3.34 g, 20 mmol, 1 eq.), 1,4-dibromobenzene (15.80 g, 67 mmol, 3.3 eq.), $K_2CO_3$ (11.06 g, 80 mmol, 4 eq.), Cu powder (0.83 g, 13 mmol, 0.66 eq.) and 18-crown-6 (1.77 g, 6.7 mmol, 0.3 eq.) in *o*-dichlorobenzene (115 mL) was degassed with nitrogen for 20 min while stirring. The reaction mixture was then refluxed under nitrogen for 24 hours. The crude mixture was filtered through an $Al_2O_3$ plug and the residue was washed with $CHCl_3$ (3x20 mL). The combined filtrates were evaporated to dryness. The residue was purified by recrystallization from hexanes to give compound **3a** (4.1 g, 64%) as a white solid.

$R_f$: 0.82 (Hex:EA = 3/1)

$^1$H-NMR (400 MHz, $CDCl_3$): δ = 8.15 (dt, J = 7.70, 0.94 Hz, 2H), 7.74 (ddd, J = 8.73, 2.85, 2.10 Hz, 2H), 7.46 (ddd, J = 8.72, 2.85, 2.10 Hz, 2H), 7.43 (td, J = 6.83, 1.24 Hz, 2H), 7.38 (dm, J = 8.14 Hz, 2H), 7.31 (ddd, J = 7.95, 6.70, 1.25 Hz, 2H) ppm.

## 9-(3-Bromophenyl)-9*H*-carbazole (3b)

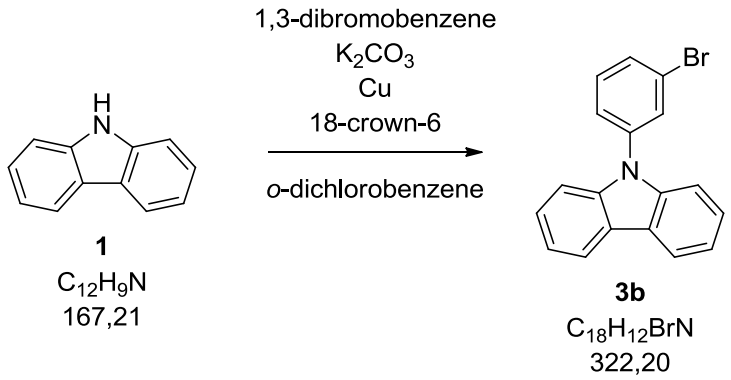


**1**
$C_{12}H_9N$
167,21

**3b**
$C_{18}H_{12}BrN$
322,20

Procedure on basis of [38]. A mixture of 9*H*-carbazole (**1**) (3.34 g, 20 mmol, 1 eq.), 1,3-dibromobenzene (15.80 g, 67 mmol, 3.3 eq.), $K_2CO_3$ (11.06 g, 80 mmol, 4 eq.), Cu powder (0.83 g, 13 mmol, 0.66 eq.) and 18-crown-6 (1.77 g, 6.7 mmol, 0.3 eq.) in *o*-dichlorobenzene (115 mL) was degassed with nitrogen for 30 min while stirring. The reaction mixture was then refluxed under nitrogen for 24 hours. The crude mixture was filtered and the residue was washed with $CHCl_3$ (3x20 mL). The combined filtrates were evaporated to dryness. The residue was purified by column chromatography (silica gel, 20% DCM in hexanes) to give compound **3b** (5.85 g, 91%) as a colorless oil.

$R_f$: 0.62 (Hex:DCM = 3/1)

$^1$H-NMR (400 MHz, $CDCl_3$): δ = 8.22 (dt, J = 7.74, 0.95 Hz, 2H), 7.83 (t, J = 1.92 Hz, 1H), 7.66 (ddd, J = 7.90, 1.88, 1.18 Hz, 1H), 7.58 (ddd, J = 7.95, 1.94, 1.17 Hz, 1H), 7.53-7.48 (m, 5H), 7.41-7.37 (m, 2H) ppm.

$^{13}$C NMR (400 MHz, $CDCl_3$) δ = 140.33, 138.92, 130.87, 130.20, 129.85, 125.98, 125.40, 123.41, 123.06, 120.25, 120.22, 109.43 ppm.

## 9-(2-Bromophenyl)-9*H*-carbazole (3c)

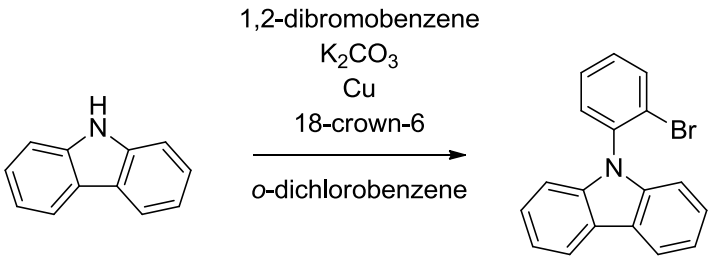


**1**
$C_{12}H_9N$
167,21

**3c**
$C_{18}H_{12}BrN$
322,20

Procedure adapted from [38]. A mixture of 9*H*-carbazole (**1**) (3.34 g, 20 mmol, 1 eq.), 1,2-dibromobenzene (15.80 g, 67 mmol, 3.3 eq.), $K_2CO_3$ (11.06 g, 80 mmol, 4 eq.), Cu powder (0.83 g, 13 mmol, 0.66 eq.) and 18-crown-6 (1.77 g, 6.7 mmol, 0.3 eq.) in *o*-dichlorobenzene (115 mL) was degassed with nitrogen for 30 min while stirring. The reaction mixture was then refluxed under nitrogen for 24 hours. The crude mixture was filtered through an $Al_2O_3$ plug and the residue was washed with $CHCl_3$ (3x20 mL). The combined filtrates were evaporated to dryness. The residue was purified by column chromatography (silica gel, 10% DCM in hexanes) to give compound **3c** (5.46 g, 85%) as a white solid.

$R_f$: 0.60 (Hex:EA = 6/1)

$^1$H-NMR (400 MHz, $CD_2Cl_2$): δ = 8.30 (d, J = 7.75 Hz, 2H), 7.97 (d, J = 8.03 Hz, 1 H), 7.60- 7.58 (m, 2H), 7.54 (td, J = 7.67, 1.16 Hz, 2H), 7.50-7.46 (m, 1H), 7.44 (td, J = 7.48, 0.97 Hz, 2H), 7.22 (dt, J = 8.16, 0.82 Hz, 2H) ppm.

$^{13}$C NMR (400 MHz, $CDCl_3$) δ = 140.79, 136.67, 134.13, 131.03, 130.05, 128.72, 125.89, 123.74, 123.20, 120.30, 119.95, 109.96 ppm.

## 9-(4-Bromophenyl)-3,6-di-*tert*-butyl-9*H*-carbazole (4a)

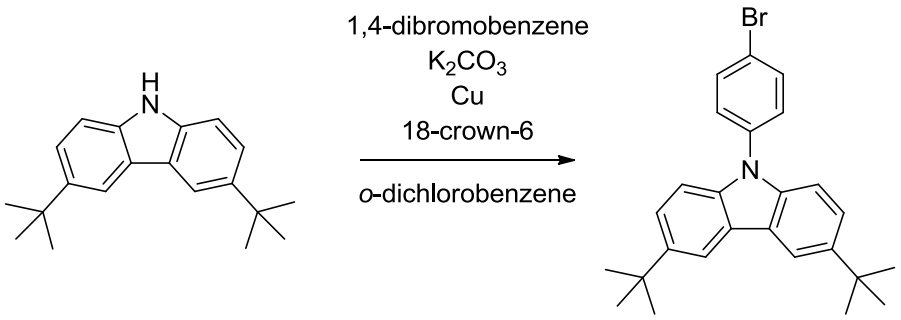


**2**
$C_{20}H_{25}N$
279,42

**4a**
$C_{26}H_{28}BrN$
434,41

Procedure according to [38]. A mixture of 3,6-di-*tert*-butyl-9*H*-carbazole (**2**) (1.68 g, 6 mmol, 1 eq.), 1,4-dibromobenzene (4.72 g, 20 mmol, 3.3 eq.), $K_2CO_3$ (3.32 g, 24 mmol, 4 eq.), Cu powder (0.25 g, 0.4 mmol, 0.66 eq.) and 18-crown-6 (0.53 g, 2 mmol, 0.3 eq.) in *o*-dichlorobenzene (32 mL) was degassed with nitrogen for 30 min while stirring. The reaction mixture was then refluxed under nitrogen overnight (190 °C oil bath temperature for 19 hours). The crude mixture was filtered and the residue was washed with $CHCl_3$ (3x20 mL). The combined filtrates were evaporated to dryness. The residue was purified by flash column chromatography (silica gel, 50% DCM in hexanes) and recrystallization from hexanes to give compound **4a** (1.5 g, 58%) as a white solid.

$R_f$: 0.88 (Hex:EA = 3/1)

$^1$H-NMR (400 MHz, $CDCl_3$): $\delta$ = 8.13 (s, 2H), 7.70 (d, J = 8.38 Hz, 2H), 7.48-7.43 (m, 4H), 7.31 (d, J = 8.66 Hz, 2H), 1.46 (s, 18H) ppm.

## 9-(3-Bromophenyl)-3,6-di-*tert*-butyl-9*H*-carbazole (4b)

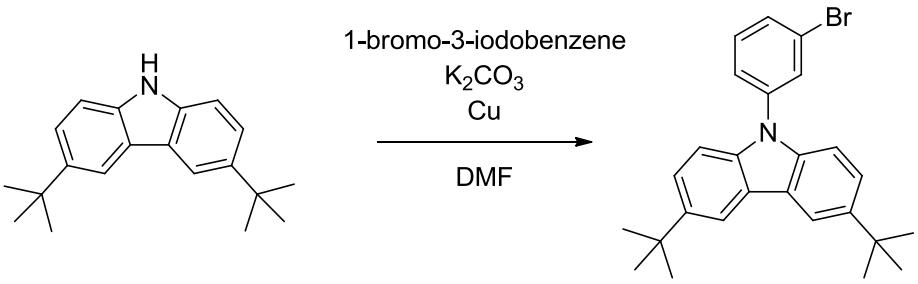


**2**
$C_{20}H_{25}N$
279,42

**4b**
$C_{26}H_{28}BrN$
434,41

Procedure adapted from [39]. A mixture of 3,6-di-*tert*-butyl-9*H*-carbazole (**2**) (1.63 g, 5.83 mmol, 1 eq.), 1-bromo-3-iodobenzene (1.7 g, 5.9 mmol, 1 eq.), $K_2CO_3$ (2.42 g, 17.5 mmol, 3 eq.), and Cu powder (1.11 g, 17.5 mmol, 3 eq.) in DMF (20 mL) was stirred at refluxing temperature overnight under nitrogen atmosphere. After cooling to room temperature the crude mixture was filtered through Celite. The filtrate was poured into water and then extracted with EA (3x30 mL). The combined organic phase was washed with water (3x30 mL), dried over $MgSO_4$ and evaporated to dryness. The residue was purified by recrystallization from hexanes to give compound **4b** (1.66 g, 66%) as a white solid.

$R_f$: 0.82 (Hex:EA = 3/1)

$^1$H-NMR (400 MHz, $CDCl_3$): δ = 8.14 (s, 2H), 7.75 (s, 1H), 7.57 (d, J = 7.86 Hz, 1H), 7.53 (d, J = 8.06 Hz, 1H), 7.48 (d, J = 7.90 Hz, 2H), 7.45 (t, J = 7.92 Hz, 1H), 7.36 (d, J = 8.64 Hz, 2H), 1.48 (s, 18H) ppm.

$^{13}$C NMR (400 MHz, $CDCl_3$) δ = 143.29, 139.60, 138.87, 130.97, 129.94, 129.67, 125.22, 123.76, 123.56, 123.11, 116.31, 109.07, 34.74, 31.99 ppm.

## E.4.3 Lithiation trial of a brominated triarylamine system

**3,6-Di-*tert*-butyl-9-(4-(trimethylsilyl)phenyl)-9*H*-carbazole (T1)**

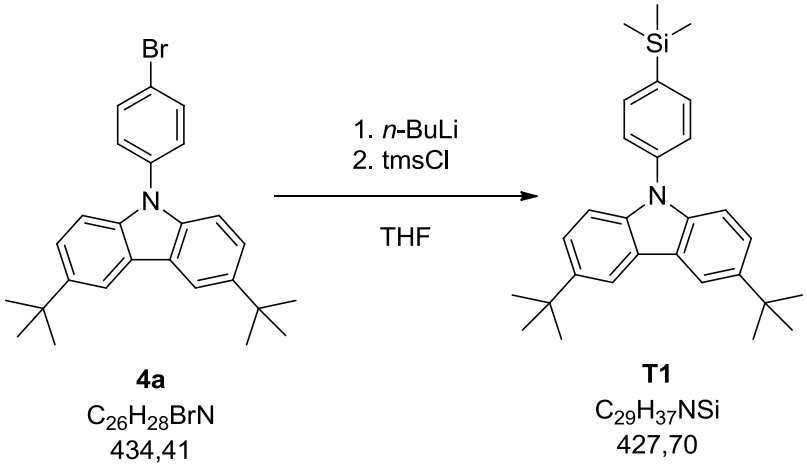


**4a**
$C_{26}H_{28}BrN$
434,41

**T1**
$C_{29}H_{37}NSi$
427,70

*n*-BuLi (0.046 mL, 0.115 mmol, 2.5 M in hexane, 1 eq.) was added dropwise to a solution of **4a** (50 mg, 0.115 mmol, 1 eq.) in THF (1 mL) at -78 °C under nitrogen atmosphere. After 2 hours of stirring at -78 °C tmsCl (0.30 mL, 25 mg, 0.230 mmol, 2 eq.) was added. The reaction mixture was allowed to warm to room temperature and stirred overnight. The solvent was evaporated under vacuum to give compound **T1** (48 mg, 98%) as a white, slightly yellowish solid.

$^1$H-NMR (400 MHz, $CDCl_3$): δ = 8.13 (d, J = 1.43 Hz, 2H), 7.72 (d, J = 8.28 Hz, 2H), 7.55 (d, J = 8.27 Hz, 2H), 7.45 (dd, J = 8.66, 1.92 Hz, 2H), 7.39 (d, J = 8.59 Hz, 2H), 1.47 (s, 18H) ppm.

## E.4.4 Preparation of the phosphine reagent

**Bis(diethylamino)chlorophosphane (7)**

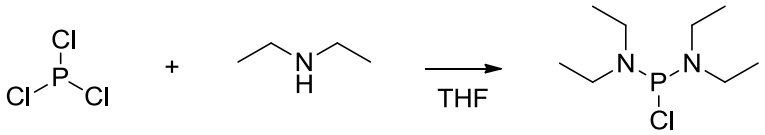


| **5** | **6** | **7** |
|---|---|---|
| $Cl_3P$ | $C_4H_{11}N$ | $C_8H_{20}ClN_2P$ |
| 137,33 | 73,14 | 210,68 |

Procedure on basis of [40]. To a solution of phosphorus trichloride (**5**) (13.73 g, 100 mmol, 1 eq.) in absolute THF (300 mL) was added diethylamine (**6**) (29.26 g, 400 mmol, 4 eq.) dropwise at -78 °C. After complete addition the solution was allowed to warm up to room temperature and stirred overnight. The reaction mixture was filtered through a Celite-plug under nitrogen using a cannula. After evaporation of the solvent under reduced pressure the crude product was distilled to give compound **7** (18.2 g, 86%) as a colorless liquid.

$^{1}$H-NMR (400 MHz, $CDCl_3$): δ = 1.12 (t, $^{3}J_{HH}$ = 7.2 Hz, 12H, $CH_3$), 3.15 (bs, 8H, $CH_2$).

$^{31}$P {$^{1}$H}-NMR (400 MHz, $CDCl_3$): δ = 160.74 (s).

$T_B$: 72 °C (8 torr).

## E.4.5 Synthesis of the dichlorophosphine precursors

### 9-(4-(Dichlorophosphino)phenyl)-9*H*-carbazole (Ia)

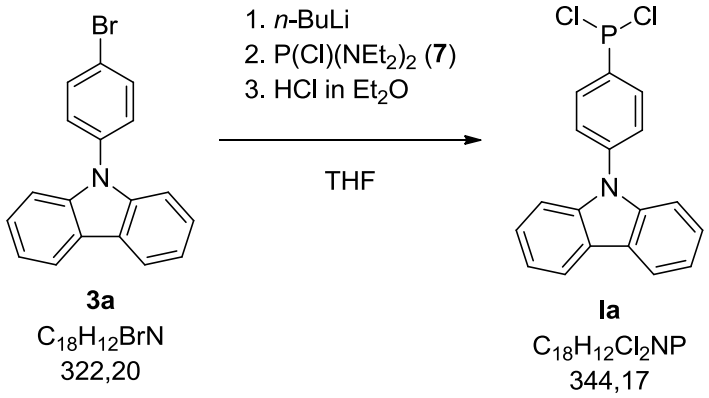


**3a**
$C_{18}H_{12}BrN$
322,20

**Ia**
$C_{18}H_{12}Cl_2NP$
344,17

Procedure adapted from [34d]. *n*-BuLi (2.43 mL, 6.2 mmol, 2.5 M in hexane, 1 eq.) was added dropwise to a solution of **3a** (2 g, 6.2 mmol, 1 eq.) in THF (50 mL) at -78 °C under nitrogen atmosphere. After 1.5 hours of stirring at -78 °C compound **7** (1.28 g, 6.2 mmol, 1 eq.) was added. The reaction mixture was allowed to warm up to room temperature and stirred overnight. Subsequently HCl (12.4 mL, 24.8 mmol, 2 M in diethyl ether, 4 eq.) was added slowly to the reaction mixture at 0 °C and stirred for 3 hours at room temperature. The diethylammonium chloride precipitate was separated using a cannula to filter the reaction mixture under nitrogen through a Celite plug which was washed with diethyl ether (3x30 mL). The solvent was evaporated under vacuum to give a yellowish milky solid which was dissolved in absolute diethyl ether and filtrated again. Compound **Ia** (1.8 g, 85%) was obtained as a yellowish milky solid.

$^{31}P$ {$^{1}H$}-NMR (400 MHz, $CDCl_3$): $\delta$ = 159.98 (s).

## 9-(3-(Dichlorophosphino)phenyl)-9*H*-carbazole (Ib)

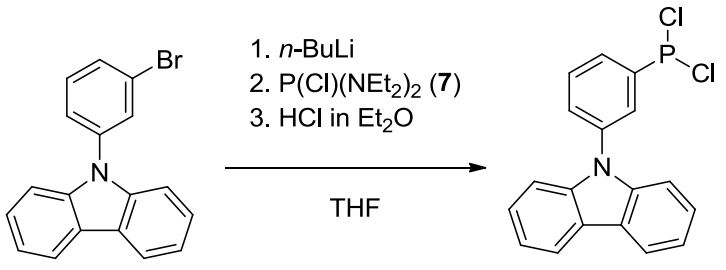


**3b**
$C_{18}H_{12}BrN$
322,20

**Ib**
$C_{18}H_{12}Cl_2NP$
344,17

Procedure adapted from [34d]. *n*-BuLi (4.34 mL, 10.86 mmol, 2.5 M in hexane, 1 eq.) was added dropwise to a solution of **3b** (3.5 g, 10.86 mmol, 1 eq.) in diethyl ether (105 mL) at -78 °C under nitrogen atmosphere. After 2 hours of stirring at -78 °C compound **7** (3.432 g, 16.29 mmol, 1.5 eq.) was added. The reaction mixture was allowed to warm up to room temperature and stirred overnight. The solvent and the excess of compound **7** were evaporated under vacuum. The residue was dissolved in absolute diethyl ether (80 mL). Subsequently HCl (27.15 mL, 54.3 mmol, 2 M in diethyl ether, 5 eq.) was added slowly to the reaction mixture at 0 °C and stirred for 2 hours at room temperature. After the addition of pentane (40 mL), the diethylammonium chloride as well as the Li-salt precipitate was separated using a cannula to filter the reaction mixture under nitrogen through a Celite plug which was washed with diethyl ether (3x30 mL). The solvent was evaporated under vacuum to give compound **Ib** (3.7 g, 99%) as a yellowish milky oil.

$^{31}P$ {$^{1}H$}-NMR (400 MHz, $CDCl_3$): $\delta$ = 159.40 (s).

$^{1}H$-NMR (400 MHz, $CDCl_3$): $\delta$ = 8.31 (d, J = 7.70 Hz, 2H), 8.00 (t, J = 8.03 Hz, 1H), 7.81 (d, J = 7.59 Hz, 1H), 7.75 (d, J = 6.69, 1H), 7.60 (d, J = 3.79 Hz, 5H), 7.53-7.47 (m, 2H) ppm.

## 9-(2-(Dichlorophosphino)phenyl)-9*H*-carbazole (Ic)

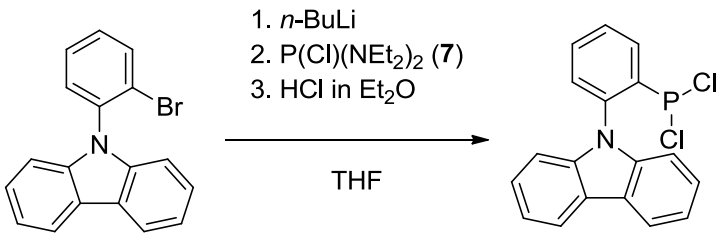


**3c**
$C_{18}H_{12}BrN$
322,20

**Ic**
$C_{18}H_{12}Cl_2NP$
344,17

Procedure adapted from [34d]. *n*-BuLi (2.96 mL, 7.4 mmol, 2.5 M in hexane, 1 eq.) was added dropwise to a solution of **3c** (2.38 g, 7.4 mmol, 1 eq.) in THF (45 mL) at -78 °C under nitrogen atmosphere. After 2 hours of stirring at -78 °C compound **7** (1.56 g, 7.4 mmol, 1 eq.) was added. The reaction mixture was allowed to warm up to room temperature and stirred overnight. Subsequently HCl (14.8 mL, 29.6 mmol, 2 M in diethyl ether, 4 eq.) was added slowly to the reaction mixture at 0 °C and stirred for 1.5 hours at room temperature. The solvent was evaporated under vacuum and replaced with dry diethyl ether (60 ml). The diethylammonium chloride as well as the Li-salt precipitate was separated using a cannula to filter the reaction mixture under nitrogen through a Celite plug which was washed with diethyl ether (2x30 mL). The solvent was evaporated under vacuum to give compound **Ic** (2.5 g, 99%) as a yellowish milky oil.

$^{31}P$ {$^{1}H$}-NMR (400 MHz, $CDCl_3$): $\delta$ = 155.42 (s).

## 9-(3-(Dichlorophosphino)phenyl)-3,6-di-*tert*-butyl-9*H*-carbazole (IIb)

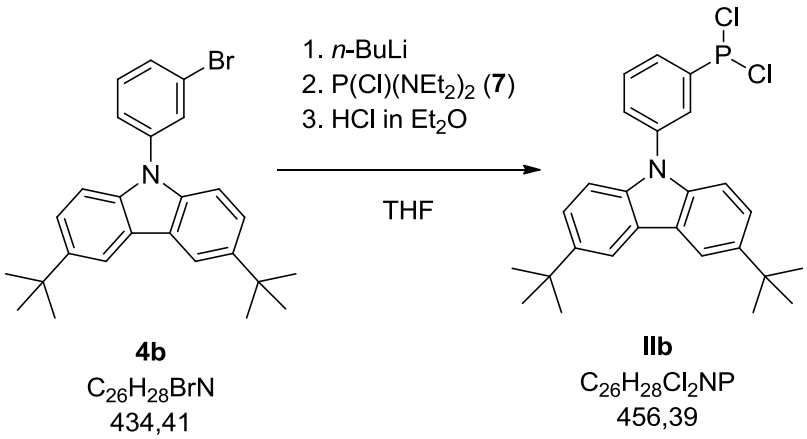


**4b**
$C_{26}H_{28}BrN$
434,41

**IIb**
$C_{26}H_{28}Cl_2NP$
456,39

Procedure adapted from [34d]. *n*-BuLi (1.53 mL, 3.82 mmol, 2.5 M in hexane, 1 eq.) was added dropwise to a solution of **4b** (1.66 g, 3.82 mmol, 1 eq.) in THF (50 mL) at -78 °C under nitrogen atmosphere. After 1.5 hours of stirring at -78 °C compound **7** (0.805 g, 3.82 mmol, 1 eq.) was added. The reaction mixture was allowed to warm up to room temperature and stirred overnight. Subsequently HCl (7.6 mL, 15.3 mmol, 2 M in diethyl ether, 4 eq.) was added slowly to the reaction mixture at 0 °C and stirred for 5 hours at room temperature. The solvent was evaporated under vacuum and replaced with dry diethyl ether (60 ml). The diethylammonium chloride as well as the Li-salt precipitate was separated using a cannula to filter the reaction mixture under nitrogen through a Celite plug which was washed with diethyl ether (2x30 mL). The solvent was evaporated under vacuum to give compound **IIb** (1.7 g, 98%) as a white foam.

$^{31}P$ {$^{1}H$}-NMR (400 MHz, $CDCl_3$): δ = 159.48 (s).

$^{1}H$-NMR (400 MHz, $CDCl_3$): δ = 8.27-8.23 (m, 2H), 7.94 (t, J = 8.29 Hz, 1H), 7.82 (d, J = 7.13 Hz, 1H), 7.75 (d, J = 7.13, 1H), 7.58 (dd, J = 7.88, 1.82 Hz, 2H), 7.57 (s, 1H), 7.46 (d, J = 8.71 Hz, 2H), 1.57 (s, 18H) ppm.

## 2-(Dichlorophosphino)indolo[3,2,1-*jk*]-carbazole (IIIa)

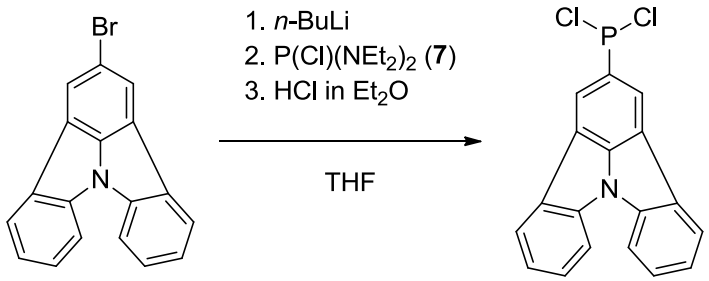


**8a**
$C_{18}H_{10}BrN$
320,18

**IIIa**
$C_{18}H_{10}Cl_2NP$
342,16

Procedure adapted from [34d]. *n*-BuLi (1.5 mL, 3.75 mmol, 2.5 M in hexane, 1 eq.) was added dropwise to a solution of **8a** (1.2 g, 3.75 mmol, 1 eq.) in THF (60 mL) at -78 °C under nitrogen atmosphere. After 1.5 hours of stirring at -78 °C compound **7** (0.790 g, 3.75 mmol, 1 eq.) was added. The reaction mixture was allowed to warm up to room temperature and stirred overnight. Subsequently HCl (7.5 mL, 15 mmol, 2 M in diethyl ether, 4 eq.) was added slowly to the reaction mixture at 0 °C and stirred for 2 hours at room temperature. The diethylammonium chloride precipitate was separated using a cannula to filter the reaction mixture under nitrogen through a Celite plug which was washed with diethyl ether (3x30 mL). The solvent was evaporated under vacuum to give a yellowish milky solid which was dissolved in absolute diethyl ether and filtrated again. Compound **IIIa** (1.25 g, 98%) was obtained as an orange milky solid.

$^{31}P$ {$^{1}H$}-NMR (400 MHz, $CDCl_3$): $\delta$ = 167.07 (s).

## E.5 Synthesis of OLED compounds – acceptor systems

### E.5.1 Synthesis of bithiophene systems

**3,3',5,5'-Tetrabromo-2,2'-bithiophene (10)**

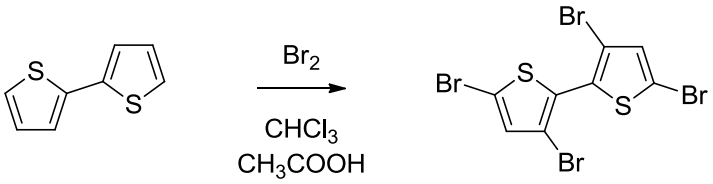


**9**
$C_8H_6S_2$
166,26

**10**
$C_8H_2Br_4S_2$
481,85

Procedure adapted from [41]. Bithiophene (**9**) was distilled under reduced pressure (100 °C, 0.4 mbar). Bithiophene (**9**) (24.8 g, 149 mmol, 1 eq.), chloroform (270 mL) and glacial acetic acid (119 mL) was charged in a 1 L 3-neck-round bottom flask. The reaction mixture was cooled down to 0 °C and $Br_2$ (29 mL, 90.45 g, 580 mmol, 3.9 eq) was added slowly (over 1.5 hrs) using a dropping funnel and wash traps filled with water for the gas outlet. After the addition the residue material in the dropping funnel was washed into the round bottom flask with chloroform (20 mL). After replacing the dropping funnel with a reflux condenser the reaction mixture was allowed to warm up to RT and refluxed overnight. During cooling a precipitate was formed which was separated by filtration. The filter cake was washed with KOH (10% solution). The organic solution and the KOH solution were combined and separated using a separation funnel. The organic layer was once again washed with KOH (10% solution) and brine and then dried over anhydrous $Na_2SO_4$. The solvent was evaporated under vacuum leaving a yellow solid which was purified by recrystallization from ethanol giving compound **10** (53.3 g, 74%) as yellow crystalline solid.

$R_f$: 0.19 (EA)

$^1$H-NMR (400 MHz, $CDCl_3$): $\delta$ = 7.05 (s, 2H) ppm.

## 3,3'-Dibromo-2,2'-bithiophene (11)

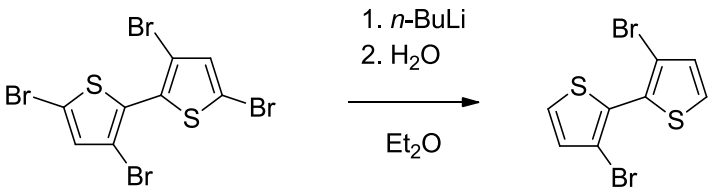


**10**
$C_8H_2Br_4S_2$
481,85

**11**
$C_8H_4Br_2S_2$
324,06

Procedure adapted from [42]. *n*-BuLi (8.3 mL, 20.75 mmol, 2.5 M in hexane, 2 eq.) was added dropwise to a solution of compound **10** (5 g, 10.38 mmol, 1 eq.) in THF (100 mL) at -78 °C under nitrogen atmosphere. After 2 hours of stirring at -78 °C water (5 mL) was added. The reaction mixture was allowed to warm up to room temperature and stirred overnight. The solvent was evaporated under vacuum and the residue was purified by recrystallization to give compound **11** (2.1 g, 62%) as a white, slightly yellowish solid.

$R_f$: 0.42 (Hex)

$^1$H-NMR (400 MHz, $CDCl_3$): $\delta$ = 7.41 (d, J = 5.3, 2H), 7.08 (d, J = 5.3 Hz, 2H) ppm.

## 3,3'-Dibromo-5,5'-dibutyl-2,2'-bithiophene (12)

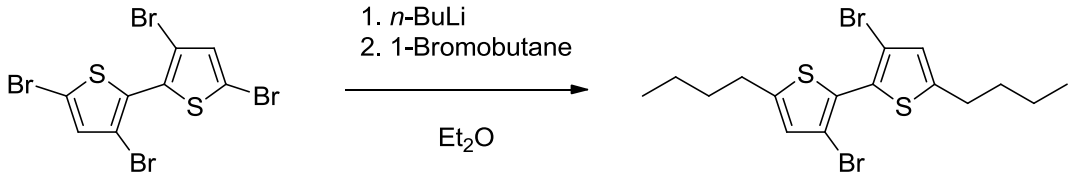


**10**
$C_8H_2Br_4S_2$
481,85

**12**
$C_{16}H_{20}Br_2S_2$
436,27

Procedure adapted from [34d]. *n*-BuLi (9.2 mL, 23 mmol, 2.5 M in hexane, 2 eq.) was added dropwise to a solution of compound **10** (5.52 g, 11.5 mmol, 1 eq.) in THF (100 mL) at -78 °C under nitrogen atmosphere. After 15 min of stirring at -78 °C 1-bromobutane (2.46 mL, 3.152 g, 23 mmol, 2 eq) was added. The reaction mixture was allowed to warm up to room temperature really slowly and stirred overnight. The solvent was evaporated under vacuum and replaced with hexanes (80 mL). The solution was filtrated through a Celite plug. The solvent was once more removed under vacuum and the residue was purified by flash column chromatographie to give compound **12** (4.2 g, 84%) as a yellowish oil.

$R_f$: 0.50 (Hex)

$^1$H-NMR (400 MHz, $CDCl_3$): $\delta$ = 6.75 (s, 2H), 2.79 (t, J = 7.59 Hz, 4H), 1.67 (quin, J = 7.65 Hz, 4H), 1.42 (hex, J = 7.50 Hz, 4H), 0.95 (t, J = 7.35 Hz, 6H) ppm.

## E.5.2 Test reaction - Synthesis of a basic dithienophosphole oxide

**4-Phenyl-4*H*-phospholo[3,2-*b*:4,5-*b'*]dithiophene 4-oxide (14)**

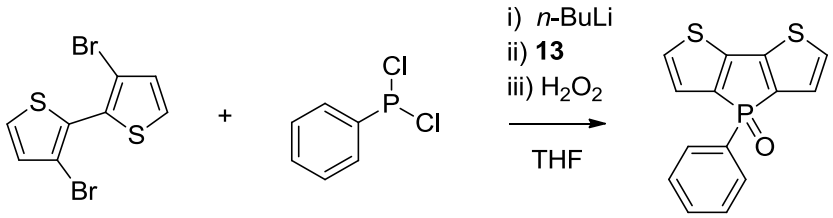


**11**
$C_8H_4Br_2S_2$
324,06

**13**
$C_6H_5Cl_2P$
178,98

**14**
$C_{14}H_9OPS_2$
288,32

Procedure adapted from [34d]. To a solution of **11** (1 g, 3.086 mmol, 1 eq.) in dry diethyl ether (120 mL) was added *n*-BuLi (3.86 mL, 6.17 mmol, 1.6 M in hexane, 2 eq.) dropwise at -78 °C under nitrogen atmosphere. After 1.5 hrs of stirring at -78 °C compound **13** (0.552 g, 3.086 mmol, 1 eq.) was added slowly to the solution and the resulting mixture was allowed to warm quickly to room temperature. After an hour of stirring at room temperature the reaction mixture was filtrated trough an $Al_2O_3$ plug. Water (50 mL) and an excess of $H_2O_2$ (30%, 2 mL) was added to the yellow filtrate. After stirring overnight the layers were separated and the aqueous layer was washed with diethyl ether (2x30 mL). The combined organic phases were dried over $MgSO_4$ before the solvent was removed and the residue was purified by column chromatography (silica gel, ethyl acetate) giving compound **14** as a light yellowish solid (0.6 g, 70 %).

$R_f$: 0.17 (EA)

## E.6 Synthesis of the novel dithienophosphole oxides

### E.6.1 2,2'-Bithiophene-based dithienophosphole oxides

**4-(4-(9*H*-Carbazol-9-yl)phenyl)-4*H*-phospholo[3,2-*b*:4,5-*b*']dithiophene 4-oxide (Va)**

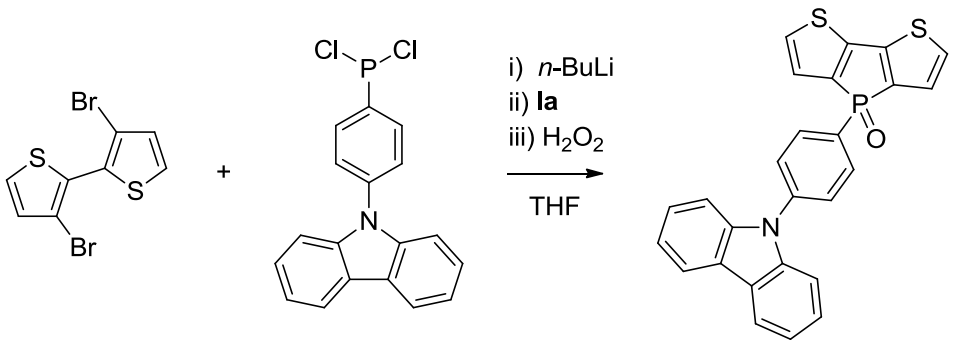


**11**
$C_8H_4Br_2S_2$
324,06

**Ia (*para*)**
$C_{18}H_{12}Cl_2NP$
344,17

**Va (*para*)**
$C_{26}H_{16}NOPS_2$
453,52

Procedure adapted from [34d]. To a solution of **11** (1 g, 3.086 mmol, 1 eq.) and TMEDA (0.94 mL, 0.72 g, 6.17 mmol, excess) in dry diethyl ether (80 mL) was added *n*-BuLi (2.47 mL, 6.17 mmol, 2.5 M in hexane, 2 eq.) dropwise at -78 °C under nitrogen atmosphere. After 2 hrs of stirring at -78 °C a solution of compound **Ia** (0.75 g, 2.24 mmol, 0.73 eq.) in THF (35 mL) was added slowly to the solution and the resulting mixture was allowed to warm quickly to room temperature. After an hour of stirring at room temperature the solvent was removed under vacuum. The residue was dissolved in chloroform (60 mL) and an excess of $H_2O_2$ (30%, 2 mL) was added. After stirring for 2 hours the solution was dried over $MgSO_4$ before the solvent was removed and the residue was purified by column chromatography (silica gel, ethyl acetate) giving compound **Va** as a light yellowish solid (130 mg, 13 %).

$R_f$: 0.34 (EA)

$^1$H NMR (400 MHz, $CD_2Cl_2$) δ = 8.14 (d, J = 7.65 Hz, 2H), 7.94 (dd, J = 12.81, 8.33 Hz, 2H), 7.68 (dd, J = 8.38, 2.33 Hz, 2H), 7.44 (t, J = 8.02 Hz, 2H), 7.41 (m, 2H), 7.40 (dd, J = 4.80, 3.31 Hz, 2H), 7.30 (t, J = 6.94 Hz, 2H), 7.26 (dd, J = 4.88, 2.33 Hz, 2H) ppm.

$^{13}$C NMR (400 MHz, $CD_2Cl_2$) δ = 146.34 (d, J = 24.34 Hz), 141.97 (d, J = 3.51 Hz), 140.65 (s), 139.28 (d, J = 112.33 Hz), 133.03 (d, J = 12.05 Hz), 129.27 (d, J = 108.25 Hz), 129.25 (d, J = 14.86 Hz), 127.34 (d, J = 13.32 Hz), 126.55 (s), 126.28 (d, J = 14.49 Hz), 124.07 (s), 120.88 (s), 129.71 (s), 110.11 (s) ppm.

## 4-(3-(9*H*-Carbazol-9-yl)phenyl)-4*H*-phospholo[3,2-*b*:4,5-*b'*]dithiophene 4-oxide (Vb)

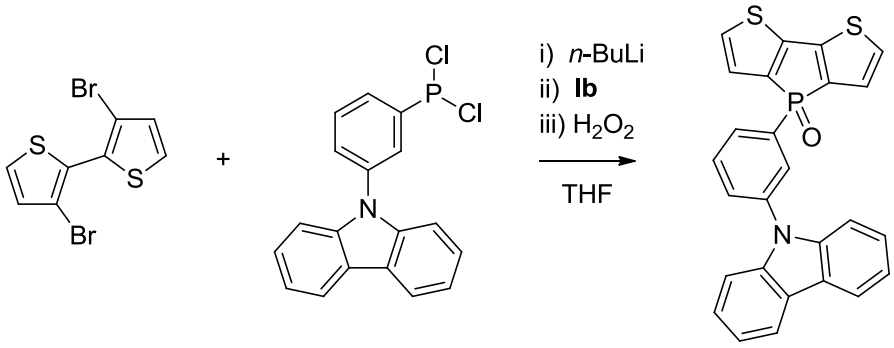


**11**
$C_8H_4Br_2S_2$
324,06

**Ib (*meta*)**
$C_{18}H_{12}Cl_2NP$
344,17

**Vb (*meta*)**
$C_{26}H_{16}NOPS_2$
453,52

Procedure adapted from [34d]. To a solution of **11** (1.41 g, 4.358 mmol, 1 eq.) in dry diethyl ether (150 mL) was added *n*-BuLi (3.49 mL, 8.716 mmol, 2.5 M in hexane, 2 eq.) dropwise at -78 °C under nitrogen atmosphere. After 2 hrs of stirring at -78 °C a solution of compound **Ib** (1.5 g, 4.358 mmol, 0.73 eq.) in THF (40 mL) was added slowly to the solution and the resulting mixture was allowed to warm quickly to room temperature. After two hours of stirring at room temperature an excess of water (120 mL) and $H_2O_2$ (30%, 2 mL) was added. After stirring over night the organic phase was separated and dried over $MgSO_4$ before the solvent was removed and the residue was purified by column chromatography (silica gel, ethyl acetate) giving compound **Vb** as a white, slightly yellowish solid (0.81 g, 41 %).

$R_f$: 0.45 (EA)

$^1$H NMR (400 MHz, $CD_2Cl_2$) δ = 8.12 (dd, J = 7.81, 0.66 Hz, 2H), 7.86 (ddt, J = 12.81, 7.37, 1.34 Hz, 1H), 7.83 (dt, J = 13.34, 1.44 Hz, 1H), 7.77 (dm, J = 7.52 Hz, 1H), 7.70 (td, J = 7.63, 3.56 Hz, 1H), 7.36-7.39 (m, 4H), 7.30-7.31 (m, 2H), 7.28-7.29 (m, 2H), 7.24 (dd, J = 4.92, 2.39 Hz, 2H) ppm.

$^{13}$C NMR (400 MHz, $CD_2Cl_2$) δ = 146.37 (d, J = 24.46 Hz), 140.76 (s), 139.16 (d, J = 112.47 Hz), 138.71 (d, J = 15.70 Hz), 133.14 (d, J = 105.90 Hz), 131.07 (d, J = 13.96 Hz), 130.91 (d, J = 2.75 Hz), 129.98 (d, J = 10.34 Hz), 129.34 (d, J = 15.08 Hz), 129.03 (d, J = 12.24 Hz), 126.47 (s), 126.17 (d, J = 14.52 Hz), 123.86 (s), 120.71 (s), 120.69 (s), 109.85 (s) ppm.

$^{31}$P {$^1$H}-NMR (400 MHz, $CDCl_3$): δ = 17.82 (s) ppm.

## 4-(2-(9*H*-Carbazol-9-yl)phenyl)-4*H*-phospholo[3,2-*b*:4,5-*b'*]dithiophene 4-oxide (Vc)

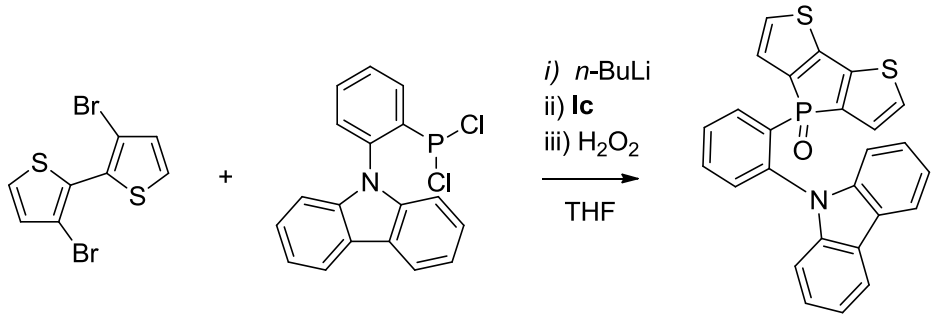


**11**
$C_8H_4Br_2S_2$
324,06

**Ic (*ortho*)**
$C_{18}H_{12}Cl_2NP$
344,17

**Vc (*ortho*)**
$C_{26}H_{16}NOPS_2$
453,52

Procedure adapted from [34d]. To a solution of **11** (1 g, 3.086 mmol, 1 eq.) and TMEDA (0.94 mL, 0.72 g, 6.17 mmol, excess) in dry diethyl ether (120 mL) was added *n*-BuLi (2.47 mL, 6.17 mmol, 2.5 M in hexane, 2 eq.) dropwise at -78 °C under nitrogen atmosphere. After 2 hrs of stirring at -78 °C a solution of compound **Ic** (1.06 g, 3.086 mmol, 1 eq.) in THF (35 mL) was added slowly to the solution and the resulting mixture was allowed to warm quickly to room temperature. After an hour of stirring at room temperature the solvent was removed under vacuum. The residue was dissolved in chloroform (60 mL) and stirred overnight in an open round-bottom-flask. Since TLCs did not show complete oxidation an excess of $H_2O_2$ (30%, 1.5 mL) was added. After stirring for 1 hour the solution was dried over $MgSO_4$ before the solvent was removed *in vacuo* and the residue was purified by column chromatography (silica gel, ethyl acetate) giving compound **Vc** as a light yellowish solid (353 mg, 25 %). Single crystals, suitable for X-ray-crystallography, were obtained by slow evaporation from a $CD_2Cl_2$-solution.

$R_f$: 0.51 (EA)

$^1$H NMR (400 MHz, $CD_2Cl_2$) δ = 8.82 (ddd, J = 13.19, 7.75, 1.56 Hz, 1H), 7.87 (m, 1H), 7.86 (d, J = 7.45 Hz, 2H), 7.79 (t, J = 7.56 Hz, 1H), 7.23 (t, J = 6.43 Hz, 1H), 7.11 (td, J = 7.40, 1.10 Hz, 2H), 7.06 (td, J = 7.45, 1.2 Hz, 2H), 6.76 (dd, J = 4.76, 3.54 Hz, 2H), 6.68 (dd, J = 4.86, 2.26 Hz, 2H), 6.44 (d, J = 8.28 Hz, 2H) ppm.

$^{13}$C NMR (400 MHz, $CD_2Cl_2$) δ = 145.60 (d, J = 25.55 Hz), 142.19 (s), 138.69 (d, J = 5.96 Hz), 137.67 (d, J = 115.67 Hz), 137.08 (d, J =7.30 Hz), 134.45 (d, J = 2.26 Hz), 132.68 (d, J = 101.71 Hz), 131.80 (d, J = 7.70 Hz), 130.24 (d, J = 11.30 Hz), 128.09 (d, J = 15.56 Hz), 125.89 (s), 125.22 (d, J = 15.16 Hz), 123.21 (s), 120.03 (s), 119.83 (s), 110.01 (s) ppm.

$^{31}$P {$^1$H}-NMR (400 MHz, $CDCl_3$): δ = 12.93 (s) ppm.

## 4-(3-(3,6-Di-*tert*-butyl-9*H*-carbazol-9-yl)phenyl)-4*H*-phospholo[3,2-*b*:4,5-*b*'] dithiophene 4-oxide (VIb)

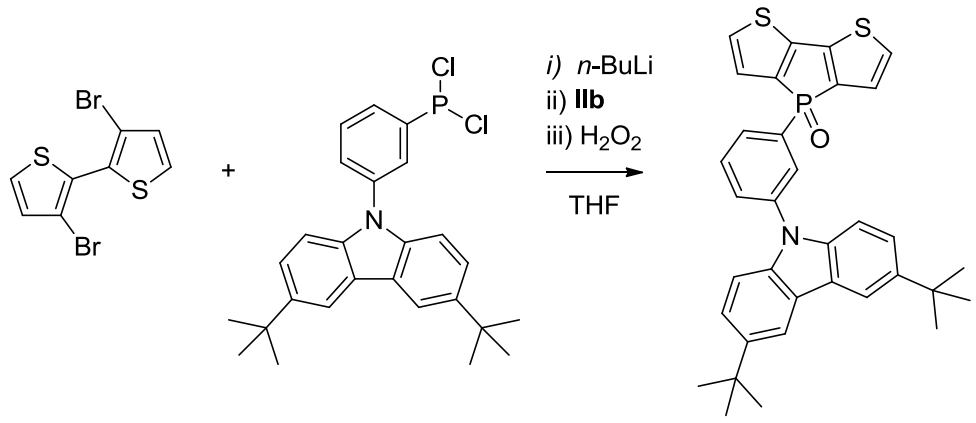


| **11** | **IIb (*meta*)** | **VIb (*meta*)** |
|---|---|---|
| $C_8H_4Br_2S_2$ | $C_{26}H_{28}Cl_2NP$ | $C_{34}H_{32}NOPS_2$ |
| 324,06 | 456,39 | 565,73 |

Procedure adapted from [34d]. To a solution of **11** (0.62 g, 1.91 mmol, 1 eq.) and TMEDA (0.58 mL, 0.44 g, 3.82 mmol, excess) in dry THF (75 mL) was added *n*-BuLi (1.53 mL, 3.82 mmol, 2.5 M in hexane, 2 eq.) dropwise at -78 °C under nitrogen atmosphere. After 2 hrs of stirring at -78 °C a solution of compound **IIb** (0.87 g, 1.91 mmol, 1 eq.) in THF (30 mL) was added slowly to the solution and the resulting mixture was allowed to warm quickly to room temperature. After 1.5 hours of stirring at room temperature the solvent was removed under vacuum. The residue was dissolved in chloroform (60 mL) and an excess of $H_2O_2$ (30%, 1 mL) was added. After stirring for 1 hour the organic layer was separated and dried over $MgSO_4$ before the solvent was removed and the residue was purified by column chromatography (silica gel, DCM : MeCN = 20:1) giving compound **VIb** as a light yellowish solid (185 mg, 17 %).

$R_f$: 0.22 (EA:Hex = 1:1), , 0.23 (DCM : MeCN = 20:1)

$^1$H NMR (400 MHz, $CD_2Cl_2$) δ = 8.13 (sd, J = 1.82 Hz, 2H), 7.86-7.77 (m, 2H), 7.75 (dm, J = 8.20 Hz, 1H), 7.68 (td, J = 7.70, 3.68 Hz, 1H), 7.44 (dd, J = 8.68, 1.84 Hz, 2H), 7.38 (dd, J = 4.83, 3.39 Hz, 2H), 7.23-7.25 (m, 4H), 1.45 (s, 18H) ppm.

$^{13}$C NMR (400 MHz, $CD_2Cl_2$) δ = 146.41 (d, J = 24.07 Hz), 143.83 (s), 139.25 (d, J = 15.90 Hz), 139.02 (d, J = 112.67 Hz), 139.09 (s), 132.76 (d, J = 106.19 Hz), 130.97 (d, J = 14.00 Hz), 130.58 (d, J = 2.81 Hz), 129.43 (d, J = 10.35 Hz), 129.36 (d, J = 15.16 Hz), 128.63 (d, J = 12.23 Hz), 126.20 (d, J = 14.53 Hz), 124.18 (s), 123.89 (s), 116.77 (s), 109.29 (s), 35.03 (s), 32.09 (s) ppm.

$^{31}$P {$^1$H}-NMR (400 MHz, $CDCl_3$): δ = 17.97 (s) ppm.

## 4-(Indolo[3,2,1-*jk*]carbazol-2-yl)-4*H*-phospholo[3,2-*b*:4,5-*b*']dithiophene 4-oxide (VIIa)

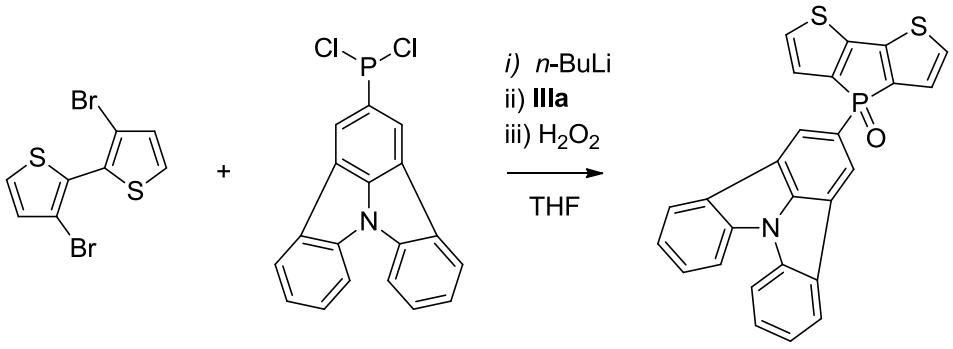


**11**
$C_8H_4Br_2S_2$
324,06

**IIIa**
$C_{18}H_{10}Cl_2NP$
342,16

**VIIa**
$C_{26}H_{14}NOPS_2$
451,50

Procedure adapted from [34d]. To a solution of **11** (0.5 g, 1.53 mmol, 1 eq.) in dry THF (60 mL) was added *n*-BuLi (1.22 mL, 3.06 mmol, 2.5 M in hexane, 2 eq.) dropwise at -78 °C under nitrogen atmosphere. After 2 hrs of stirring at -78 °C a solution of compound **IIIa** (0.52 g, 1.53 mmol, 1 eq.) in THF (15 mL) was added slowly to the solution and the resulting mixture was allowed to warm quickly to room temperature. After an hour of stirring at room temperature the solvent was removed under vacuum. The residue was dissolved in chloroform (60 mL) and an excess of $H_2O_2$ (30%, 2 mL) was added. After stirring for 2 hours the organic phase was separated and dried over $MgSO_4$ before the solvent was removed and the residue was purified by column chromatography (silica gel, DCM : MeCN = 5:1) giving compound **VIIa** as a light yellowish solid (73 mg, 10 %).

$R_f$: 0.26 (DCM : MeCN = 5:1)

$^1$H NMR (400 MHz, $CD_2Cl_2$) δ = 8.46 (d, J = 13.06 Hz, 2H), 8.15 (d, J = 7.78 Hz, 2H), 7.95 (d, J = 8.06 Hz, 2H), 7.62 (t, J = 7.74 Hz, 2H), 7.40 (t, J = 7.74 Hz, 2H), 7.37 (dd, J = 4.74, 3.47 Hz, 2H), 7.20 (dd, J = 4.78, 2.30 Hz, 2H) ppm.

$^{13}$C NMR (400 MHz, $CD_2Cl_2$) δ = 146.18 (d, J = 1.86 Hz), 145.98 (d, J = 23.63 Hz), 140.63 (d, J = 111.05 Hz), 139.58 (s), 129.60 (s), 129.07 (d, J = 14.80 Hz), 128.08 (s), 126.23 (d, J = 14.48 Hz), 123.95 (s), 123.74 (d, J = 108.36 Hz), 122.86 (s), 122.78 (d, J = 14.51 Hz), 119.30 (d, J = 17.11 Hz), 112.87 (s) ppm.

$^{31}$P {$^1$H}-NMR (400 MHz, $CDCl_3$): δ = 22.23 (s) ppm.

## E.6.2 5,5'-Dibutyl-2,2'-bithiophene-based dithienophosphole oxides

**4-(4-(9*H*-Carbazol-9-yl)phenyl)-2,6-dibutyl-4*H*-phospholo[3,2-*b*:4,5-*b*']dithiophene 4-oxide (VIIIa)**

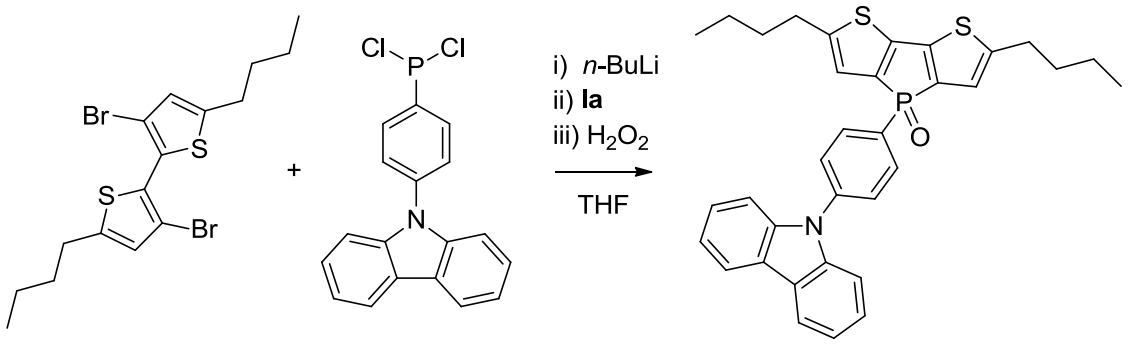


| **12** | **Ia (*para*)** | **VIIIa (*para*)** |
|---|---|---|
| $C_{16}H_{20}Br_2S_2$ | $C_{18}H_{12}Cl_2NP$ | $C_{34}H_{32}NOPS_2$ |
| 436,27 | 344,17 | 565,73 |

Procedure adapted from [34d]. To a solution of **12** (0.8 g, 1.83 mmol, 1 eq.) and TMEDA (0.58 mL, 0.45 g, 3.87 mmol, excess) in dry diethyl ether (73 mL) was added *n*-BuLi (1.46 mL, 3.66 mmol, 2.5 M in hexane, 2 eq.) dropwise at -78 °C under nitrogen atmosphere. After 2 hrs of stirring at -78 °C a solution of compound **Ia** (0.63 g, 1.83 mmol, 1 eq.) in abs. diethyl ether (and a few drops of THF) (30 mL) was added slowly to the solution and the resulting mixture was allowed to warm quickly to room temperature. After an hour of stirring at room temperature the solvent was removed under vacuum. The residue was dissolved in chloroform (60 mL) and an excess of $H_2O_2$ (30%, 2 mL) was added. After stirring for 1.5 hours the organic phase was separated and dried over $MgSO_4$ before the solvent was removed and the residue was purified by column chromatography (silica gel, ethyl acetate and hexanes, 1:1) giving compound **VIIIa** as a yellowish solid (375 mg, 36 %).

$R_f$: 0.26 (EA:Hex = 1:1)

$^1$H NMR (400 MHz, $CD_2Cl_2$) δ = 8.14 (d, J = 7.69 Hz, 2H), 7.94 (dd, J = 12.68, 8.34 Hz, 2H), 7.67 (dd, J = 8.41, 2.36 Hz, 2H), 7.46 (d, J = 8.17 Hz, 2H), 7.42 (ddd, J = 8.22, 7.01, 1.08 Hz, 2H), 7.23 (td, J = 7.36, 0.99 Hz, 2H), 6.91 (st, J = 1.03 Hz, 2H), 2.85 (t, J = 7.63 Hz, 4H), 1.69 (quin, J = 7.56 Hz, 4H), 1.42 (hex, J = 7.41 Hz, 4H), 0.95 (t, J = 7.5 Hz, 6H) ppm.

$^{13}$C NMR (400 MHz, $CD_2Cl_2$) δ = 150.61 (d, J = 14.37 Hz), 144.21 (d, J = 24.31 Hz), 141.71 (d, J = 3.18 Hz), 140.68 (s), 137.39 (d, J = 112.52 Hz), 133.01 (d, J = 12.06 Hz), 130.07 (d, J = 107.26 Hz), 127.27 (d, J = 13.17 Hz), 126.53 (s), 124.05 (s), 122.69 (d, J = 14.30 Hz), 120.85 (s), 120.71 (s), 110.11 (s), 34.06 (s), 30.46 (s), 22.51 (s), 13.93 (s) ppm.

$^{31}$P {$^1$H}-NMR (400 MHz, $CDCl_3$): δ = 19.23 (s) ppm.

## 4-(3-(9*H*-Carbazol-9-yl)phenyl)-2,6-dibutyl-4*H*-phospholo[3,2-*b*:4,5-*b*']dithiophene 4-oxide (VIIIb)

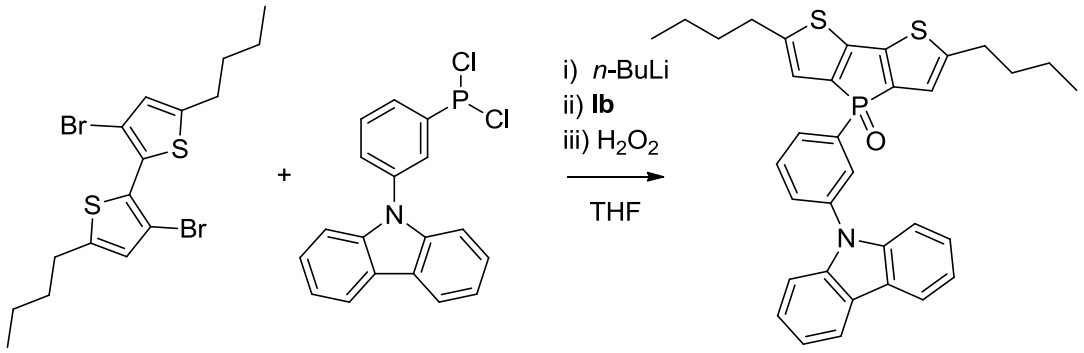


| **12** | **Ib (*meta*)** | **VIIIb (*meta*)** |
|---|---|---|
| $C_{16}H_{20}Br_2S_2$ | $C_{18}H_{12}Cl_2NP$ | $C_{34}H_{32}NOPS_2$ |
| 436,27 | 344,17 | 565,73 |

Procedure adapted from [34d]. To a solution of **12** (1.394 g, 3.196 mmol, 1 eq.) in dry diethyl ether (110 mL) was added *n*-BuLi (2.56 mL, 6.392 mmol, 2.5 M in hexane, 2 eq.) dropwise at -78 °C under nitrogen atmosphere. After 2 hrs of stirring at -78 °C a solution of compound **Ib** (1.1 g, 3.196 mmol, 1 eq.) in a 1:1 mixture of abs. Ether and abs. THF (13 mL) was added slowly to the solution and the resulting mixture was allowed to warm quickly to room temperature. After an hour of stirring at room temperature the solvent was removed under vacuum. The residue was dissolved in hexanes (60 mL) and an excess of $H_2O_2$ (30%, 2 mL) was added. After stirring for 2 hours the organic phase was separated and dried over $MgSO_4$ before the solvent was removed and the residue was purified by column chromatography (silica gel, ethyl acetate and hexanes, 1:1) giving compound **VIIIb** as a light yellowish solid (0.55 g, 30 %).

$R_f$: 0.63 (EA), 0.25 (EA:Hex = 1:1)

$^1$H NMR (400 MHz, $CD_2Cl_2$) δ = 8.13 (d, J = 7.77 Hz, 2H), 7.88 (ddt, J = 12.60, 7.34, 1.36 Hz, 1H), 7.81 (dt, J = 13.86, 1.42 Hz, 1H), 7.76 (dm, J = 8.03, 1.40 Hz, 1H), 7.71 (td, J = 7.60, 3.43 Hz, 1H), 7.38 (ddd, J = 8.21, 7.00, 1.20 Hz, 2H), 7.31 (d, J = 8.05 Hz, 2H), 7.29 (ddd, J = 7.90, 6.86, 1.00 Hz, 2H), 6.89 (st, J = 1.00 Hz, 2H), 2.82 (t, J = 7.65 Hz, 4H), 1.66 (quin, J = 7.57 Hz, 4H), 1.39 (hex, J = 7.41 Hz, 4H), 0.92 (t, J = 7.34 Hz, 6H) ppm.

$^{13}$C NMR (400 MHz, $CD_2Cl_2$) δ = 150.74 (d, J = 14.43 Hz), 144.27 (d, J = 24.37 Hz), 140.76 (s), 138.61 (d, J = 15.45 Hz), 137.19 (d, J = 112.53 Hz), 133.78 (d, J = 104.57 Hz), 130.97 (d, J = 13.69 Hz), 130.64 (d, J = 2.65 Hz), 130.06 (d, J = 10.13 Hz), 128.93 (d, J = 12.35 Hz), 126.46 (s), 123.86 (s), 122.56 (d, J = 14.34 Hz), 120.69 (s, 2C), 109.88 (s), 34.06 (s), 30.43 (s), 22.49 (s), 13.90 (s) ppm.

$^{31}$P {$^1$H}-NMR (400 MHz, $CDCl_3$): δ = 19.07 (s) ppm.

## 4-(2-(9*H*-Carbazol-9-yl)phenyl)-2,6-dibutyl-4*H*-phospholo[3,2-*b*:4,5-*b*']dithiophene 4-oxide (VIIIc)

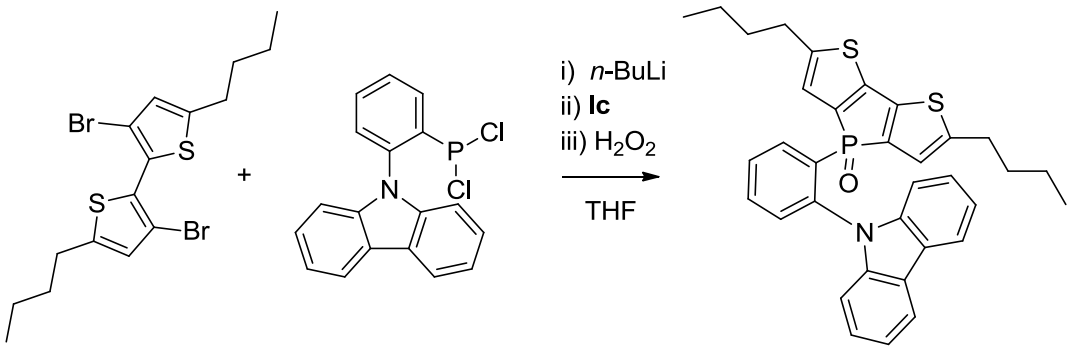


| **12** | **Ic (*ortho*)** | **VIIIc (*ortho*)** |
|---|---|---|
| $C_{16}H_{20}Br_2S_2$ | $C_{18}H_{12}Cl_2NP$ | $C_{34}H_{32}NOPS_2$ |
| 436,27 | 344,17 | 565,73 |

Procedure adapted from [34d]. To a solution of **12** (1 g, 2.29 mmol, 1 eq.) and TMEDA (0.69 mL, 0.53 g, 4.58 mmol, excess) in dry THF (90 mL) was added *n*-BuLi (1.83 mL, 4.58 mmol, 2.5 M in hexane, 2 eq.) dropwise at -78 °C under nitrogen atmosphere. After 2 hrs of stirring at -78 °C a solution of compound **Ic** (0.79 g, 2.29 mmol, 1 eq.) in THF (35 mL) was added slowly to the solution and the resulting mixture was allowed to warm quickly to room temperature. After an hour of stirring at room temperature the solvent was removed under vacuum. The residue was dissolved in chloroform (60 mL) and stirred overnight in an open round-bottom-flask. Since TLCs did not show complete oxidation an excess of $H_2O_2$ (30%, 1.5 mL) was added. After stirring for 1 hour the solution was dried over $MgSO_4$ before the solvent was removed *in vacuo* and the residue was purified by column chromatography (silica gel, ethyl acetate and hexanes, 1:1) giving compound **VIIIc** as a light yellowish solid (220 mg, 17 %).

$R_f$: 0.69 (EA)

$^1$H NMR (400 MHz, $CD_2Cl_2$) δ = 8.70 (ddd, J = 13.03, 7.72, 1.36 Hz, 1H), 7.88 (m, 2H), 7.83 (t, J = 7.63 Hz, 1H), 7.76 (t, J = 7.51 Hz, 1H), 7.19 (dd, J = 6.30 Hz, 1H), 7.08-7.14 (m, J = 5.4, 3.61 Hz, 4H), 6.47 (dd, J = 5.73, 2.94 Hz, 2H), 6.34 (s, 2H), 2.48 (t, J =7.45 Hz, 4H), 1.49 (quin, J = 7.37 Hz, 4H), 1.34 (hex, J = 7.34 Hz, 4H), 0.92 (t, J = 7.29 Hz, 6H) ppm.

$^{13}$C NMR (400 MHz, $CD_2Cl_2$) δ = 149.42 (d, J = 14.83 Hz), 143.79 (d, J = 25.46 Hz), 142.36 (s), 138.77 (d, J = 5.76 Hz), 136.92 (d, J = 7.12 Hz), 135.70 (d, J = 115.99 Hz), 134.16 (d, J = 2.16 Hz), 133.35 (d, J = 100.27 Hz), 131.65 (d, J = 7.64 Hz), 130.09 (d, J = 11.00 Hz), 125.59 (s), 123.36 (s), 121.96 (d, J = 14.84 Hz), 119.92 (s), 119.82 (s), 110.30 (s), 33.49 (s), 30.13 (s), 22.57 (s), 13.93 (s) ppm.

$^{31}$P {$^1$H}-NMR (400 MHz, $CDCl_3$): δ = 14.08 (s) ppm.

## 4-(3-(3,6-Di-*tert*-butyl-9*H*-carbazol-9-yl)phenyl)-2,6-dibutyl-4*H*-phospholo[3,2-*b*:4,5-*b*'] dithiophene 4-oxide (IXb)

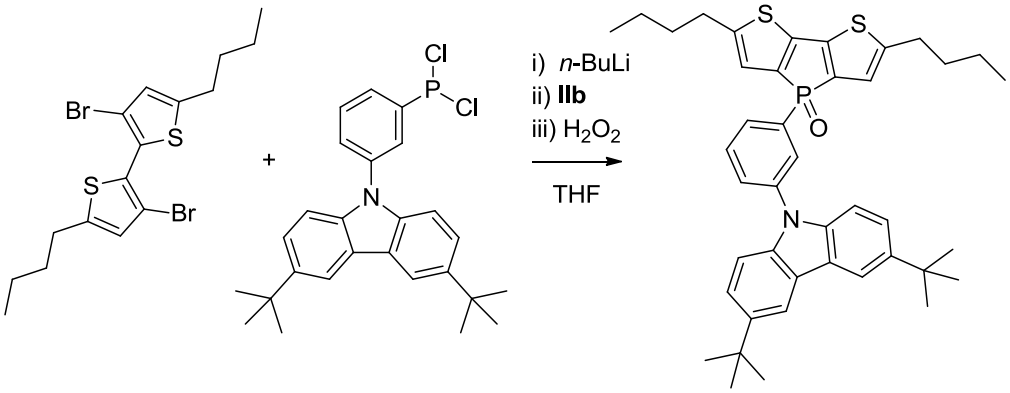


| **12** | **IIb (*meta*)** | **IXb (*meta*)** |
|---|---|---|
| $C_{16}H_{20}Br_2S_2$ | $C_{26}H_{28}Cl_2NP$ | $C_{42}H_{48}NOPS_2$ |
| 436,27 | 456,39 | 677,94 |

Procedure adapted from [34d]. To a solution of **12** (0.83 g, 1.91 mmol, 1 eq.) and TMEDA (0.58 mL, 0.44 g, 3.82 mmol, excess) in dry THF (75 mL) was added *n*-BuLi (1.53 mL, 3.82 mmol, 2.5 M in hexane, 2 eq.) dropwise at -78 °C under nitrogen atmosphere. After 2 hrs of stirring at -78 °C a solution of compound **IIb** (0.87 g, 1.91 mmol, 1 eq.) in THF (30 mL) was added slowly to the solution and the resulting mixture was allowed to warm quickly to room temperature. After 1.5 hours of stirring at room temperature the solvent was removed under vacuum. The residue was dissolved in chloroform (60 mL) and an excess of $H_2O_2$ (30%, 1 mL) was added. After stirring for 1 hour the organic layer was separated and dried over $MgSO_4$ before the solvent was removed and the residue was purified by column chromatography (silica gel, DCM : MeCN = 20:1) giving compound **IXb** as a light yellowish solid (0.47 g, 36 %).

$R_f$: 0.32 (DCM : MeCN = 20:1)

$^1$H NMR (400 MHz, $CD_2Cl_2$) δ = 8.13 (sd, J = 1.78 Hz, 2H), 7.84 (ddt, J = 12.63, 7.34, 1.24 Hz, 1H), 7.78 (dt, J = 13.99, 1.35 Hz, 1H), 7.75 (dm, J = 8.80 Hz, 1H), 7.68 (td, J = 7.65, 3.52 Hz, 1H), 7.43 (dd, J = 8.68, 1.93 Hz, 2H), 7.25 (d, J = 8.66 Hz, 2H), 6.89 (st, J = 1.00 Hz, 2H), 2.82 (t, J = 7.65 Hz, 4H), 1.66 (quin, J = 7.57 Hz, 4H), 1.44 (s, 18H), 1.39 (hex, J = 7.42 Hz, 4H), 0.92 (t, J = 7.35 Hz, 6H) ppm.

$^{13}$C NMR (400 MHz, $CD_2Cl_2$) δ = 150.72 (d, J = 14.11 Hz), 144.29 (d, J = 24.38 Hz), 143.78 (s), 139.11 (d, J = 15.57 Hz), 139.07 (s), 137.11 (d, J = 112.61 Hz), 133.44 (d, J = 104.91 Hz), 130.88 (d, J = 13.86 Hz), 130.25 (d, J = 2.84 Hz), 129.56 (d, J = 10.12 Hz), 128.47 (d, J = 12.41 Hz), 124.14 (s), 123.88 (s), 122.57 (d, J = 14.14 Hz), 116.76 (s), 109.31 (s), 35.02 (s), 34.05 (s), 32.10 (s), 30.43 (s), 22.50 (s), 13.91 (s) ppm.

$^{31}$P {$^1$H}-NMR (400 MHz, $CDCl_3$): δ = 19.18 (s) ppm.

## 4-(Indolo[3,2,1-*jk*]carbazol-2-yl)-2,6-dibutyl-4*H*-phospholo[3,2-*b*:4,5-*b*'] dithiophene 4-oxide (Xa)

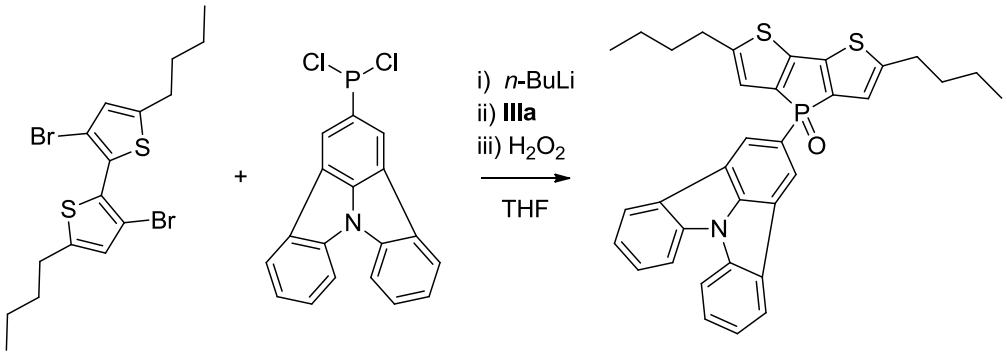


**12**
$C_{16}H_{20}Br_2S_2$
436,27

**IIIa**
$C_{18}H_{10}Cl_2NP$
342,16

**Xa**
$C_{34}H_{30}NOPS_2$
563,71

Procedure adapted from [34d]. To a solution of **12** (0.97 g, 2.22 mmol, 1 eq.) in dry THF (90 mL) was added *n*-BuLi (1.78 mL, 4.44 mmol, 2.5 M in hexane, 2 eq.) dropwise at -78 °C under nitrogen atmosphere. After 2 hrs of stirring at -78 °C a solution of compound **IIIa** (0.76 g, 2.22 mmol, 1 eq.) in THF (20 mL) was added slowly to the solution and the resulting mixture was allowed to warm quickly to room temperature. After an hour of stirring at room temperature the solvent was removed under vacuum. The residue was dissolved in chloroform (60 mL) and an excess of $H_2O_2$ (30%, 2 mL) was added. After stirring for 2 hours the organic phase was separated and dried over $MgSO_4$ before the solvent was removed and the residue was purified by column chromatography (silica gel, DCM : MeCN = 20:1) giving compound **Xa** as a light yellowish solid (152 mg, 12 %).

$R_f$: 0.34 (DCM : MeCN = 20:1)

$^1$H NMR (400 MHz, $CD_2Cl_2$) δ = 8.45 (d, J = 12.91 Hz, 2H), 8.15 (d, J = 7.80 Hz, 2H), 7.94 (d, J =8.08 Hz. 2H), 7.61 (t, J = 7.74 Hz, 2H), 7.40 (t, J = 7.48 Hz, 2H), 6.85 (s, 2H), 2.81 (t, J = 7.57 Hz, 4H), 1.66 (quin, J = 7.52 Hz, 4H), 1.39 (hex, J = 7.38 Hz, 4H), 0.92 (t, J = 7.34 Hz, 6H) ppm.

$^{13}$C NMR (400 MHz, $CD_2Cl_2$) δ = 150.43 (d, J = 13.97 Hz), 146.09 (d, J = 1.95 Hz), 143.85 (d, J = 23.74 Hz), 139.54 (s), 138.68 (d, J = 111.21 Hz), 129.64 (s), 128.00 (s), 124.49 (d, J = 106.92 Hz), 123.91 (s), 122.80 (s), 122.77 (d, J = 14.37 Hz), 122.67 (d, J = 14.17 Hz), 119.22 (d, J = 16.70 Hz), 112.84 (s), 34.03 (s), 30.44 (s), 22.49 (s), 13.91 (s) ppm.

$^{31}$P {$^1$H}-NMR (400 MHz, $CDCl_3$): δ = 23.33 (s) ppm.

# Bibliography


[1] (a) M. Stolar, T. Baumgartner, *New Journal of Chemistry* **2012**, *36*, 1153-1160; (b) Y. Tao, C. Yang, J. Qin, *Chemical Society Reviews* **2011**, *40*, 2943-2970.

[2] (a) I. F. Perepichka, D. F. Perepichka, John Wiley & Sons, Ltd, **2009**; (b) B. Valeur, M. N. Berberan-Santos, *Molecular Fluorescence: Principles and Applications*, Wiley, **2013**; (c) J. R. Lakowicz, *Principles of Fluorescence Spectroscopy*, Springer, **2007**; (d) K. Müllen, U. Scherf, *Organic Light Emitting Devices: Synthesis, Properties and Applications*, Wiley, **2006**; (e) T. A. Skotheim, J. R. Reynolds, *Handbook of Conducting Polymers: Conjugated Polymers*, Taylor & Francis, **2007**.

[3] (a) Y. Matano, H. Imahori, *Organic & biomolecular chemistry* **2009**, *7*, 1258-1271; (b) M. G. Hobbs, T. Baumgartner, *European Journal of Inorganic Chemistry* **2007**, *2007*, 3611-3628; (c) T. Baumgartner, R. Réau, *Chemical reviews* **2006**, *106*, 4681-4727; (d) A. Fukazawa, S. Yamaguchi, *Chemistry – An Asian Journal* **2009**, *4*, 1386-1400; (e) M. Shimizu, H. Tatsumi, K. Mochida, K. Oda, T. Hiyama, *Chemistry – An Asian Journal* **2008**, *3*, 1238-1247; (f) J. Hou, H.-Y. Chen, S. Zhang, G. Li, Y. Yang, *Journal of the American Chemical Society* **2008**, *130*, 16144-16145; (g) M. Elbing, G. C. Bazan, *Angewandte Chemie International Edition* **2008**, *47*, 834-838; (h) M. J. Bosdet, W. E. Piers, *Canadian Journal of Chemistry* **2009**, *87*, 8-29; (i) C. R. Wade, A. E. Broomsgrove, S. Aldridge, F. P. Gabbai, **2010**; (j) F. Jäkle, *Chemical reviews* **2010**, *110*, 3985-4022.

[4] S. R. Forrest, *Nature* **2004**, *428*, 911-918.

[5] oled.at, http://www.oled.at/lg-zeigt-finales-design-vom-55em9600-oled-tv-in-monaco/, 20.05. **2014**

[6] (a) S. Reineke, F. Lindner, G. Schwartz, N. Seidler, K. Walzer, B. Lussem, K. Leo, *Nature* **2009**, *459*, 234-238; (b) Y. Sun, N. C. Giebink, H. Kanno, B. Ma, M. E. Thompson, S. R. Forrest, *Nature* **2006**, *440*, 908-912.

[7] Wikipedia, http://commons.wikimedia.org/wiki/File:OLED_EarlyProduct.JPG, 20.05. **2014**

[8] Y. Zhou, C. Fuentes-Hernandez, J. Shim, J. Meyer, A. J. Giordano, H. Li, P. Winget, T. Papadopoulos, H. Cheun, J. Kim, *Science* **2012**, *336*, 327-332.

[9] Y.-H. Tak, K.-B. Kim, H.-G. Park, K.-H. Lee, J.-R. Lee, *Thin Solid Films* **2002**, *411*, 12-16.

[10] Y. Shirota, H. Kageyama, *Chemical reviews* **2007**, *107*, 953-1010.

[11] (a) S. Kappaun, C. Slugovc, E. J. List, *International journal of molecular sciences* **2008**, *9*, 1527-1547; (b) N. J. Lundin, A. G. Blackman, K. C. Gordon, D. L. Officer, *Angewandte Chemie International Edition* **2006**, *45*, 2582-2584.

[12] M. A. Baldo, D. F. O'Brien, M. E. Thompson, S. R. Forrest, *Physical Review B* **1999**, *60*, 14422-14428.

[13] T. G. Chasteen, http://www.files.chem.vt.edu/chem-ed/quantum/jablonsk.html, 25.04. **2014**

[14] (a) S. Lamansky, P. Djurovich, D. Murphy, F. Abdel-Razzaq, H.-E. Lee, C. Adachi, P. E. Burrows, S. R. Forrest, M. E. Thompson, *Journal of the American Chemical Society* **2001**, *123*, 4304-4312; (b) M. A. Baldo, S. Lamansky, P. E. Burrows, M. E. Thompson, S. R. Forrest, *Applied Physics Letters* **1999**, *75*, 4-6; (c) C. Adachi, M. A. Baldo, S. R. Forrest, M. E. Thompson, *Applied Physics Letters* **2000**, *77*, 904-906; (d) M. A. Baldo, D. F. O'Brien, Y. You, A. Shoustikov, S. Sibley, M. E. Thompson, S. R. Forrest, *Nature* **1998**, *395*, 151-154.

[15] (a) M. A. Baldo, C. Adachi, S. R. Forrest, *Physical Review B* **2000**, *62*, 10967-10977; (b) C. Ulbricht, B. Beyer, C. Friebe, A. Winter, U. S. Schubert, *Advanced Materials* **2009**, *21*, 4418-4441; (c) Y. Chi, P.-T. Chou, *Chemical Society Reviews* **2010**, *39*, 638-655.

[16] S. J. Yeh, M. F. Wu, C. T. Chen, Y. H. Song, Y. Chi, M. H. Ho, S. F. Hsu, C. H. Chen, *Advanced Materials* **2005**, *17*, 285-289.

[17] S. Reineke, M. Thomschke, B. Lüssem, K. Leo, *Reviews of Modern Physics* **2013**, *85*, 1245-1293.
[18] A. Chaskar, H.-F. Chen, K.-T. Wong, *Advanced Materials* **2011**, *23*, 3876-3895.
[19] S.-H. Eom, Y. Zheng, E. Wrzesniewski, J. Lee, N. Chopra, F. So, J. Xue, *Applied Physics Letters* **2009**, *94*, -.
[20] Y.-K. Huang, T.-H. Jen, Y.-T. Chang, N.-J. Yang, H.-H. Lu, S.-A. Chen, *ACS Applied Materials & Interfaces* **2010**, *2*, 1094-1099.
[21] M.-H. Tsai, T.-H. Ke, H.-W. Lin, C.-C. Wu, S.-F. Chiu, F.-C. Fang, Y.-L. Liao, K.-T. Wong, Y.-H. Chen, C.-I. Wu, *ACS Applied Materials & Interfaces* **2009**, *1*, 567-574.
[22] P. K. Koech, E. Polikarpov, J. E. Rainbolt, L. Cosimbescu, J. S. Swensen, A. L. Von Ruden, A. B. Padmaperuma, *Organic Letters* **2010**, *12*, 5534-5537.
[23] (a) W. Xie, Y. Zhao, C. Li, S. Liu, *Solid-State Electronics* **2007**, *51*, 1129-1132; (b) S. H. Kim, J. Jang, J. Y. Lee, *Applied Physics Letters* **2007**, *91*, 083511-083511-083513; (c) M. E. Kondakova, T. D. Pawlik, R. H. Young, D. J. Giesen, D. Y. Kondakov, C. T. Brown, J. C. Deaton, J. R. Lenhard, K. P. Klubek, *Journal of Applied Physics* **2008**, *104*, 094501-094501-094517.
[24] M.-Y. Lai, C.-H. Chen, W.-S. Huang, J. T. Lin, T.-H. Ke, L.-Y. Chen, M.-H. Tsai, C.-C. Wu, *Angewandte Chemie International Edition* **2008**, *47*, 581-585.
[25] Z. Ge, T. Hayakawa, S. Ando, M. Ueda, T. Akiike, H. Miyamoto, T. Kajita, M.-a. Kakimoto, *Advanced Functional Materials* **2008**, *18*, 584-590.
[26] F.-M. Hsu, C.-H. Chien, C.-F. Shu, C.-H. Lai, C.-C. Hsieh, K.-W. Wang, P.-T. Chou, *Advanced Functional Materials* **2009**, *19*, 2834-2843.
[27] C.-H. Chien, L.-R. Kung, C.-H. Wu, C.-F. Shu, S.-Y. Chang, Y. Chi, *Journal of Materials Chemistry* **2008**, *18*, 3461-3466.
[28] M. Guan, Z. Chen, Z. Bian, Z. Liu, Z. Gong, W. Baik, H. Lee, C. Huang, *Organic Electronics* **2006**, *7*, 330-336.
[29] (a) Y. Tao, Q. Wang, Y. Shang, C. Yang, L. Ao, J. Qin, D. Ma, Z. Shuai, *Chemical Communications* **2009**, 77-79; (b) Y. Tao, Q. Wang, L. Ao, C. Zhong, J. Qin, C. Yang, D. Ma, *Journal of Materials Chemistry* **2010**, *20*, 1759-1765.
[30] D.-H. Lee, Y.-P. Liu, K.-H. Lee, H. Chae, S. M. Cho, *Organic Electronics* **2010**, *11*, 427-433.
[31] S. J. Su, E. Gonmori, H. Sasabe, J. Kido, *Advanced Materials* **2008**, *20*, 4189-4194.
[32] P. Kautny, D. Lumpi, Y. Wang, A. Tissot, J. Bintinger, E. Horkel, B. Stoeger, C. Hametner, H. Hagemann, D. Ma, *Journal of Materials Chemistry C* **2014**.
[33] (a) E. Mattmann, F. Mercier, L. Ricard, F. Mathey, *The Journal of organic chemistry* **2002**, *67*, 5422-5425; (b) E. Mattmann, D. Simonutti, L. Ricard, F. Mercier, F. Mathey, *The Journal of Organic Chemistry* **2001**, *66*, 755-758; (c) E. Mattmann, F. Mathey, A. Sevin, G. Frison, *The Journal of Organic Chemistry* **2002**, *67*, 1208-1213; (d) C. Romero-Nieto, T. Baumgartner, *Synlett* **2013**, *24*, 920-937.
[34] (a) Y. Dienes, S. Durben, T. Kárpáti, T. Neumann, U. Englert, L. Nyulászi, T. Baumgartner, *Chemistry-A European Journal* **2007**, *13*, 7487-7500; (b) T. Neumann, Y. Dienes, T. Baumgartner, *Organic letters* **2006**, *8*, 495-497; (c) T. Baumgartner, W. Bergmans, T. Kárpáti, T. Neumann, M. Nieger, L. Nyulászi, *Chemistry-A European Journal* **2005**, *11*, 4687-4699; (d) C. J. Chua, Y. Ren, T. Baumgartner, *Organic Letters* **2012**, *14*, 1588-1591.
[35] (a) R. A. Krüger, T. J. Gordon, T. C. Sutherland, T. Baumgartner, *Journal of Polymer Science Part A: Polymer Chemistry* **2011**, *49*, 1201-1209; (b) T. Baumgartner, W. Wilk, *Organic letters* **2006**, *8*, 503-506; (c) S. Durben, Y. Dienes, T. Baumgartner, *Organic letters* **2006**, *8*, 5893-5896; (d) T. Baumgartner, T. Neumann, B. Wirges, *Angewandte Chemie International Edition* **2004**, *43*, 6197-6201.
[36] (a) D. R. Bai, T. Baumgartner, *Organometallics* **2010**, *29*, 3289-3297; (b) D. R. Bai, C. Romero-Nieto, T. Baumgartner, *Dalton Transactions* **2010**, *39*, 1250-1260; (c) Y. Dienes, M. Eggenstein, T. Neumann, U. Englert, T. Baumgartner, *Dalton Transactions* **2006**, 1424-1433.

[37] (a) Y. Ren, W. H. Kan, V. Thangadurai, T. Baumgartner, *Angewandte Chemie International Edition* **2012**, *51*, 3964-3968; (b) C. Romero-Nieto, M. Marcos, S. Merino, J. Barberá, T. Baumgartner, J. Rodríguez-López, *Advanced Functional Materials* **2011**, *21*, 4088-4099.
[38] Y. Liu, M. Nishiura, Y. Wang, Z. Hou, *Journal of the American Chemical Society* **2006**, *128*, 5592-5593.
[39] H.-Y. Chen, C.-T. Chen, C.-T. Chen, *Macromolecules* **2010**, *43*, 3613-3623.
[40] B. Gschwend, University Basel **2009**.
[41] H. Meng, W. Huang, *The Journal of Organic Chemistry* **2000**, *65*, 3894-3901.
[42] J. Ohshita, M. Nodono, H. Kai, T. Watanabe, A. Kunai, K. Komaguchi, M. Shiotani, A. Adachi, K. Okita, Y. Harima, K. Yamashita, M. Ishikawa, *Organometallics* **1999**, *18*, 1453-1459.
[43] Bruker, *APEXII, SAINT and SADABS. Bruker Analytical X-ray Instruments, Inc. , Madison, Wisconsin, USA.*, **2008**.
[44] L. Palatinus, G. Chapuis, *Journal of Applied Crystallography* **2007**, *40*, 786-790.
[45] M. D. V. Petricek, L. Palatinus, *JANA2006. Institute of Physics, Praha, Czech Republic.*, **2006**.